



Computer Aided Production Engineering

edited by
Antoni Świć
Jerzy Lipski

M
O
N
O
G
R
A
F
I
E

Computer Aided Production Engineering

Monografie – Politechnika Lubelska



Lublin University of Technology
Mechanical Engineering Faculty
ul. Nadbystrzycka 36
20-618 LUBLIN

Computer Aided Production Engineering

edited by
Antoni Świć
Jerzy Lipski



Politechnika Lubelska
Lublin 2013

Reviewers:

Prof. D. Sc. Eng. Wiktor Taranenko

D. Sc. Eng. Marian Marek Janczarek, Assoc. Prof.

Publication approved by the Rector of Lublin University of Technology

© Copyright by Lublin University of Technology 2013

ISBN: 978-83-63569-72-3

Publisher: Lublin University of Technology
ul. Nadbystrzycka 38D, 20-618 Lublin, Poland

Realization: Lublin University of Technology Library
ul. Nadbystrzycka 36A, 20-618 Lublin, Poland
tel. (81) 538-46-59, email: wydawca@pollub.pl
www.biblioteka.pollub.pl

Printed by : TOP Agnieszka Łuczak, Włocławek, Poland
www.agencjatorp.pl

Impression: 80 copies

OLENA KRESTIANPOL

1. Systematic and Structural Approach to the Formation of Flexible Manufacturing Systems for Packaging.....	9
Introduction	9
1.1. Flexible manufacturing systems of packing	9
1.2. Development of multisubject packaging FMS	12
1.3. Development of multiroute packaging FMS	16
1.4. General principles of packaging FMS design	17
Conclusions	18
References	19

BOGDAN PALCHEVSKY, TARAS VARANITSKY

2. Genetic-Based Approach to the Functional-Modular Structure Design of Packaging Machines.....	20
Introduction	20
2.1. Creating a topological graph structure packing machine	20
2.2. Building a matrix of packing machine structure	23
2.3. Mathematical Model.....	24
2.4. Optimization method with use of genetic algorithm	26
2.5. Example of practical implementation.....	27
References	31

PIOTR PENKALA

3. Analysis of spinning of conical vessels.....	32
Introduction	32
3.1. Assumptions stress analysis process	33
3.2. Design of tools trajectory	35
3.3. Influence of technological parameters on the spinning process	35
3.3.1. Speed stencil.....	35
3.3.2. Feed of working rollers	36
3.3.3. Radius of working rolls	36
3.3.4. Roll diameter grooving.....	36
3.3.5. The thickness of sheet metal disc	36
3.3.6. Diameter of steel disc	37

3.4. Numerical Analysis in Simufact Forming 11.0	37
3.4.1. Spinning parameters used in numerical analysis	37
3.4.2. Analyses spinning process in the first phase.....	37
Conclusions.....	40
References.....	40
<i>JACEK DOMIŃCZUK, JAKUB SZABELSKI</i>	
4. Analysis of energetic properties of the surface layer – overview of methods for measuring the contact angle and the surface free energy	42
Introduction.....	42
4.1. The work of Adhesion	43
4.2. Surface energy	44
4.3. Methods For Determining The Contact Angle	44
4.4. Methods of Determining Surface Energy of Solid.....	46
4.5. The Fowkes methods	48
4.6. The Extended (Hydrogen Bridges) Fowkes method.....	49
4.7. The method by Owens, Wendt, Rabel and Kaelble	49
4.8. The Wu method.....	50
4.9. The Van Oss-Good’s method.....	51
4.10. Surface free energy research.....	51
Conclusions.....	52
References.....	53
<i>PIOTR JAREMEK</i>	
5. The roller cones selection criteria and the ways of their classification.....	55
5.1. Design features of the roller cone and their purpose.....	55
5.2. The ways of roller cones identification.....	58
Conclusions.....	65
Reference	65
<i>VIKTOR MARCHUK, ANATOLIU TKACHUK, STANISLAV PRYSTUPA</i>	
6. Thermophysical analysis process diamond smoothing	67
Conclusions.....	73
References.....	74

MAREK SUKOP, VLADIMIR BALAZ, RUDOLF JANOS, JAROMIR JEZNY

7. Higher speeds of data between computers and mobile robots based on increase in the number of transmitters (robosoccer)	75
Introduction	75
7.1. The standard configuration the transmitting device	75
7.2. Using more transmitters	76
Conclusions	79
References	80

JOZEF VARGA, KAMIL MADÁČ, LADISLAV VARGOVCIK

8. Walking and turning of swivel walker	81
Introduction	81
8.1. Analysis of walking for swivel walker	82
8.2. Analysis of turning swivel walker	83
8.3. Modular conception of swivel walker	84
Conclusions	85
References	85

VLADIMÍR BALÁŽ, MAREK VAGAŠ, MIKULÁŠ HAJDUK, JÁN SEMJON

9. Modular training system in virtual reality environment - MSEVR.....	87
Introduction	87
9.1. Virtual Laboratory	88
Conclusions	93
References	93

KRZYSZTOF JĘDRZEJEK

10. Stock price forecasting using collective intelligence	95
10.1. Introduction	95
10.2. Efficient Market Hypothesis.....	95
10.3. Stock price forecasting	96
10.4. Investor psychology and human interaction in forecasting process	98
10.5. Methodology	99
10.5.1. Collective Intelligence.....	99
10.5.2. User collaboration methods.....	100

10.6. Methodology and experiment	102
10.6.1. Experiment principle.....	102
10.6.2. Algorithm.....	103
10.6.3. Experiment results	104
Conclusions.....	106
References.....	107
<i>JAROSŁAW ZUBRZYCKI</i>	
11. Automation of shafts machining about low rigidity	110
Introduction.....	110
11.1. Identification of dynamic system of cutting processing for shafts with control realized using longitudinal feed.....	110
11.2. Output mathematical model	112
11.3. Analysis of the possibilities of simplifying mathematical models.....	114
11.4. Empirical investigation of the static and dynamic characteristics of machine dynamic system	118
Conclusions.....	123
References:.....	124
<i>RUDOLF JANOS, MIKULAS HAJDUK, MAREK SUKOP, VLADIMIR BALÁŽ</i>	
12. Requirements for agent - rescue robot	126
Introduction.....	126
12.1. Requirements for Rescue Service Robots.....	126
12.2. Requirements of Transport	127
12.3. Working Tasks Requirements.....	128
12.4. Conclusion	129
References.....	129
<i>VLADIMÍR BALÁŽ, MAREK VAGAŠ, JÁN SEMJON, MIKULÁŠ HAJDUK</i>	
13. Design of automated robotized system with two robots	131
Introduction.....	131
13.1. Automated robotized system for assembly	131
Conclusions.....	135
References.....	136

1. Systematic and Structural Approach to the Formation of Flexible Manufacturing Systems for Packaging

Introduction

Development and implementation of flexible manufacturing systems (FMS) means a new phase of technological improvements in production. Currently, FMS has not reached the potentially inherent level of technical and economic efficiency. Getting to develop the FMS, its designers often leave aside the question of its optimality, but in the extent of their knowledge, experience and ingenuity are looking for a solution that they feel to be the best.

Most FMS have several disadvantages that result from lack of a common approach and wide preliminary elaboration of FMS projects in general. Absence of a unified approach to the formation of organizational and technological FMS structures often leads to a simple adoption of engineering solutions with unjustified material costs.

Creating the FMS in packaging production, in particular, requires high investment costs and attracting a large number of highly qualified specialists. Possibilities of achieving FMS efficiency at this level of development are closely related to the improvement of their design process. Engineering, technology and organization of production are laid at this stage. That's why the undeliberate decisions or mistakes in the design become difficult or impossible to remove at further operation of FMS.

Design of FMS at this stage of their development is not possible without the active use of information technology on the basis of a systematic approach. Nowadays there is a tendency of understanding and generalization of FMS design experience in various industries. The intensive work is underway to identify the specific systematic approach in designing FMS of packaging production and use of the optimization synthesis methodology for the structure of FMS.

1.1. Flexible manufacturing systems of packing

Automatic packaging is a set of processes for the connection of product with containers and auxiliary packaging means that are conducted without human intervention. Packing machine or system of machines in this case should form the container, prepare it for the filling in with substance, measure the required dose, upload the dose in a container and carry out sealing and labelling.

Flexible automatic packaging is the listed above set of processes complemented by machine readjustment that provides flexibility in the production system.

* Dr inż. Olena Krestianpol, Lutsk National Technical University, 75 Lvivska str., 43018 Lutsk, Tel.: +380 (332) 767395, e-mail: pac@tf.dtu.lutsk.ua

There are the following aspects of flexibility:

- subject flexibility that provides production of various packages by one FMS (or changing the dose, type of packaging material, the nature of sealing and labeling, etc.);
- flexibility in terms of output - the ability to adapt to daily changes in production volumes caused by the downtime, seasonal changes caused by specific product and annual changes caused by market conditions.

There are two options the control of which provides various aspects of flexibility: product and process of manufacture, i.e., in case of packaging, package and packaging process. In the first case we obtain the subject FMS, in the second – the operational one.

Subject FMS is created of the machines that perform complete processing of parts or packaging of similar goods, such as shaft processing, production of PET bottles, packaging bulk products and more.

Operational FMS is created of the machines that perform homogeneous technological operations on products, such as pressure working, injection molding, packing viscous products and the like.

The evolutionary process of creating packaging FMS can be divided into two stages. The first stage is mainly introduced by FMS, quite similar to automated high-volume production complexes in engineering. These were the first generation of FMS for manufacturing of packages, which do not differ in form, but differ in dose.

The basic principle, which is implemented in the FMS of the second generation, is the integration of operations on the basis of group technology of packaging, which has similar manufacturing operations and conversions. Such FMS are used to form packages, that have different purposes, but with structural and technological similarities.

Tab. 1.1 Types of packaging manufacturing systems

Flexibility level	Type of manufacturing system	Number of package types	FMS equipment characteristics	Organization form
None	one-subject one-route FMS-0	one	Special	Mass-production automatic line
Low	one-subject multiroute FMS-1	one	Specialized	FMC changing route when external conditions change
Medium	multisubject multiroute FMS-2	Group	Versatile	FML of versatile machines and single route
High	multisubject multiroute FMS-3	Group	Versatile	FML of versatile machines and changeable route

We can assume that production systems increase their flexibility from one-subject one-route production system of mass production (e.g., automated line for beer packaging), through one-subject multiroute FMS-1 and multisubject one-route FMS-2 to multisubject and multiroute FMS-3.

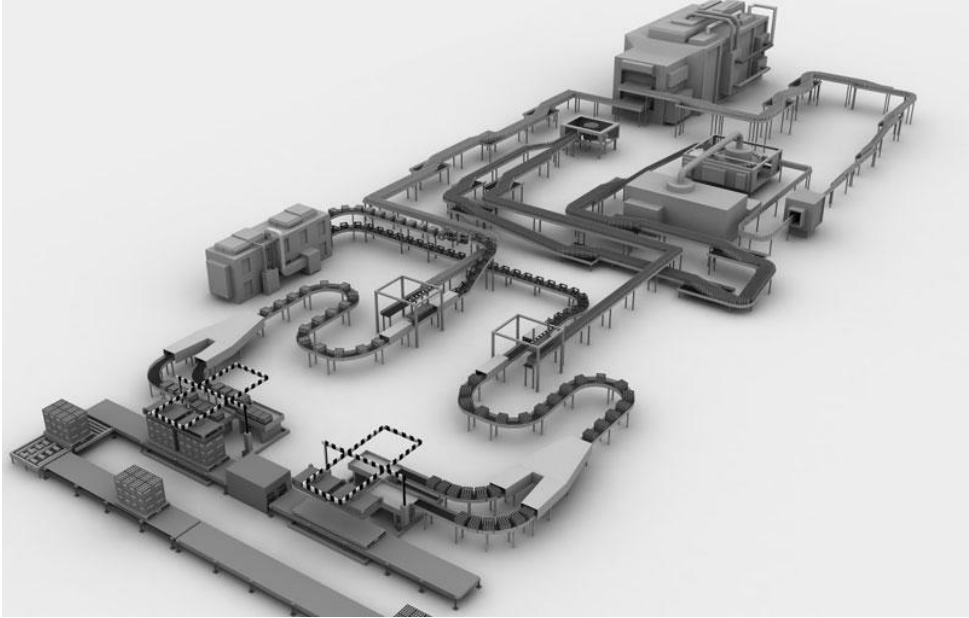


Fig.1.1. Example one-subject one-route production system of mass production of beer (60000 bottles per hour)

FMS-1 appears when the process allows several options for the sequence of operations. In this case, a change in external conditions may change the sequence of operations. The organizational form of such FMS – one-subject flexible automated station – flexible manufacturing cell with specialized machines (Fig. 1.2).

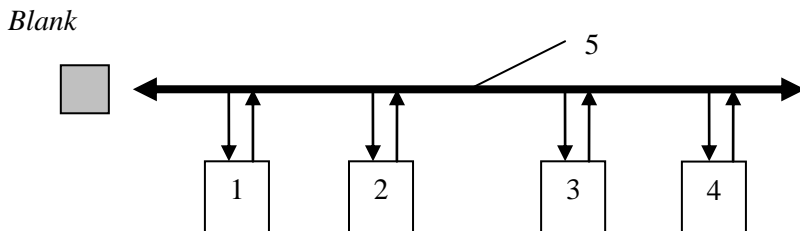


Fig.1.2. one-subject multiroute FMS-1 with FMC organization
1-4 – technological machines, 5 – transportation route

1.2. Development of multisubject packaging FMS

One of the first and main features that indicate the possibility of creating multisubject FMS is the ability to manufacture various packages in a common stream. It is necessary to examine the similarity of their design and develop a method of grouping the same so that the duration of the process of readjustment was the lowest.

In this case, the processes are considered together with the readjustment process and packing machine must have such property as flexibility, that is to be versatile and mobile.

The process of readjustment is one of the main in flexible manufacturing; it has the same characteristics as the technological processes, that are structure, different levels of complexity and automation, duration characteristics and more.

Creating a FMS is impossible without interaction of the technological and readjustment processes. Since these processes are linked, they form one common process that is the basis for optimizing the design of the machines in the FMS.

The basis of a systematic approach is grouping of products and the development of the system model based on modular-element description of each product, creating a system based on this model of group packaging process and forming the structure of FMS and its elements - highly versatile packaging machines.














As an example, consider the application of this approach to the forming of multisubject FMS for packing of powders. The most common for consumer is a soft film package made of the body in the form of sleeve, bottom of different configurations, with an open neck, with or without flaps.

The polymeric packets are produced of different types and sizes. Selecting a package depends on its purpose, type of packaged product, its volume, mass, etc. There are several designs of package (Table 1.2).

The "library of standard structural and technological elements" was designed to create a system model for group of packages and to facilitate the design of group process of package manufacturing in a common stream. The first step is determining a set of structural elements of package (Fig. 1.3 a). Each package may have a set of various structural elements according to the type. The generalized package (Fig. 1.3b), on which the group and process of manufacturing in a common stream is created contains elements common to all the above types of packets. These elements are denoted as a_1 , a_2 , ..., a_{10} respectively. The size of the package is also important because the film width and magnitude of pulling depends on it.

Based on the structural elements of a generalized package the system model is constructed for the group of products. We can assume that the system model of package design group is set, all the real packages in the group being the subsets thereof.

Tab. 1.2. Types of packets

Packet type	Appearance	Characteristics
A		“cushion”-type
B		Folded top, gusset bottom, flapping bottom seam
A/B		Folded top and bottom. Used for “bag in box” package
C		Flat bottom, bent bottom seam
D		Flat bottom, bent bottom seam, mechanically shaped facets
D/B		Gusset bottom, flapping bottom seam, mechanically shaped facets
E		Flat top and bottom
F		Flat bottom, seamed facets “Stabilo”.
F/B		Flat bottom, seamed facets, flapping bottom seam
F/E		Flat top and bottom, seamed facets, bent top and bottom seam
F/P		Seamed facets, flapping top and bottom seam
I		One or multiple openings
J		“Doy Pack”-type, may comprise fastener

Since the implementation of each structural element of package a_{ij} should be performed by a certain technological conversion, the FMS for making the entire group of packets should have the technological capabilities to implement N technological conversions

$$N = \sum_{i=1}^n \sum_{j=1}^{m_i} a_{ij} ,$$

Where a_{ij} – j -th element of the i -th package design,

n – number of package types in a group.

m – number of elements in a packet.

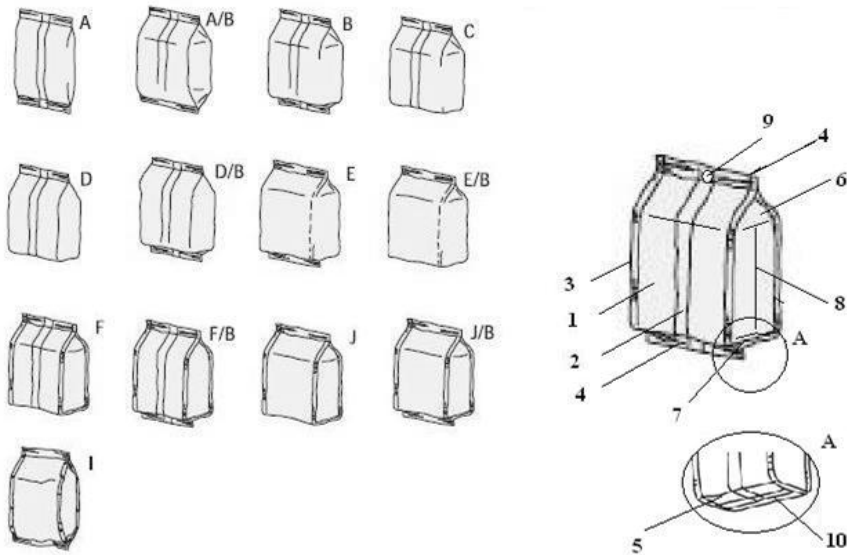


Fig. 1.3 Typical packet designs and a generalized package
1 – body, 2 – longitudinal seam, 3 – facet seam, 4 – transverse seam,
5 – bottom, 6 – top fold, 7 – bottom fold, 8 – side folds,
9 – opening, 10 – bent seam

As in real conditions each of the technological machines can implement several conversions, the total number of conversions for which the FMS is created can be significantly reduced. Moreover, the higher versatility of the equipment, the deeper the decrease, the less pieces of equipment in the FMS and the simpler is its structure.

After the distinguishing of conversions, the analysis of need of their implementation for each type of package and creating generalized technological operation of package forming is conducted. It is based on the sequence of transformations needed to create a generalized package. Obviously, this generalized process operation should ensure the formation of structural elements inherent in all types of package in a specified sequence and implementation of

support functions. The given summary technological operation covers all possible conversions undertaken during formation of package with all structural elements.

This completes the goal the multisubject FMS is to achieve - providing the implementation of all functions of package formation in a common stream. For this purpose the FMS should have sufficiently wide versatility. To increase the versatility of FMS two ways exist:

- expanding the functionality of machines or functional modules in FMS i.e. by complication of their designs for obtaining multisubject one-route structure;
- placing additional functional elements in the FMS - machines or functional modules, creating multisubject multiroute structure.

For example, the versatile vertical packing machine Pitpack-Smart allows automatic packaging of loose, granular, crystalline and powdered food and non-food products in packages of any type of the above.



Fig. 1.4 Pitpack-Smart versatile packaging machine

On the machine you can generate different types of packages: "cushion"-type package, package with a flat bottom, and choose the type of longitudinal seam – "overlap" or "butt". The maximum width of the package is 200 mm, height – 320mm, flat bottom perimeter not more than 400 mm. The machine has a productivity of 90 packages per minute. It can work with different types of dispensers (weight, volume, screw and multihead).

Basing on the desired performance of FMS, the number of basic equipment is calculated. In this case, 3 packaging machines and packaging machine for forming group packaging in shrink bags (Fig. 1.5) are installed.

Flexibility depends on many structural features. If there is great number of components and they are branched, it would seem, we should expect high flexibility of the system as a great number of ways to go through the process is possible, but this is not always the case. Duplication of operations carried out on similar technological machines and other mechanisms of the system, reduces the load of equipment and efficiency of the whole system falls. However, the introduction of redundant elements in FMS leads to significant changes in its structure, which changes the nature of the linkages and makes synchronization of components more complex. In this regard, it seems appropriate to introduce functional redundancy at a lower level, i.e. at the level of individual functional modules of the equipment. This enhances the functionality of FMS without changing its structure.

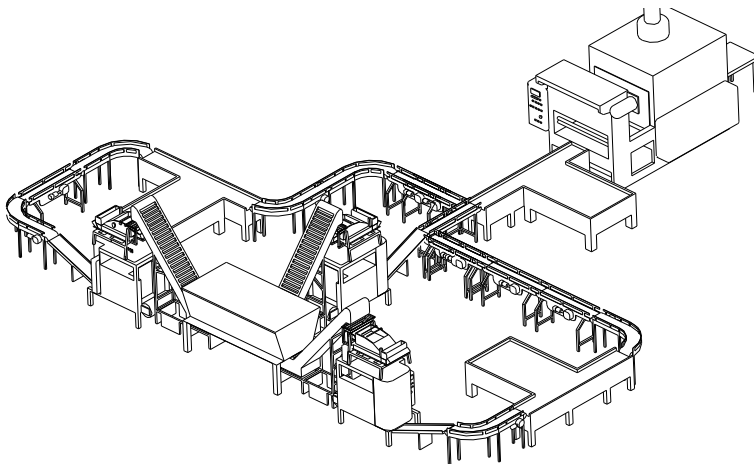


Fig. 1.5 FMS for packing granular substances

In this case distributing the package group between machines is rational, making them partially specialized and providing fewer adjustments for each machine in the FMS.

1.3. Development of multiroute packaging FMS

Consider the example multisubject multiroute FMS for packing viscous products in glass jars with two types of closures - CKO type and Twist-off. For this purpose the structure of FMS has two closing machines of different types, each for their jars. In this case, depending on the type of packaging, cans after dosing are on Route 1 or Route 2.

The basis of any system is the structure that is relatively stable connections between the elements. When designing structures the search of relationships between structure properties and pattern of element connection in it, through which the system becomes a single whole, plays an important role. These bonds are material (containers and auxiliary packaging means) and information flows.

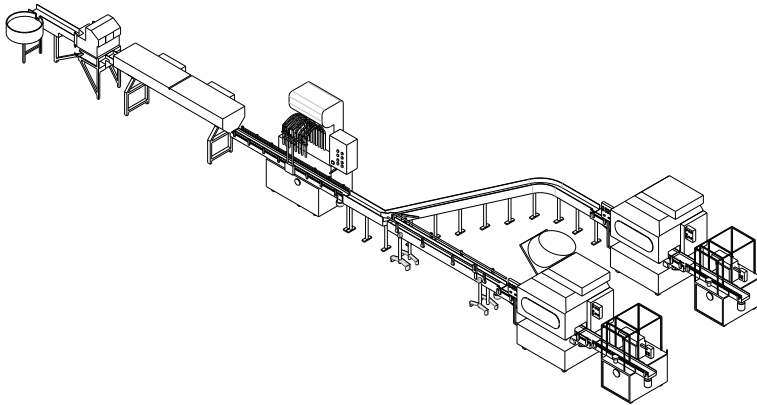


Fig. 1.6. Multisubject multiroute FMS for packing viscous substances

1.4. General principles of packaging FMS design

Theoretical foundations of optimal design of FMS are based on scientifically sound methods that allow forming a general set of technically feasible options for a given input, conducting a comparative analysis and selection thereof up to identify the best option.

Creating highly efficient technological machines systems of is one of the most challenging tasks of modern production through multiversion of possible solutions in the process development, selection of machines and facilities to create the process lines.

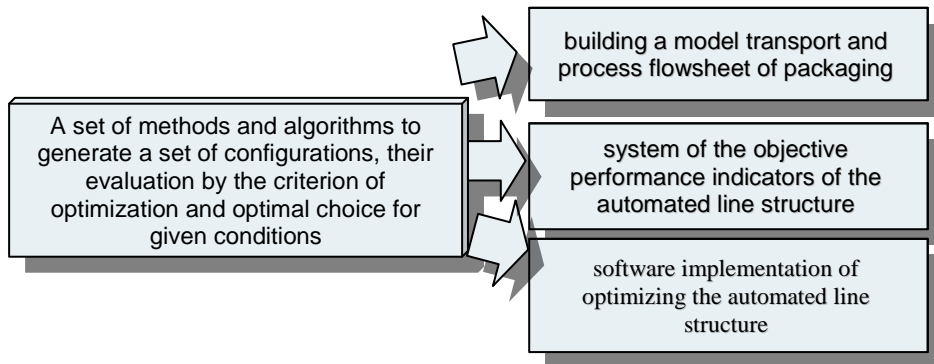


Fig. 1.7 Scheme of technological line design process

The method of synthesis is based on extensive use of information design technology. It allows to find a set of technically feasible options for processes and FMS layouts by generating multiple options, their evaluation and directed search for the best using the computer (Fig. 1.8).

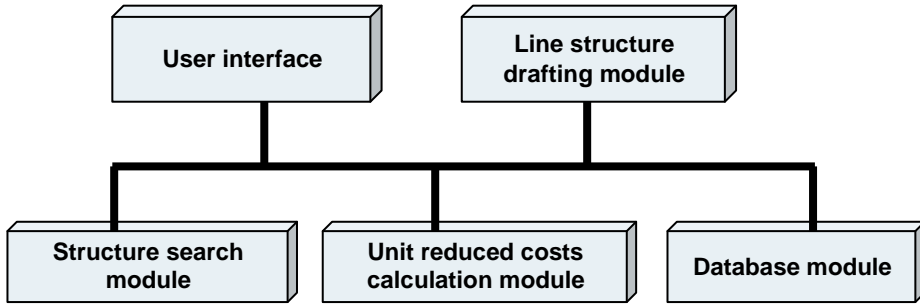


Fig. 1.8 Scheme of computer-aided optimization synthesis of packaging line

The developed system of virtual design of technological lines allows obtaining electronic layout of the line, which determines the scheme of the line with regard to dimensions of storage and transporting equipment (Fig. 1.9).

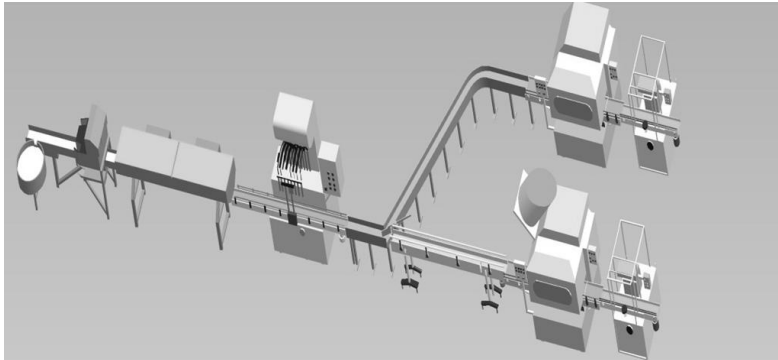


Fig. 1.9 Virtual model of packaging FMS

Conclusions

After analyzing the evolution of packaging production FMS, we can note the following major trends of further development.

1. Unitization of technological machines with standardized functional modules paves the way for the creation of packaging systems. They provide the implementation of two different properties of technological systems, the ability to work in the one-route and polyroute options and the concentration of almost all conversions of packaging (packaging preparation, dosing, sealing, labeling, handling, etc.) in a technological system.

2. Use of the method of intellectual adaptation to changing production situation for the automatic diagnosis of complex process equipment and automatic troubleshooting.

3. Standardization and unification of hardware and software of FMS based on the principles of modularity and aggregation. Creating effective FMS with

minimal cost to their design, implementation and operation is impossible without a wider and deeper standardization of all FMS components, design solutions, structures and technology, software and so on

4. The transition from traditional scheduling to dynamic production planning according to the needs of today's products on the basis of methods of optimal computer-aided planning. Substantial increase of the timeliness factor importance in carrying out the order. Minimizing logistical stocks of FMS.

5. The transition from single-level computer networks while creating automated systems to multi-level FMS, based on the Open Systems architecture.

References

- [1] Пальчевський Б.О. Автоматизація технологічних процесів (виготовлення і пакування виробів.-Львів: Світ, 2007.-392 с.
- [2] Пальчевський Б.О. Технологічні основи гнучкого автоматизованого виробництва.-Львів: Світ,1994.-201 с.
- [3] Крестьянполь О.А. Принципи побудови ГВС пакувального виробництва / Технологічні комплекси: Науковий журнал.- Луцьк: видавництво Луцького НТУ, 2010, №1, с.152-159.
- [4] Крестьянполь О.А. Особливості проектування ГВС пакувального виробництва / Технологічні комплекси: Науковий журнал.- Луцьк: видавництво Луцького НТУ, 2011, №1(3), с.128-133.

Systematic and structural approach to the formation of flexible manufacturing systems for packaging

Abstract: The paper presents a systematic approach to the design of flexible manufacturing systems at the stage of their development with the active use of information technology. The types of packaging manufacturing systems are distinguished on the basis of their flexibility and the trends for their development are listed.

Key words: packaging, machine, flexible, manufacturing system, structure

Systemowo-strukturalne podejście do formacji elastycznych systemów produkcji opakowań

Streszczenie: Przedstawiono systematyczne podejście do projektowania elastycznych systemów produkcyjnych na etapie poprzez aktywne zastosowanie technologii informacyjnych. Wyróżniono rodzaje układów dla produkcji opakowań na podstawie ich elastyczności oraz tendencję do ich rozwoju są wymienione.

Słowa kluczowe: pakowanie, maszyna, elastyczny, system produkcyjny, struktura

2. Genetic-Based Approach to the Functional-Modular Structure Design of Packaging Machines

Introduction

Most of the packaging devices, especially packaging machines with modular structure are made by collecting various components of the simpler structure than the final product (Fig. 2.1). The synthesis of such a structure is the choice of what components should be added together to get a result in the construction with the necessary parameters. The method presented in this paper aims to systematize the process of structural synthesis of packaging machine with a main focus on its versatility, taking also into account productivity, cost, reliability, weight and overall performance. This approach aims to provide the designer feedback on possible designs of packaging machine before detailed design stage.

In this method, the design of packaging machine is obtained by optimization structure synthesis of a set of heterogeneous functional modules (FMs). This process includes three stages:

1. Creating a topological graph of the packing machine structure based on a set of elementary technological operations (ETO) and their corresponding functional modules;
2. Building the two-dimensional matrices for genetic coding of packing machine structure on the basis of topological graph;
3. Optimizing the formed matrix using a genetic algorithm with regard to the above criteria and consistency of the packing process.

The issue of synthesis of topological graph of the packing machine structure is considered as a discrete optimization problem that is solved by means of genetic algorithm.

2.1. Creating a topological graph structure packing machine

Fig. 2.2 shows the course of forming the packing machine structure matrix. At the beginning the distinct parts of the packaging process are distinguished – the elementary technological operations (Fig. 2.2a). Each ETO is an action, which results in a new element of package to be formed or changing the shape, position or properties of the existing one.

* Prof. dr. hab. inż. Bogdan Palchevskiy, Lutsk National Technical University, 75 Lvivska str., 43018 Lutsk, Tel.: +380 (332) 767395, e-mail: pac@tf.dtu.lutsk.ua

** Mgr inż. Taras Varanitskyi, Lutsk National Technical University, 75 Lvivska str., 43018 Lutsk, Tel.: +380 (332) 767395, e-mail: varanitskyi@i.ua

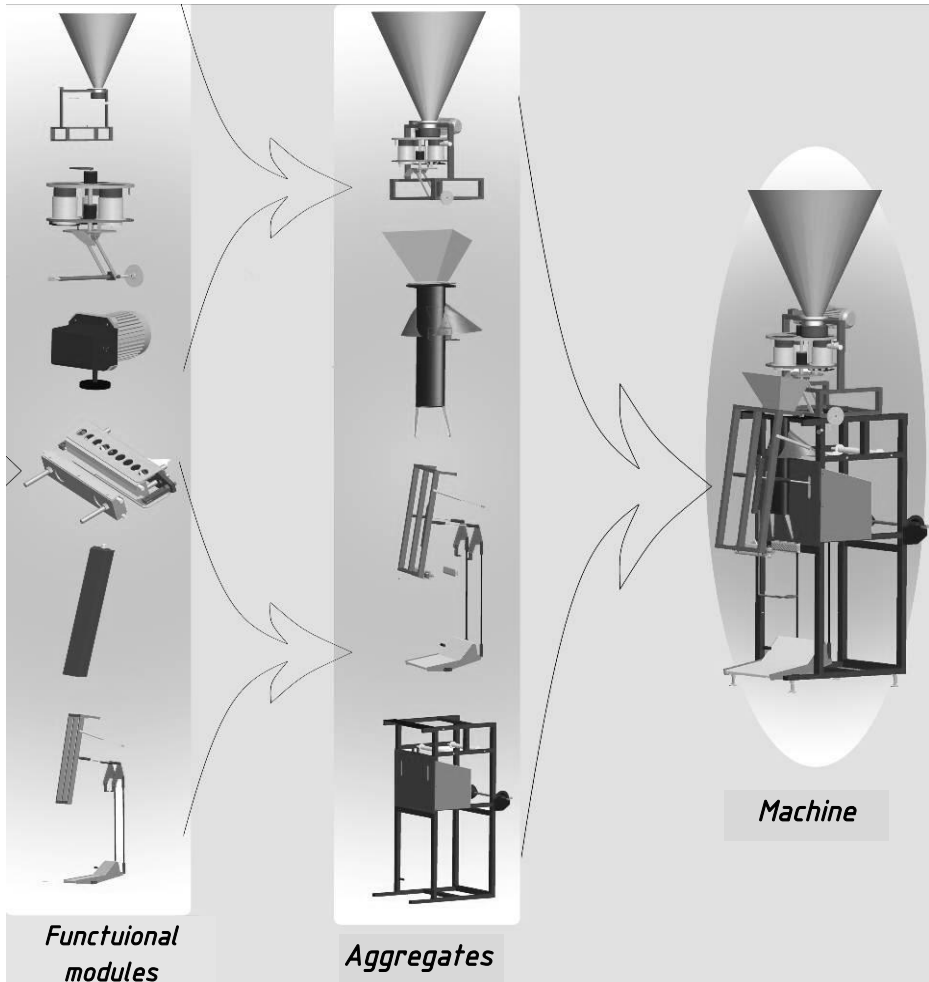


Fig. 2.1. Scheme of the packing machine decomposition

Next, each ETO should be put in correspondence with a specific functional module (Fig. 2.2b). In view of technology or possible design of FM a separate ETO is not always performed apart so it is necessary to combine ETOs into sets. Each set describes a certain type of FM. For example, a set of ETO "to weld a longitudinal seam" and "move film sleeve" match to design of the roller mechanisms for longitudinal welding. Thus two types of functional modules that implement ETO sets are different, if these sets have at least one different ETO. Obviously, the set may contain only one ETO. Sets of ETO significantly expand the number of FM designs that are used during the synthesis of structure packing machine.

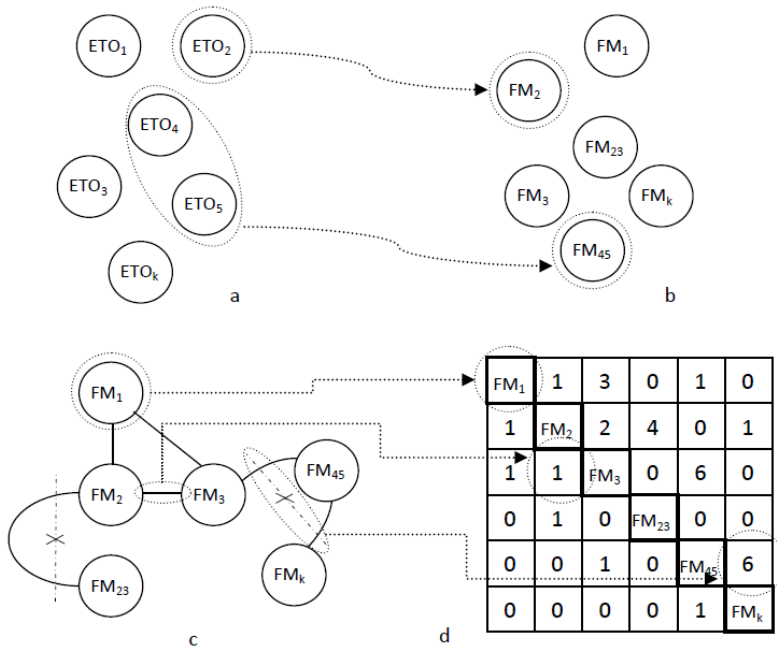


Fig. 2.2. Course of forming the packing machine structure matrix

Each vertex in the graph is given a number. The numbering is carried out in accordance to a set of ETO, which the appropriate FM implements: first in the sequence of operations of a generalized process and then two digits – a combination of numbers of single ETO. Thus the obtained set of vertices of the structure topological graph includes the FM, presented by two types of sets: single and paired ETO.

The next step is ordering the vertices: placing them in certain sequence and establishing connections between them (Fig. 2.2c). This process tends to generate a graph that describes the structure of the packaging machine and is performed in the following way:

1. A vertex that has the smallest number, usually 1, is selected from the set.
2. The value of degree is generated for each vertex. It is a natural number, limited to a certain value.
3. Steps 1 and 2 are repeated until the k vertices are collected. The maximum number of vertices in the graph k is limited by the number of structural elements in a family of products.

The generated graph should be checked on several grounds. The main purpose of this test is to set those options that represent actual allowable structures of packing machine. Their separation will greatly accelerate the optimization process, reducing costs to process options that go beyond the space of feasible solutions.

Graph must be connected. Obviously, the machine cannot consist of a set of functional modules that are not linked, even if each of them separately can provide the relevant operations of package forming. Therefore a disconnected graph does not depict acceptable structure at all. In validation process all graphs the degree of at least one vertex is zero are discarded immediately, while others are checked by any known method (e.g. Kruskal's algorithm) for connectivity.

Graph must be simple, i.e. it should not contain loops or multiple bonds. The loop in this case means that the manufacture of the product may be stuck in one position in the machine. Multiple bond between the vertices of the graph leads to the loss of uniqueness in determining relative positions of FM in the machine. This problem is solved by creating a structure matrix: its completion is organized in a way that eliminates the appearance of loops and multiple bonds.

The FM describing the graph should implement all the ETO necessary for the formation of all structural elements of a product family in a given sequence. The longest path in the graph must include all ETO necessary for making at least one type of product. Otherwise the basic aim of the machine – producing the necessary range of products – is not provided.

As a result the topological graph of packing machine structure shows all its working positions and options the product routes in the machine.

2.2. Building a matrix of packing machine structure

A matrix of packing machine structure is obtained by sequential cellpadding of the two-dimensional array. Each cell of the matrix is associated with the corresponding vertex of topological structure graph. The matrix size is $k \times k$ elements. The adjacency matrix by which undirected graphs are usually describe is taken as a basis. However, a way its completion is modified the gain an opportunity to describe not only the interconnections between the vertices of the graph, but also the characteristics of arcs and the vertices themselves. A matrix of packing machine structure (Fig. 2.2d) can be divided into three parts, each comprising an encoded description of certain aspects of the structure of the packaging machine.

The first part is represented by cells that are below and to the left of the main diagonal of the matrix. The content of cells is based on the topological graph of structure and describes the links between the FMs in the machine. Filling of this part is performed likewise cellpadding of classical adjacency matrix and fully describes the process of generating the graph. Since the topological graph of packing machine structure is a simple graph, the cells can only take values 0 or 1.

The second part of the matrix structure - is the cells that are above and to the right of the main diagonal. As usual adjacency matrix for an undirected graph is symmetric, it was decided to use these cells for expanding the characteristics of the graph. They show the actual links between FMs in a machine. Each cell in this part describes mutual position of a pair of FMs to which it relates. The value of the cell is a number that describes a one-way communication between the modules in the sequence of their connection.

There may be six types of such links:

- Placement along the vertical axis,
- Placement along the horizontal axis,
- Placement along the inclined axis,
- Placement in a circle with a vertical axis of rotation,
- Placement in a circle with a horizontal axis of rotation,
- Placement in a circle with oblique rotation axis.

Therefore, each cell gains value from 1 to 6. So 6^x connection methods between the neighbouring FMs can be specified.

The third part of the matrix – its main diagonal – describes the FM types included in the structure of the machine. Cells contain information about the design of FM and thus set of ETO it performs. The value of a cell consists of two digits. They point to the ETO implemented by a particular module. In case a set consists of one ETO, a zero is written in place of the second one. Filling of cells of the main diagonal is conducted according to the order of the process of packing. That is, cell a_{11} describes the FM, a set of ETO for which necessarily contains the first operation. Further cells respectively contain the entire set of ETO required for the formation of all structural elements from a given family of packages.

Thus, each cell of the main diagonal of the matrix of structure meets specific FM and its corresponding diagonal cells - additionally describe the location and characteristics of FM.

2.3. Mathematical Model

Optimization synthesis of structure can be considered as a problem of creation of the graph. In such case the elements of the machine structure correspond to vertices, and the links between them – to edges that connect two or more vertices. Therefore, the whole structure can be represented as a graph $G = (V, E)$, where V – the set of vertices, E – set of edges. The problem of synthesis optimization then can be described as finding the optimal set P of nodes V , such that the objective function $f(P)$ is maximized.

It should be noted that the number of vertices k , which form the best option is not defined in general. However, a set of characteristics F for each FM should be specified in order to get the opportunity to fully evaluate the various options of structure.

Thus, the optimization problem can be put as:

Given G a topological graph of structure, F a set of characteristics for each FM, and k the number of vertices. Find a vector x , which determines the optimal set of FM, the vector v - way to link FMs and vector y - description of each FM, subject to $p(x, v, y)$ – the objective function that defines the quality of packing machine structure.

The objective function assesses the structure of the following criteria:

- Versatility – increased by introducing a FM, carrying out new functions into the structure of packing machine and depends on the combination method thereof;
- Productivity – rises by increasing the number of FMs;
- Reliability – reduced when FM, carrying out new features introduced into the structure of packing machine and depends on the combination method thereof.

To assess a packaging machine according to the criterion of universality, the total number of types and sizes of products, which the machine can produce is calculated primarily, and on this basis the coefficient of universality is determine. This value is determined by the structure of the machine and the set structural elements of products that specific FM produces. In general, the ratio of universality is the product of the coefficients of universality for serial and parallel connection of FMs. Thus arbitrarily complex TM is reduced to a chain of series-connected parts. Several FM, which operate in parallel or sequentially on the same level are considered as one group.

To evaluate the productivity of packaging machine the theoretical quantity of product it produces during a specified time is calculated. Raising the value of this parameter can be achieved by increasing the number of FM as the slowest ETO, as well as throughout the whole packing machine.

Reliability of a packaging machine is estimated by the availability function. This value is calculated based on the known factors of availability for each FM and the method of connection thereof. Thus in case of serial connection, the reliability of a machine declines. This shortcoming can be partially removed by reserving FM on operations where there the failures are most often.

The following objective function is a result of combining the criteria:

$$f(x, v, y) = w_1 \cdot \left(1 - \left(\prod_{j=1}^{\alpha} (1 - K_{y_j})\right) \cdot \prod_{j=1}^{\beta} \frac{1}{\sum_{i=1}^q \left(\frac{1}{1 - K_{y_i}}\right)}\right) + w_2 \cdot \left(\frac{1}{T_{\max}}\right) + w_3 \cdot \left(\frac{1}{1 + \sum_{i=1}^k \left(\frac{1}{K_{r_i}} - 1\right)}\right),$$

where $x=(x_i) - x_i$ is a variable that refers to the presence of the edge e_i in the x ,

$v=(v_i) - v_i$ is a variable that represents the weight coefficient of the edge e_i in the set x ,

$y=(y_i) - y_i$ is a variable that refers to the characteristics of the FM for the correspondent vertex,

w_i – weights of partial criteria

α and β – number of series-connected FM and parallel connected sets of FM respectively,

K_{y_i} – actor universality of the i -th FM

q – number of parallel-connected FM

T_{\max} – the duration of the longest ETO

K_{r_i} – availability factor of i -th FM

k – number of FMs in the packaging machine.

2.4. Optimization method with use of genetic algorithm

Synthesis of a graph is NP-complete problem even using simple linear relationships for calculating the value of criteria. As a result, all known algorithms that exactly solve the problem of graph synthesis, do it for the time that depends exponentially on the size of the graph. In our case objective function is nonlinear and since we cannot afford exponential computation, heuristic algorithms are found to be suitable. More specifically, a steady-state genetic algorithm (SSGA) has been used to solve the problem approximately, which goes through the following stages:

1. Randomly create a population P of n chromosomes (encoded representation of the parameters x , v and y), estimate the value of the objective function and keep the best chromosome. Create an empty subpopulation Q

2. Select two chromosomes c_i and c_j in P with a probability $\Pr(c_i) = \frac{f_i}{\sum_{k=0}^n f_k}$,

where f_i - value of the objective function for chromosome c_i ;

3. Crossover the chromosomes c_i and c_j and generate new chromosomes c'_i and c'_j ;

4. Mutate c'_i and c'_j with a certain low probability;

5. Evaluate the objective function for c'_i and c'_j and add them to Q. If Q contains less than m chromosomes move to step 2;

6. Replace m chromosomes in P with the ones in Q and empty Q. Update the best chromosome and increment the generation counter. If the generation counter has reached a pre-specified number, terminate the process and return the best chromosome. Otherwise go to 2.

The main advantage of SSGA is empirically set prevention of premature convergence and optimal results obtained in fewer computations.

Each version of the packaging machine is encoded in a matrix structure, which is also its chromosome. Values of genes are identical and describe the same characteristics as the corresponding matrix cell.

It should be noted that the information is the first part of the chromosome refers to the vector x , the second – to the vector v , and - the third to vector y in a mathematical model. Also is necessary to stress that not every chromosome describes the "true" structure of packing machine. Eliminating some edges may not lead to destruction of the structure, so each option should be checked whether it meets the unconnected graph. Obviously, the ideal case is all the k-connected vertices.

Since chromosomes, describing the structure of packaging machine contain three types of information there is a need to configure crossing-over and mutation operators. Cross-over operator influences on each part of chromosome separately. It is performed in two steps where the first third mates with the first third, and third - with the third part of the chromosome. Such crossing takes

place in lines (Fig. 2.3), the line number being also generated randomly. Crossover is not performed for the main diagonal. Thus when deploying a matrix structure in line, we have actually multipoint crossover.

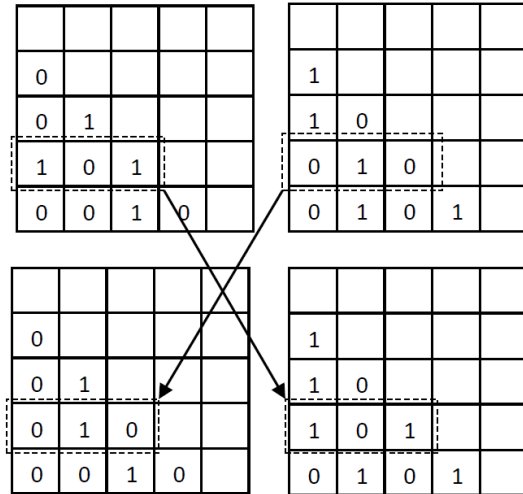


Fig. 2.3. Cross-over of two chromosomes

The mutation operator differs from the typical one by the higher probability of the second part of the chromosome.

2.5. Example of practical implementation

For example, consider the process synthesis and optimization of the structure of a packaging machine for loose products. By the condition the machine must produce a family of three types of packages: three-seam "cushion"-type package, package with a flat bottom and a bent top package. ETO set for this family of packages will be as follows:

1. Bend the film into sleeve
2. Weld the lower cross seam
4. Weld the top cross seam
5. Weld the longitudinal seam
6. Bend the bottom of the package
7. Fold the top of package
8. Cut the finished package
9. Pull a film sleeve on a step

15 sets of ETO and the same number of FM structures can be put in correspondence with the above set, namely:

- single FM1, ... FM8,
- double FM23, FM25, FM27, FM36, FM37, FM48, FM56.

The first generation of the genetic algorithm generates the following matrix of packing machine structure size 8x8:

01	0	2	0	0	0	0	0
0	25	0	1	0	3	0	0
1	0	06	0	0	5	0	0
0	1	0	36	2	0	0	0
0	0	0	1	56	0	2	4
0	1	1	0	0	04	1	0
0	0	0	0	1	1	08	0
0	0	0	0	1	0	0	37

As can be seen from the genetic code, this chromosome does not represent an acceptable construction of packaging machine because the necessary sequence of package producing process is not provided. The structure graph of the FM set has the form shown in Fig. 8.4. This also will be the rough location of FMs in the machine.

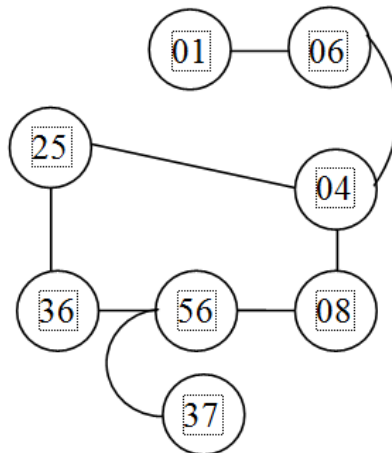


Fig. 2.4. The structure topological graph, formed at the first generation of GA

During the genetic algorithm process each part of the chromosome undergoes the following processes:

- as a result of mutations in the main diagonal the required set of ETO is determined and composition of FMs in the machine is optimized. This may also change the universality – the presence of vertices with identical ETO in sets can create the alternative ways of passing the product through the machine without its readjustment and form routes that lead to the creation of a new product type;

- genetic changes in the first part of the chromosome lead to the establishment of the required order of ETO. Basically, this process occurs due to crossing-over, mutation only accelerates finding the final result;
- the third part of the chromosome is responsible for setting such geometric relationships between FM, in which the machine design is not too cumbersome and provides a logical and efficient product passing through all positions.

Fig. 2.5 shows two couples of "matrix structure - topological graph", illustrating the possible intermediate stages of optimization synthesis of packing machine structure.

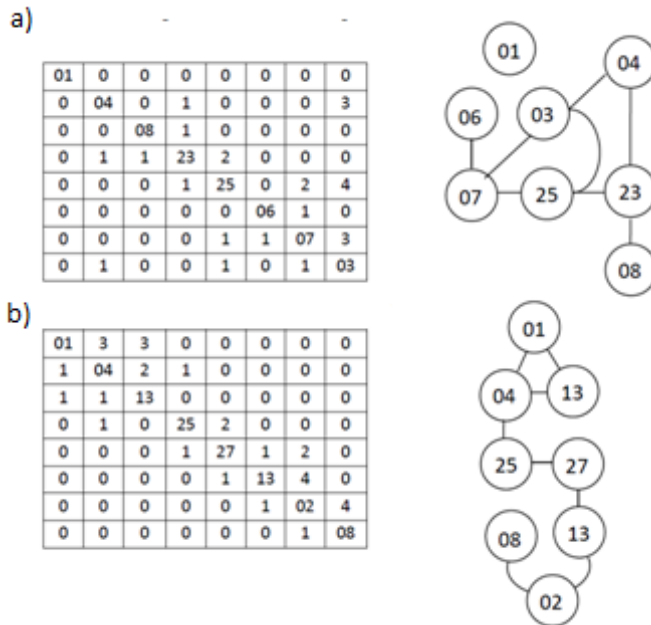


Fig. 2.5 Interim results of packing machine structure optimization synthesis using GA

The first pair (Fig. 2.5a) represents already established set of ETO. Links between modules do not describe the acceptable design of packaging machine yet. The lack of connections between some FM is evident so this structure still needs refinement so that permissible design of packaging machine could be put in correspondence to it.

The second pair (Fig. 2.5b) shows the case where the manner and types of connections between vertices of the graph can represent realistically possible machine design. However, the main diagonal of the matrix is filled chaotically: an unreasonable duplication of some ETO and the absence of others occurs. As a result of mutations, the set of encoded ETO should be reduced to the "rules" to achieve the acceptable solution of the problem.

Comparison of the interim results for multiple chromosomes on intermediate generation leads to identify trends that demonstrate how a matrix of packing machine structure mutates when approaching the optimal solution. The first trend is the location of FM numbers in ascending order along the main diagonal of the matrix. The second trend is reflected in the "clustering" of nonzero values of cells on both sides of the main diagonal. Of course, in both cases, there may be some deviation, but the preservation of classical logic and sequence of ETO for packing loose products finds confirmation in the application of genetic algorithm.

Finally, Fig. 2.6 shows a chromosome of a possible structure of packing machine, and its topological structure graph.

01	3	0	0	0	0	0	0	0
1	04	1	0	0	0	0	0	0
0	1	08	3	3	0	0	0	0
0	0	1	25	2	3	0	0	0
0	0	1	1	23	3	2	0	0
0	0	0	1	1	07	2	3	0
0	0	0	0	0	1	06	1	0
0	0	0	0	0	1	1	03	0

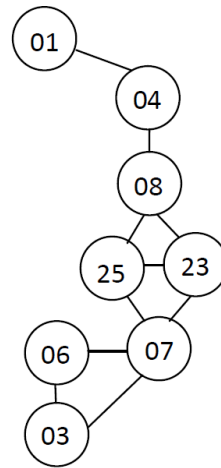


Fig. 2.6. Feasible final structure of packing machine obtained with GA

The process of packing in this case will take place in the following sequence:

- film rolled up in the sleeve moves at an angle to the longitudinal seaming mechanism,
- seamed sleeve moves to pulling mechanism that is placed vertically under the longitudinal seaming mechanism,
- before filling the blank with the product one of two mechanisms of cross seaming triggers: mesh sponge, forming both the upper seam of next package and the bottom of the previous one or the mechanism which bends the bottom of the package and welds only the bottom seam,
- next the package moves vertically downward for cutting,
- when secondary mechanism of cross seaming triggered, the filled and cut package passed horizontally to the mechanism of folding the top of package, and then - straight down - the upper cross seam is formed,
- if the folding the top of package is not necessary – the blank is immediately transmitted along an inclined trajectory to the transverse seaming mechanism.

References

- [1] Arkin Yetis F., Kazuhiro Saitou: *Decomposition-Based Assembly Synthesis Based On Structural Considerations* Proceedings of DETC'00 ASME 2000 Design Engineering Technical Conferences and Computers and Information in Engineering Conference, 2000.
- [2] Palchevskiy B., Varanitskiy T.: *Analisis Of Variability Of The Family Of Packages And The Versatile Packaging Machine Design* Applied Computer Science Vol. 8, №2, 2012, p.22-33.
- [3] Palchevskiy B.: *Avtomatyzacija technologichnykh protsesiv (vygotovlenia i pakuvannia vyrobiv)* (in Ukrainian) Svit, Lviv, 2007.

Genetic-based approach to the functional-modular structure design of packaging machines

Abstract: The paper presents a method for decomposition of packaging machine structure in order to provide the designer with choices for feasible assemblies. The aim is at providing a systematic approach to explore a large number of decompositions prior to the detailed component design phase. The structure is transformed to a graph with equivalent topology by a genetic algorithm.

Key words: packaging, machine, design, genetic algorithm, structure

Genetyczne podejście do projektowania funkcjonalno-modułowej struktury maszyn pakujących

Streszczenie: Przedstawiono metodę dekompozycji konstrukcji maszyn opakowaniowych w celu zapewnienia projektantowi wyboru możliwych zespołów. Celem jest zapewnienie systematycznego podejścia do zbadania dużej liczby dekompozycji przed etapem projektowania szczegółowych części. Struktura maszyny jest przekształcona w graf o równoważnej topologii przez algorytm genetyczny.

Słowa Kluczowe: opakowanie, maszyna, projektowanie, algorytm genetyczny, struktura

3. Analysis of spinning of conical vessels

Introduction

Spinning is the process of forming plates, where the workpiece moves ended, and the final shape of the product describes your templet. This is alternative technology for deep drawing process and is used in the manufacture of cylindrical vessels and conical. This method – compared with the processes of oil – has many valuable benefits, which include: lower energy consumption, simpler instrumentation technology and lower costs.

This process uses the ability of metal to plastic deformation without breaking the continuity of the material. Metal shaping is done with a special tool called a spinning tools or spinning reels. Modeling of material spinning method uses the principle of a simple machine called a lever two-armed. Simple lever-type machines are used by man for centuries. Their use is to increase the force required to overcome the resistance of materials because the force with which a person can interact on the environment is reduced. Figure 3.1 shows the installation phase of the plate. You can make almost any shape, depending on the needs and ideas of the designer. Metal spinning is shaping sheet metal, without excessive changes in the thickness and shape of obtaining the desired figure of revolution. Changing the thickness of the material is always present, and this phenomenon is inevitable. It should, however, see to it that these changes were minimal and did not lead to a rupture of the material. Skillfully shaping the material, you can even increase the thickness locally over the thickness of the output, this is mostly aluminum and other soft metals. In the process of crushing financial related material thickness change is intentional and specific.

Spinning process is as follows: after placing the disc centered in relation to the template and pressed it with a pressure machine is started. Lubricated surface is suitable for spinning, which is designed to reduce friction. Then specialist moves across the surface of the deformed sheet, exerting sufficient pressure.

* Dr inż. Piotr PENKAŁA, Instytut Technologicznych Systemów Informacyjnych, Wydział Mechaniczny, Politechnika Lubelska, 20-618 Lublin, ul. Nadbystrzycka 36, tel./fax.: (81)5384276, e-mail: p.penkala@pollub.pl

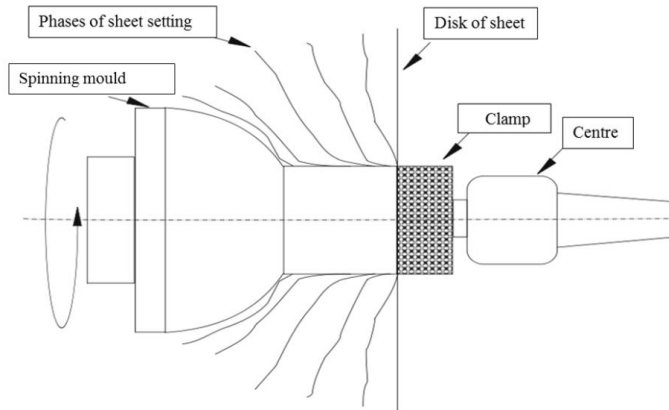


Fig. 3.1. The phases in the process of stacking plates spinning [1]

In figure 3.1 shows the successive stages of stacking plates, which can be seen as the beginning of the contact surface of the stencil with the surface pressure. The pressure on the plate should be less and less value as it approaches the piece of material already lying on the stencil with very fast moving of spinning tool uniform over the surface of the plate. Subsequent steps of the remainder of the spinning disk are designed to complete the form of packing material. The force and method of operating the working tool depend on the type of material deformed. The time required to camber one piece, smooth the surface and dimensional accuracy depends on the experience and skills of the sheet metal forming. Metal spinning is a process that requires high skills acquired at the time, many years of practice. Knowledge of the principles and processes of spinning derivatives as rotary crushing should show all engineers, not only in the fields of mechanical. Many times during the design phase is the necessity of prototype components. Implementation in this case by means of a single pumping device is too expensive. Produce an identical item by spinning it may take a few minutes, and the cost of equipment is significantly lower [2].

3.1. Assumptions stress analysis process

The occurrence of defects during the process of spinning is dependent on the type of stresses which are dependent on the direction of movement of the working rolls. When the roller moves toward the outer edge of the disc, the material stresses are compressive circumferential and radial stretching. When the working roll is moved towards the center of the disc, there is a circumferential compressive stresses and radial compression (Fig. 3.2) [3].

The most common defects during the spinning process are: creases, cracks, circumferential and radial cracks. Creasing disc may occur when the material is placed too high compressive stress (too much reformation in one phase transition tool) [3].

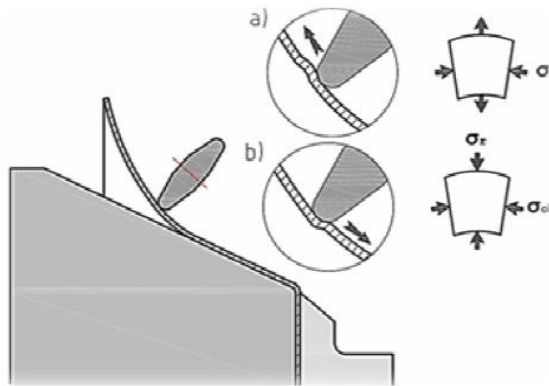


Fig. 3.2. Distribution of the stresses depending on the direction of movement of the working rollers [4]

To prevent folding to increase the number of move tool. Circumferential cracking occurs when the material is placed on a high radial tensile stress. Radial cracks occur, they are placed as high circumferential tensile stress, or if the resulting folds are crimped on the stencil [4].

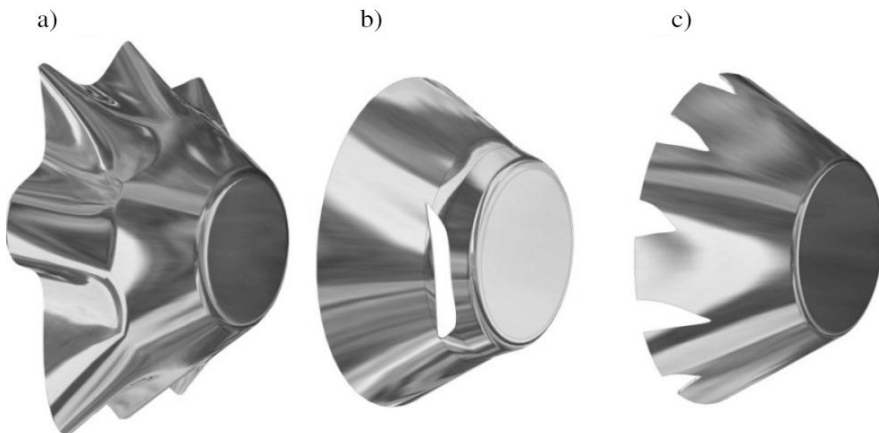


Fig. 3.3. Types of defects during spinning: a) folding, b) circumferential cracks, c) radial cracks [3]

3.2. Design of tools trajectory

Design tools trajectory of movement is currently an unsolved problem. Taken three attempts to automate the design trajectory moves through: systems with feedback parameters, and by comparison with the previous cases, H. Dierig proposed power control system for real-time tool that was designed to maintain a constant level of force on the tool. This system did not provide for a product without folding.

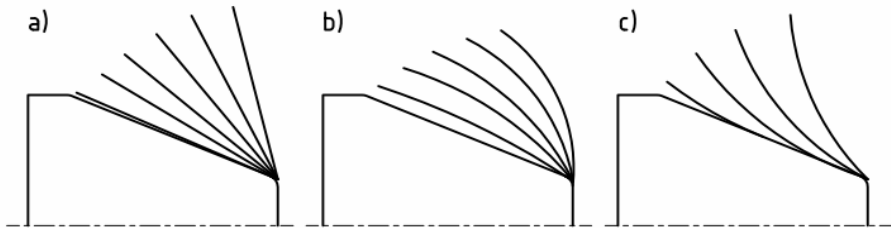


Fig. 3.4. Types of tool motion trajectories while spinning: a) linear b) convex arc c) concave arc [11]

However, G. Reil suggested the use of different forces during the whole process of the so-called fuzzy control. He found that by using this method can be reduced by thinning the wall of up to 21% compared to the uncontrolled process. Next attempt to automate the design of trajectory motion was proposed by R. Ewers, who proposed design automation tool paths based on similarity to previous cases. This approach facilitates the design tool trajectory by about 37%, but it requires a large database (Fig. 3.4) [3].

3.3. Influence of technological parameters on the spinning process

Influence of technological parameters on the spinning process. In the spinning process, there are many factors that affect the formation process of the material. By far the greatest impact are the following parameters: speed stencil roller feed rate, roll diameter, the radius of the working rolls, tool geometry, tool number of passes, thickness and diameter metal disc.

3.3.1. Speed stencil

Increasing the rotational speed of the stencil – n , with constant other parameters, thereby improving the surface roughness decreases, reducing the roundness deviation of the device and reduces the force needed for the forming. Increasing the RPM decreases the tendency to crease the material, but produces greater thinning and increases the likelihood of cracking. Turnover template – n is chosen according to the following formula:

$$n = \frac{9500 \div 32000}{D} [r / \text{min}] \quad (3.1)$$

where: D – the diameter of the disc plate in mm.

The equation shows that, there is a wide range of choice turnover template. For example, assuming the diameter of the disc $\phi 100$ mm, rotation speed stencil is in the range of 95 to 3200 r/min⁻¹.

3.3.2. Feed of working rollers

Effect of feed rollers work - the process of forming p at constant other parameters is significant. Reduction of feed improves the same parameters as the speed increases and the stencil, increases the thinning of the wall. However, the impact of this parameter on the process of formation is greater than the speed of rotation, since the change of only about 20% has been significantly affected.

3.3.3. Radius of working rolls

Selection of the appropriate radius roll – R is very important. In determining the radius of the roll should be taken into account: the type of material, thickness and size of the disc. For hard materials deform and thicker used smaller radius. Tight roll causes more thinning of the wall. Larger radius should be used for materials with good properties such as discharge DC04, 1050A aluminum.

The use of a larger radius rollers and improves the surface quality of the product reduces the out of roundness. Recommended work roll radius is:

$$R = (0.012 \div 0.05) D \quad (3.2)$$

where: D – the diameter in mm of the disc plate.

3.3.4. Roll diameter grooving

The diameter of the roll – D_r no direct connection with the formation of defects stampings. The choice of roll diameter is based on an empirical formula to ensure adequate speed roll, which may not exceed the limit speed roller bearings work:

$$D_r = 0.1 D + 120 \pm 60 \quad (3.3)$$

where: D – the diameter in mm of the disc plate.

3.3.5. The thickness of sheet metal disc

With increasing thickness of the sheet - g, reduced tendency of the material to the folding, but higher forces are needed to shape. The thin sheet metal support plate is used, as an additional supporting roller, in order to prevent loss of stability during the forming disc.

3.3.6. Diameter of steel disc

With the increase in diameter of the disc – D, it is more difficult to get the product without folding. Creases are caused by the fact that the metal disc easily loses stability at the edge of the circuit, where there is much greater linear speed. Loss of stability occurs primarily in products with high degree of forming of the surface.

3.4. Numerical Analysis in Simufact Forming 11.0

3.4.1. Spinning parameters used in numerical analysis

To perform numerical analysis program was necessary Simufact relevant parameters, the process of spinning was done by a concave arc-like spinning method. It was also necessary to set the relevant parameters:

- spindle speed: 500 r / min,
- feed speed of spinning tool: 10 mm /s,
- the contact force on the template: 20 kN.

The material used for aluminum AA6061 was spinning, with a high tensile strength and resistance to elongation corresponding to about 10%. i.e., the elements forming spinning tool form and pressure applied by a simple tool steel. Figure 10.5 shows a diagram of the submission of the tools – shaped object. The system has been modeled in Catia v5 then were transferred to the Simufact Forming v11.

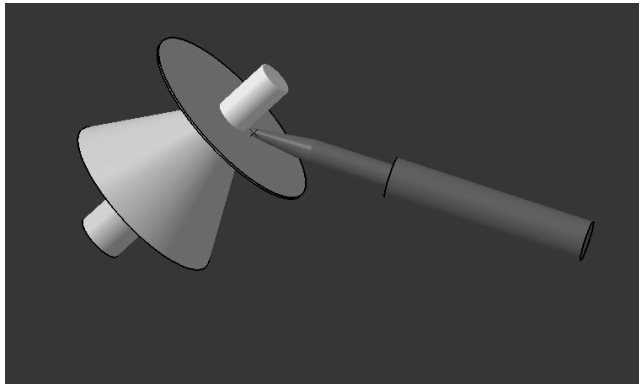


Fig. 3.5. Submission of tools and material

3.4.2. Analyses spinning process in the first phase

The first processing stage is to pre-form the bottom. Figure 3.6 shows the waveform changes in the forces acting on spinning tool function of time. The graph in the direction of the Z axis shows the changes of a force acting on the material formed perpendicular to the main axis of rotation of the elements, which operates spinning tool. In the initial phase of spinning tool dent in the form of a plate, which means that the recess of spinning tool the workpiece,

there are compressive stresses and tensile. However, a graph of force in the X axis is present torsion stress. As can be seen at this stage of the most impacting element, the forces in the Y and Z axis, this implies that the material is compressed and stretched, thus reducing the thickness of the material and extending along the surface of the mold (Fig. 3.6).

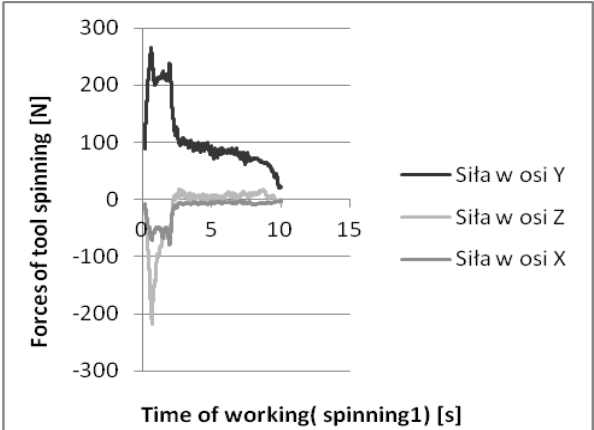


Fig.3.6. Spinning (phase 1) - chart forces as a function of time

Figure 3.7 – 3.12 shows the first phase of the spinning process, which began to form the basis spinning tool dishes. The numerical analysis shows the nature of flow – the range presented in colors from blue (no deformation) to red (highest strain) – along the mold. The nature of the deformation that the material is exposed to a significant reduction in wall thickness. The signatures of drawings describes the percentage (%) the progress of the process.

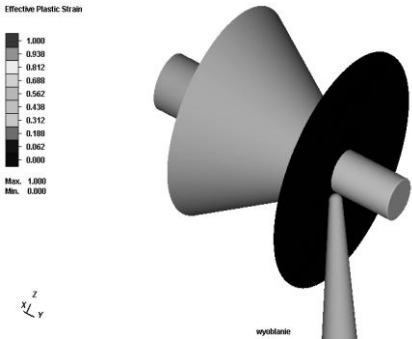


Fig. 3.7. Spinning phase 1 – the system before the process

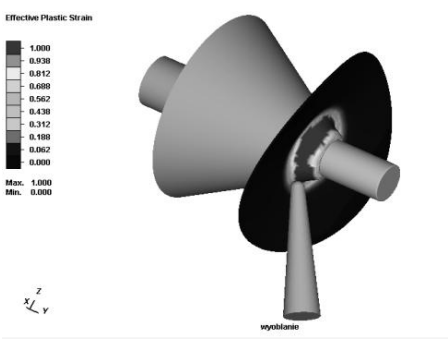


Fig. 3.8. Spinning phase 1 – 20%

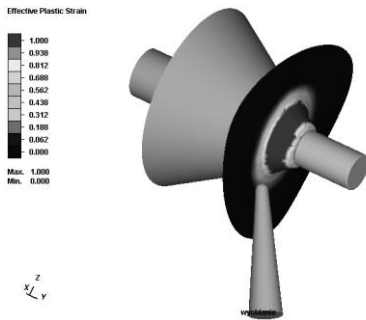


Fig. 3.9. Spinning phase 1 – 40%

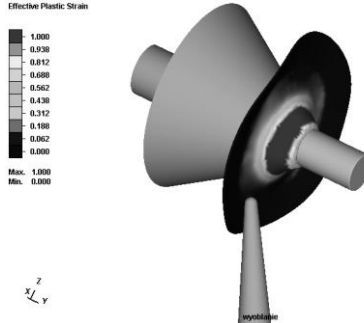


Fig. 3.10. Spinning phase 1 – 60%

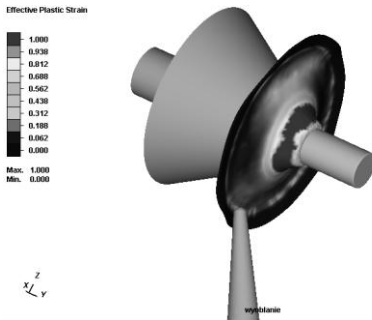


Fig. 3.11. Spinning phase 1 – 80%

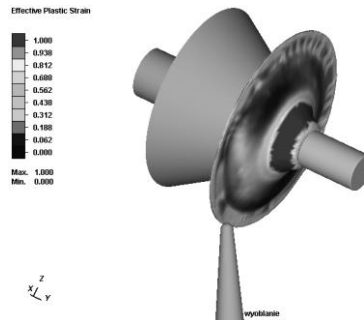


Fig. 3.12. Spinning phase 1 – 100%

The presented figures show that in the first phase of development of the conical vessel deformations are very large. In the bottom of the vessel, regardless of the progress of the maximum relative deformation is 100%, which means that in these areas may result in damage to the material in the form of broken. In the next phase of the process is a shaped material deformation has considerably less as evidenced by changes in strain as shown in Figures 3.13 and 3.14.

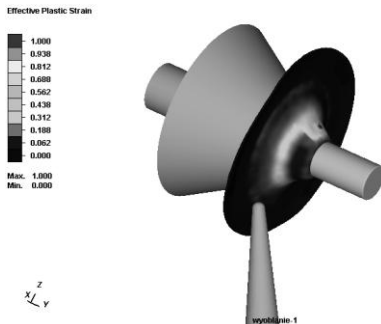


Fig. 3.13. Spinning phase 2 – 60%

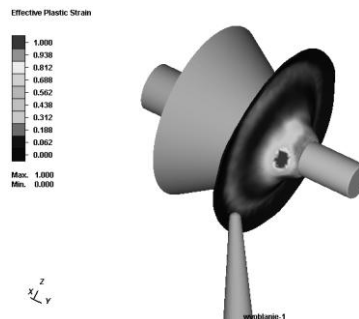


Fig. 3.14. Spinning phase 2 – 80%

The second phase of the process involves the formation of the next part of the vessel on a stencil. In this step, spinning force in the X direction and the much less significant effect on the deformation and changes in the structure of the sheet than the force corresponding to the Y-axis direction by stretching the material along the shape of the stencil. In Figures 3.13–3.14 is visible flow of material at the contact tip radius of spinning tool.

Conclusions

Based on the analyses, one can see that a very important aspects of the spinning elements of the inclined walls of the cone is the selection of the respective properties of the process, the correct speed changes underlying the wall thickness at the highest index and stretching the material (the bottom of the formed container) and corrugations present on the entire surface conical machined metal, a well selected material and shape of the casting of spinning tool scratch and smooth sheet, selection of the material properties of the workpiece to allow the tension and compression of the material without significant changes in the structure.

Based on the results of the analysis carried out in the Simufact Forming, in a very simple way, we can see how the pressure changes and of spinning tool force distribution on the surface of molded material. Should have been given very high, reaching almost 300 N force causes formation of blood. Machining simulation also presented relative deformation of the material. As can be seen in several stages most stretched sheet near the bottom of the mold at a very strong effect on the thinning of the wall thickness at this location. However, excessive stretching of the material, compared to the intact part of the further, in the middle phase of the formulation, caused the material beginning to crease. Numerical analysis confirms the possibility of errors of basic processes, in case of incorrect choice of parameters

References

- [1] Web site: <http://www.wikipedia.org>
- [2] Szwedowski P.: Wyoblancie ręczne., WNT, Warszawa, 2007.
- [3] Frąckowiak S.: Projektowanie procesów technologicznych wytłoczek osiowosymetrycznych na wyoblarkach sterowanych CNC. Instytut Obróbki Plastycznej, Poznań, 2011.
- [4] Runge M.: Spinning and Flow Forming. Leifeld GmbH, Ahlen, 1994.

Analiza procesu wyoblania naczynia o kształcie stożkowym

Streszczenie: W pracy zaprezentowano analizę procesu wyoblania naczynia o stożkowym pochyleniu ścianek. Na podstawie danych literaturowych przyjęto układ narzędziowy oraz określono średnicę półfabrykatu. Przygotowano model cyfrowy układu narzędziowego, następnie wykonano szereg analiz w programie Simufact Forming. Celem analizy numerycznej było określenie sił działających na kształtowany materiał. Wartości tych sił zostały określone w funkcji czasu trwania procesu. Analiza pozwoliła także na określenie wartości odkształceń względnych zachodzących w poszczególnych obszarach kształtowanego naczynia. Na ich podstawie można oszacować, jaki charakter błędów może powstać podczas kształtowania. Analiza numeryczna pozwala na określenie optymalnych parametrów procesu rzeczywistego.

Słowa kluczowe: wyoblanie, analiza numeryczna, odkształcenia względne, siły kształtowania

Analysis of spinning of conical vessels

Summary: The paper presents an analysis of the process of spinning conical vessel wall gradient. Based on the literature data utility system and sets the diameter of the blank. Prepared digital model of the tool, and then performed a number of analyzes in the Simufact Forming. The aim was to determine the numerical analysis of the forces acting on the material formed. The values of these forces are determined as a function of the process time. The analysis also allowed the determination of the relative deformation occurring in various areas shaped vessel. On this basis it can be estimated that the nature of errors can occur during development. Numerical analysis allows to determinate the optimal parameters of the actual process.

Keywords: forming, numerical analysis, the relative strain, force shaping

4. Analysis of energetic properties of the surface layer – overview of methods for measuring the contact angle and the surface free energy

Introduction

Wettability considered as an ability of a liquid to maintain contact with a solid surface was proven to be extremely important physical phenomenon for many applications. On the one hand – large scales examples are examined: oil recovery, spraying plant protection pesticides, water drainage from highways or cooling the industrial reactors, on the other – smaller scale, for example well know inkjet printing, or even jet-based 3D tissue printing.

Generally, three wetting states may exist (Fig.4.1). For solid-liquid-air system, complete drying would mean appearing the air layer between the solid and the liquid. The only difference between wetting and drying is that liquid and air are interchanged [1].



Fig. 4.1. Wetting stages [1]

The measure for wettability is contact angle between liquid and solid surface, which for perfectly wet solid equals 0° and perfectly non-wet – 180° . In between – partial wet solids are divided into two groups: high wettability solids $0-90^{\circ}$ and low wettability solids $90-180^{\circ}$.

Above presented fact was examined for ideal solid surfaces. For rough surfaces additional factors appear. The research on the influence of surface roughness on contact angle values were conducted [2] for Teflon surface layer treated with abrasive papers and/or diamond paste of various grid numbers.

* dr inż. Jacek Domińczuk, Instytut Technologicznych Systemów Informatycznych, Wydział Mechaniczny Politechnika Lubelska, ul. Nadbystrzycka 36, 20-618 Lublin, tel. 81 538 45 85 e-mail: j.dominczuk@pollub.pl

** mgr inż. Jakub Szabelski, Instytut Technologicznych Systemów Informatycznych, Wydział Mechaniczny Politechnika Lubelska, ul. Nadbystrzycka 36, 20-618 Lublin, tel. 81 538 45 85 e-mail: j.szabelski@pollub.pl

It was observed that with increasing surface roughness the static contact angle was also increasing. Large amount of air entrapped inside the rough surface seems to be a reason of these phenomenon (Fig.11.2c – heterogeneous wetting). By measuring the diameters of contact perimeter of the attached drop, it was observed that the perimeter increases with the surface roughness. The Teflon surface is super-hydrophobic solid [3]. Other case would be a super-hydrophilic solids which is wetted homogeneously (Fig. 4.2b).

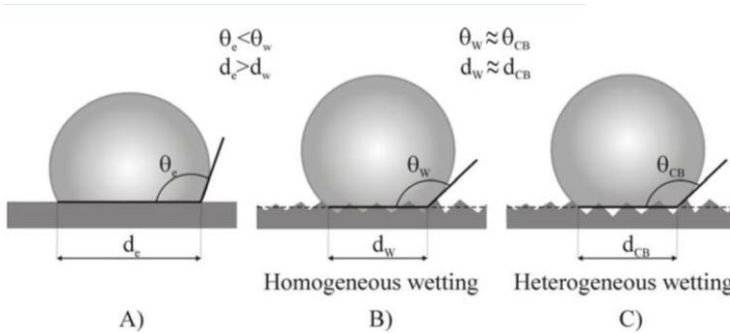


Fig. 4.2. Surface roughness of the hydrophilic and hydrophobic solids versus contact angle values using sessile drop method [2]

4.1. The work of Adhesion

Wettability is also very important property of adhesives. It determines the value of adhesion – that is the adhesives wetting ability [4]. The work of adhesion, which characterises the surface state, can be determined by measuring the wetting angle between the drop of liquid and a solid surface. It is understood as the surface free energy required to achieve a reversible phase equilibrium in constant pressure and temperature conditions (Fig. 4.3).

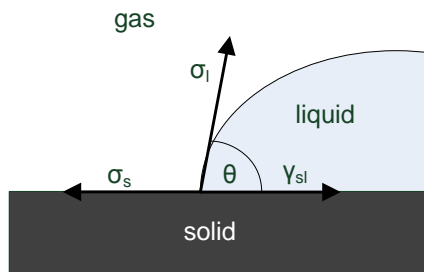


Fig. 4.3. Contact angle of a liquid droplet wetted to a surface

The formula takes the form of the Young-Dupre equation.

$$W_{sl} = \sigma_l (1 + \cos \theta) \quad (4.1)$$

where: σ_l – surface tension of the liquid [mJ/m^2], θ – wetting angle (contact angle). The wetting angle is measured between the solid surface and tangent to

a liquid meniscus curve on the liquid-solid contact surface. Drawing from the aforementioned definition, it would seem that the choice of a surface treatment operation which will provide the highest work of adhesion is the most advantageous. In practice, however, it appears that in certain cases (e.g. with an oxide film on a steel surface) low adhesive joint strength is observed regardless of high surface energy state [5, 6].

4.2. Surface energy

Surface energy can be considered as an indicator of non-equilibrium of cohesive forces between molecules inside and at the surface of the body. It constitutes an inseparable characteristic of a surface, additionally, its value and distribution is determined by the type of chemical bonds (type of body). The value of Surface Energy is the difference between the total energy of all surface atoms or molecules and their potential energy, if they were situated inside the body. Surface energy may be considered as a quantity of work needed to transfer atoms or molecules from within the body to its surface. In the case of critical state (i.e. a two-phase, one-component, system where physical properties of both phases in equilibrium state become identical, for critical pressure and temperature), surface energy equals zero as a result of lack of phase difference, therefore the disappearance of the surface. It is important that surface energy is not considered as the energy of molecules and atoms constituting the surface, because for example: the surface molecules energy increases with temperature increase while surface energy decreases and for critical temperature equals to zero [7].

4.3. Methods For Determining The Contact Angle

Contact angle measurement depending on drop type

A contact angle can be measured on static or dynamic drops. The first method is based on measuring a constant volume drops produced before measurement (Fig. 4.4a). Even though the volume is constant – the angle can vary with time due to liquid evaporation or reaction between solid surface and liquid (chemical or physical). The accuracy of the results obtained using above motioned method can be interfered by local surface irregularities (dirt, inhomogeneous surface), that is – if measurement spot on the surface is not chosen exactly the same every time. This error can be averaged out in the dynamic drop method (Fig. 4.4b). If drop volume changes during the measurement – “advancing” (drop volume increases) or “retreating” (drop volume decreases) angles are measured. The main problem within the method is the flow rate of liquid. It cannot be too high in order to establish the dynamic equilibrium of surface and in the same time it cannot be too slow – so the drop surface doesn't vary in time – as in static method. Flow rate range of: 5 to 15 ml/min is recommended. Other issue is that some not fully rigid surface materials (e.g. rubber) are better being tested with static measurements, because dynamic

contact angles are poorly reproducible. The contact angle measurements are conducted using the goniometer (Fig. 4.5), which includes the camera to obtain drop shape and computer software to analyze it and calculate the angle.

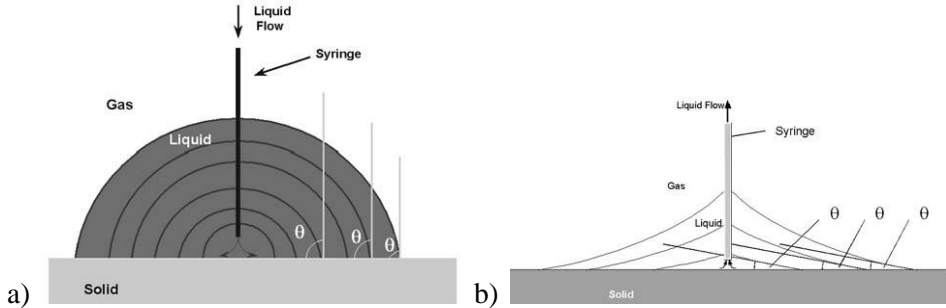


Fig. 4.4. - Measurement of contact angle: a) static, b) dynamic [8]

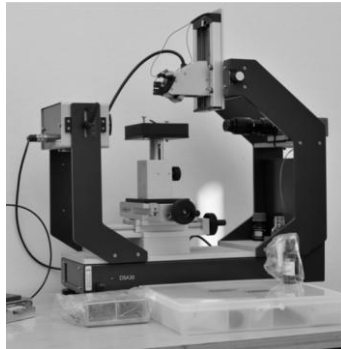


Fig. 4.5. Goniometer – equipment for visual estimation of drop shape

The computer aided drop shape evaluation methods

The computer software determines the shape of the drop and the contact line (baseline) with the solid by analysing the grey level values of captured image pixels. After that – in order to describe it more accurately, the root of the secondary derivative of the brightness levels is calculated to receive the point of greatest changes of brightness. The received drop shape is adapted to fit in one of mathematical models used to calculate the contact angle as tangent at the intersection of the drop contour line with the solid surface line. The simplest method is usage of general conic section equation to describe the complete profile of a sessile drop. The derivative of this equation at the intersection point of the contour line with the baseline gives the slope at the 3-phase contact point and therefore the contact angle.

Other tangent method uses only the part of contour which lies near the baseline, which therefore has to be high quality image. It is adapted to fit a polynomial function of the type $y = a + bx + c\sqrt{x} + \frac{d}{\ln x} + \frac{e}{x^2}$ (the result

of numerous theoretical simulations). The contact angle is determined using the iteratively adapted parameters. This method is sensitive to distortions in the phase contact area caused by contaminants or surface irregularities at the sample surface. It is also suitable for dynamic contact angles.

Another method bases on enclosing the contour line by a rectangle which is then regarded as a segment of a circle. It allows calculating the contact angle from the height-width relationship of the enclosing rectangle. The method is more accurate for smaller drops as they are more similar to the theoretically assumed spherical cap form, but is not suitable for dynamic drops (while the needle is still in the drop). The main disadvantage of it is that the drops are regarded as symmetric. Even when there are differences between the two sides – results obtained using this method will be the same.

Similar to rectangle method but a bit more resilient to the “needle is still in the drop” problem is method that fits the drop shape to a segment of a circle. The contact angle is calculated by fitting it to a circular segment function.

The most accurate method for calculating the contact angle is the Young–Laplace fitting, which takes into account the fact that it is not just interfacial effects which produce the drop, but it also is distorted by the weight of the liquid. The method allows also calculating the interfacial tension for contact angles above 30°. The same as the rectangular, this model also considers a drop as symmetric, and cannot be used for dynamic contact angles (needle in the drop).

4.4. Methods of Determining Surface Energy of Solid

The work of adhesion is considered (according to Dupré) as a function of surface tensions of liquid, surface tensions of solid and the interfacial tension between those phases γ_{ij} :

$$W_{sl} = \sigma_s + \sigma_l - \gamma_{sl} \quad (4.2)$$

Below presented models were introduced over last six decades. All of them allow obtaining value of surface energy of solid basing on its relations to the contact angle. Except the first one (Zisman method), the main difference between them is the assumption of form of equation for the interfacial tension between solid and liquid.

The Zisman method

In the Zisman method the surface energy of the solid is determined by using the critical surface tension of the liquid. The method is based on a revised version of the Antonow method which was later found not sufficiently accurate to be used in practise, assuming that the interfacial tension is determined by the difference between the surface tensions ($\gamma_{12} = |\sigma_1 - \sigma_2|$). The Zisman method assumes that the difference between work of cohesion W_{sl} for the formation of the interface boundary and work of cohesion W_{ll} for the formation of a liquid surface is considered as the spreading pressure $S_{|s}$:

$$S_{lls} = W_{sl} - W_{ll} \quad (4.3)$$

There for: solid is wetted completely when the spreading pressure is positive; not be wetted completely - when negative.

Using the Young-Dupre equation describing the relationship between the work of cohesion W_{sl} , the contact angle θ and the surface tension of the liquid (Equation 1), and according to Dupré (who defined W_{ll} as $2 \cdot \sigma_l$), for contact angle of 0° ($\cos\theta=1$) the work of cohesion equals the work of adhesion and there for spreading pressure equals 0. Contact angle of 0° is called the limiting angle for spreading (=complete wetting).

By plotting $\cos\theta$ against the surface tension for various liquids and extrapolating the compensation curve to $\cos\theta=1$ – the critical surface tension σ_{crit} (the surface energy of the solid) is obtained [8].

Later it was discovered that the linear relationship can only be applied when the relationship between the disperse and polar interactions is the same between the solid and the liquid that is why other methods should be used for determining the surface energy.

Equation of State method

The equation of state was obtained during the search for a method of determining the surface energy of a solid from a single contact angle measurement by using a liquid with known surface tension.

The second equation (besides the Young Dupre's one – 4.1) describing the surface energy of the solid as a function of the interfacial tension solid/liquid and the surface tension of the liquid was obtained empirically after multiple research measurements of contact angle:

$$\gamma_{sl} = \sigma_l + \sigma_s - 2\sqrt{\sigma_l \cdot \sigma_s} \cdot e^{-0,0001247(\sigma_l - \sigma_s)^2} \quad (4.4)$$

Combining the equation of state and Young's equation gave the equation for calculating the surface tension of the solid σ_s from a single contact angle if the surface tension of liquid σ_l is known:

$$\cos\theta = -1 + 2\sqrt{\frac{\sigma_s}{\sigma_l}} \cdot e^{-\beta(\sigma_l - \sigma_s)^2} \quad (4.5)$$

The method does not include separation of surface energy to polar and disperse fraction. In was experimentally proven that those fractions have to be considered when measuring surface energy. Using the state equations produces inaccurate result especially when polar interactions are present and dominant.

4.5. The Fowkes methods

By using the Fowkes method the polar and disperse fractions of the surface free energy of a solid can be obtained. The method is based on a combination of the knowledge of Fowkes (who first calculated the disperse fraction only) and after Owens, Wendt, Rabel and Kaelble research – was able to determine also the polar fraction.

The Fowkes method requires purely disperse liquid to calculate polar fraction. By combination of Young equation (Equation 4.1) and the surface tension equation of Fowkes for the disperse fraction of the interactions:

$$\gamma_{sl} = \sigma_s + \sigma_l - 2\sqrt{\sigma_s^D \cdot \sigma_l^D} \quad (4.6)$$

the equation for the contact angle was obtained:

$$\cos\theta = 2\sqrt{\sigma_s^D} \cdot \frac{1}{\sqrt{\sigma_l^D}} - 1 \quad (4.7)$$

which considered as $y=ax+b$ straight line equation, and after plotting $\cos\theta$ against $1/\sqrt{\sigma_l^D}$ allows obtaining “a” factor – that is – the disperse fraction of surface energy.

As $\cos\theta$ cannot be smaller than -1 and $1/\sqrt{\sigma_l^D}$ smaller than zero: the line must intercept the ordinate at the point (0;-1) – it is possible to determine the disperse fraction from a single contact angle (several purely disperse liquids give more accurate results) [8].

For calculation of the polar fraction, the initial Equation 10.6 for the disperse fraction of the interactions is further extended by polar fraction:

$$\gamma_{sl} = \sigma_s + \sigma_l - 2\left(\sqrt{\sigma_s^D \cdot \sigma_l^D} + \sqrt{\sigma_s^P \cdot \sigma_l^P}\right) \quad (4.8)$$

The work of adhesion is obtained by adding polar and disperse fractions:

$$W_{sl} = W_{sl}^D + W_{sl}^P \quad (4.9)$$

A combination of above presented Equations and Young-Dupre Eq. 0, produces:

$$W_{sl}^P = \sigma_l \cdot (\cos\theta + 1) - 2\sqrt{\sigma_s^D \cdot \sigma_l^D} \quad (4.10)$$

Having W_{sl}^P calculated and using the fact that the polar work of adhesion is a geometric mean of the polar fractions of the surface tensions (acc. 4.8), that is:

$$W_{sl}^P = 2\sqrt{\sigma_l^P \sigma_s^P} \quad (4.11),$$

one can obtain polar fraction of the surface energy of the solid $\sqrt{\sigma_s^P}$ using the same method as before – plotting W_{sl}^P against $2\sqrt{\sigma_1^P}$ and obtaining the “a” parameter of straight line equation – that is the slope [8]. As before – one measurement is enough to calculate the polar fraction but still more measurements give more accurate results.

4.6. The Extended (Hydrogen Bridges) Fowkes method

The Fowkes method was also extended by adding one more fraction – the hydrogen bridges fraction W_{sl}^H :

$$W_{sl} = W_{sl}^D + W_{sl}^P + W_{sl}^H \quad (4.12)$$

The disperse fraction is determined as before (Equation 21), the same with the polar fraction calculations (Equation 10) – with one exception only: liquids of known polar and disperse surface tension fractions ($\sigma_1^P > 0$) and hydrogen bridge fraction $\sigma_1^H = 0$ are required.

Measurements of contact angles to calculate the hydrogen bridge fraction require liquids with all fractions known and hydrogen bridge fraction $\sigma_1^H < 0$. Equation 20 is extended by the polar fraction and hydrogen bridge fraction (as Equation 8). The same as before – the required fraction of the work of adhesion, i.e. the fraction W_{sl}^H resulting from the hydrogen bridges, can be calculated for each contact angle by subtracting the known fractions:

$$W_{sl}^H = \sigma_1 \cdot (\cos\theta + 1) - 2 \left(\sqrt{\sigma_s^D \cdot \sigma_1^D} + \sqrt{\sigma_s^P \cdot \sigma_1^P} \right) \quad (4.13)$$

Calculations of hydrogen bridge fraction of the solids surface energy are conducted in a same manner as for polar fraction that it is considered as a geometric mean of the hydrogen bridge fractions of the surface tensions (see Equation 11). Plotting one value against other allows obtaining the “a” parameter of straight line equation (slope – that is hydrogen bonds fraction of the surface energy of the solid).

4.7. The method by Owens, Wendt, Rabel and Kaelble

Owens, Wendt, Rabel and Kaelble method is very similar to Fowkes one. The difference is that Fowkes began his calculations from surface tension equation and purely dispersive liquid, obtained disperse fraction of surface free energy and then expanded the surface tension equation by polar fraction and calculated it using liquid of known disperse and polar fractions. Owens, Wendt, Rabel and Kaelble calculated both fractions of solids surface energy in a single step using the contact angles of two liquids with known disperse and polar fractions of the surface tension.

OWENS and WENDT build a system of equations that contained: surface tension equation (Equation 4.8) and YOUNG's equation:

$$\sigma_s = \gamma_{sl} + \sigma_l \cdot \cos\theta \quad (4.14)$$

Kaelble solved the system using two liquids and calculated the mean values of the resulting values for the surface energy. Rabel, as it was presented before, used equation for straight line $y=ax+b$ to analyze polar and disperse fractions. Plotting y against x he obtained $\sqrt{\sigma_s^P}$ as slope and $\sqrt{\sigma_s^D}$ as y -intercept: "b" [8]. The transposed equation used in this analysis:

$$\frac{(1+\cos\theta) \cdot \sigma_l}{2\sqrt{\sigma_l^P}} = \sqrt{\sigma_s^P} \cdot \sqrt{\frac{\sigma_l^P}{\sigma_l^D}} + \sqrt{\sigma_s^D} \quad (4.15)$$

4.8. The Wu method

The Wu method requires two test liquids with known polar and disperse fractions, one of them must have $\sigma_l^P > 0$. Instead of using the geometric mean of the surface tensions to combine dispersive and polar fractions he used the harmonic mean which was proven to be more accurate:

$$\gamma_{sl} = \sigma_s + \sigma_l - 4 \left(\frac{\sigma_l^D \cdot \sigma_s^D}{\sigma_l^D + \sigma_s^D} + \frac{\sigma_l^P \cdot \sigma_s^P}{\sigma_l^P + \sigma_s^P} \right) \quad (4.16)$$

Above presented equation combined with Young's equation (10.14) one obtains:

$$\sigma_l(\cos\theta + 1) - 4 \left(\frac{\sigma_l^D \cdot \sigma_s^D}{\sigma_l^D + \sigma_s^D} + \frac{\sigma_l^P \cdot \sigma_s^P}{\sigma_l^P + \sigma_s^P} \right) = 0 \quad (4.17)$$

The calculations after measuring contact angles for both liquids base on the analysis of system of equation for each liquid. The resulting equations after a factor analysis:

$$(b_1 + c_1 - a_1)\sigma_s^D\sigma_s^P + c_1(b_1 - a_1)\sigma_s^D + b_1(c_1 - a_1)\sigma_s^P - a_1b_1c_1 = 0 \quad (4.18)$$

$$(b_2 + c_2 - a_2)\sigma_s^D\sigma_s^P + c_2(b_2 - a_2)\sigma_s^D + b_2(c_2 - a_2)\sigma_s^P - a_2b_2c_2 = 0 \quad (4.19)$$

where variables: $a_1, b_1, c_1, a_2, b_2, c_2$ express the following terms:

$$a_1 = \frac{1}{4}\sigma_{l,1}(\cos\theta_1 + 1), b_1 = \sigma_{l,1}^D, c_1 = \sigma_{l,1}^P - \text{for } 1^{\text{st}} \text{ liquid,}$$

$$a_2 = \frac{1}{4}\sigma_{l,2}(\cos\theta_2 + 1), b_2 = \sigma_{l,2}^D, c_2 = \sigma_{l,2}^P - \text{for } 2^{\text{nd}} \text{ liquid,}$$

A quadratic equations produce two solutions for both σ_s^P and σ_s^D – the physically correct result must be therefore selected. The easiest case is when negative sign fraction is obtained – the solution is incorrect. If both solutions seem correct – the criterion behind selecting the correct one bases on answers on following questions: which of two is expected from a knowledge of the properties of the substance, which of them is similar to results obtained with

other pairs of liquids, which is closest to results obtained by calculations using other methods. The final result of the surface energy is the arithmetic mean of the part-results (if there were more than two liquids involved).

4.9. The Van Oss-Good's method

The method allows obtaining polar and disperse fractions of surface energy but instead of before presented method – calculating the polar fraction in one piece – it is divided into two subfractions. By using Lewis acid-base model the polar fraction is represented by an electron acceptor fraction σ^+ (electron receiving fraction – acid) and an electron donor σ^- (electron donor fraction – base). The surface tension equation 6, extended by this feature and converted to include contact angle:

$$(1 + \cos\theta)\sigma_l = 2 \left(\sqrt{\sigma_s^D \cdot \sigma_l^D} + \sqrt{\sigma_s^+ \cdot \sigma_l^-} + \sqrt{\sigma_s^- \cdot \sigma_l^+} \right) \quad (4.20)$$

The method requires measurements of at least 3 liquids contact angles. Two of them must have a known acid and base fraction $\sigma_l^- > 0$ and $\sigma_l^+ > 0$. For one of liquids equal acid and base fractions $\sigma_l^- = \sigma_l^+$ is required (i.e. water).

4.10. Surface free energy research

In order to improve the overall surface energy of different materials – multiple research project were taken. Some researchers focus into mechanical surface treatment methods, some into modifying chemical structure of surface layer.

The measurements on the individual components of surface free energy according to Owens and Wendt method were conducted [9] for various surface treatment methods, for example: processing with abrasive tool, additional degreasing or water rinsing. Result of calculations were compared to the joint strength (Fig. 4.6, Table 4.1).

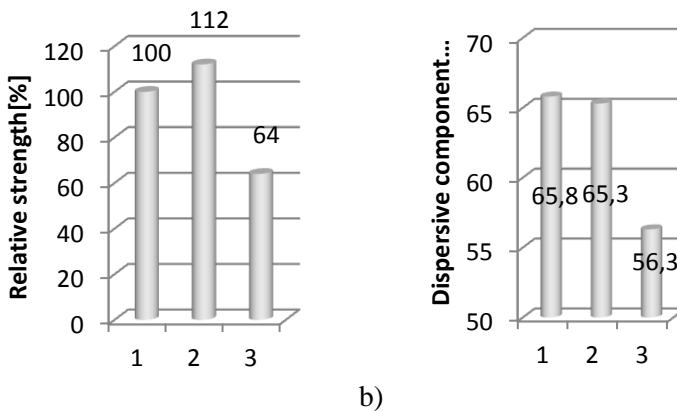


Fig. 4.6. The comparison of adhesive joint strength with a) a dispersive component of free energy for steel 1.0426 b): 1 - after processing with P320 abrasive tool, 2 - after processing with P320 abrasive tool and degreasing with Loctite 7061, 3 - after processing with P320 abrasive tool and water rinsing [9]

Table 4.1. The component values of free surface energy for 1.0426 steel and comparison of adhesive joint strength after additional treatment methods [9]

Surface condition	Surface free energy [mJ/m ²]	Non-polar component [mJ/m ²]	Polar component [mJ/m ²]	Adhesive Joint strength compared to abrasive tool treatment only [%]
P320	66,28	65,76	0,52	100
P320 degraded	67,94	65,32	2,63	112
P320 rinsed	65,54	56,31	9,23	64

The research was conducted in order to estimate the influence of ozonization process on energy properties of surface layer [10]. The obtained results show that for polyamide PA6, the ozonization process allows increasing the surface free energy by ca. 10% after 30 min. of surface treatment and by ca. 15% after 1h. There for ozonization can be an alternative for traditional means of energetic activation of surface layer of plastics (Fig. 4.7).

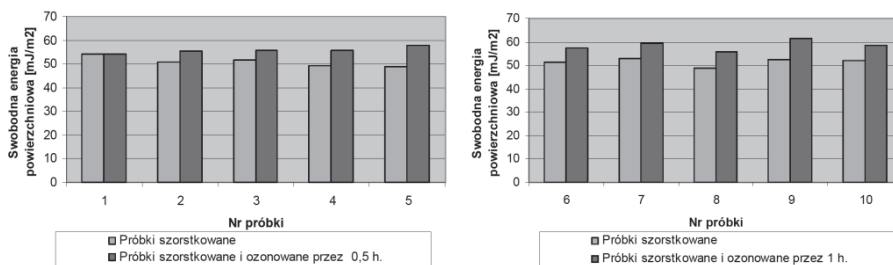


Fig. 4.7. The increase of surface free energy after ozoning process: for time: a) 30min., b) 1 h [10]

Other research into possible increase in surface energy were conducted for example for polyethylene which was activated by aluminium trihydrate [11].

Conclusions

Several existing methods for calculating the surface free energy developed over years are still widely used in research tests. One can distinguish simple ones – but not as accurate, and complicated – but much more precise. Some allow separating the energy into two fractions (disperse and polar components) some even into three (hydrogen bonds). Still – all of them are used – depending on results researches need to obtain. The paper presents also sample research projects which focused on improving energetic state of surface layer (surface free energy) – that used the contact angle measurements and surface energy calculations.

References

- [1] Bonn D., Eggers J., Indekeu J., Meunier J., Rolley E.: Wetting and spreading, *REVIEWS OF MODERN PHYSICS*, VOLUME 81, APRIL–JUNE 2009.
- [2] Krasowska M., Terpilowski K., Chibowski E., Malysa K.: Apparent Contact Angles and Time of the Three Phase Contact Formation by the Bubble Colliding With Teflon Surfaces of Different Roughness, *Physicochemical Problems of Mineral Processing*, 40 (2006), 293-306.
- [3] José Bic, Uwe Thiele, David Quéré: Wetting of textured surfaces, *Colloids and Surfaces A: Physicochemical and Engineering Aspects*, 206 (2002) 41–46.
- [4] Kuczmaszewski J.: Fundamentals of metal-metal adhesive joint design. Lublin University of Technology: Polish Academy of Sciences, Lublin Branch, 2006.
- [5] Wiącek Z. Badania wpływu stanu powierzchni metali lekkich na jakość połączeń adhezyjnych. Wydawnictwo Politechniki Lubelskiej, Mechanika 40, Lublin, 1987.
- [6] Melograna J. D., Grenestedt J. L., Maroun W. J.: Adhesive tongue-and-groove joints between thin carbon fiber laminates and steel. *Composites: Part A* 34 (2003).
- [7] Jacek Domińczuk, Jakub Szabelski,: Surface layer energy state and its influence on adhesive strength. Aspects of fracture and cutting mechanics of materials. Lubelskie Towarzystwo Naukowe, Lublin 2010.
- [8] KRUSS Software for Drop Shape Analysis for contact angle measurement systems, KRUSS GmbH, Hamburg 2012.
- [9] Domińczuk J., Szabelski J.: Measurements of the work of adhesion for different structural materials typical surface treatment methods, *Management and Control of Manufacturing Processes*, Lubelskie Towarzystwo Naukowe, Lublin 2011.
- [10] Kłonica M., Kuczmaszewski J.: Forming of polymeric material surface energy properties in ozonization process, *Technical Transactions – Mechanics*, Wydawnictwo Politechniki Krakowskiej, Issue 3/2009.
- [11] Samujło B., Rudawska A.: Influence of Polyethylene Modification by Aluminium Trihydrate on the Surface Free Energy Value, *Teka Kom. Bud. Ekspl. Masz. Elektrotech. Bud. – OL PAN*, 2008, pp. 153–158.

Analysis of energetic properties of the surface layer – overview of methods for measuring the contact angle and the surface free energy

Abstract: The paper describes methods of measuring the contact angle used further in calculation of the surface free energy of surface layer of examined materials. The phenomenon of wettability is presented and its three states are described. Methods of obtaining components of the surface free energy based on measurements of geometrical shape of drop were shown. Sample results of the surface free energy measurements after selected surface treatment operations are presented.

Keywords: wettability, contact angle, surface free energy, measurements

Analiza właściwości energetycznych warstwy wierzchniej – przegląd metod pomiaru kąta zwilżania i wyznaczania energii powierzchniowej

Streszczenie: W pracy opisano metody pomiaru kąta zwilżania wykorzystywanego do określenia energii powierzchniowej warstwy wierzchniej badanych materiałów. Opisano zjawisko zwilżalności i jego trzy stany. Zaprezentowano metody wyznaczania składowych energii powierzchniowej w oparciu o pomiary geometryczne kształtu kropli. Przedstawiono przykładowe wyniki pomiarów energii powierzchniowej uzyskane po wybranych sposobach przygotowania warstwy wierzchniej.

Słowa kluczowe: zwilżalność, kąt zwilżania, energia powierzchniowe, pomiary

5. The roller cones selection criteria and the ways of their classification

Drilling boreholes in the earth's crust is made primarily to determine the geological structure, the search for deposits, a more accurate examination and diagnosis and output of liquid and gaseous mineral resources. The holes are drilled for the purpose of research, engineering, hydro geological wells, to collect soil samples and determine its type prior to the implementation of the foundations for building structures. They are also made in underground and surface mining. The holes are drilled by mechanical crushing the rocks. Depending on how it is made, we distinguish impact and rotary drilling. Impact drilling is to drill rig crushing rocks, striking the bottom of the drilled hole. Rotary drilling is the cutting, grinding or crushing rocks by the rotating drill. The dynamic development of the global drilling in the last century was made possible by the introduction and application of large - scale rotary drilling method, for which a huge perspectives opened in 1909 and today present invention of H. Hughes, the founder of the world's first roller cone. Since then, it has undergone a number of design modifications in order to improve the geometry of the teeth, bearings, nozzle caps, shape of forgings and lubrication method of the bearings. Were changed the grades of steel and production technology this tool. Therefore all over the world the most common and most used are drill bits. Due to the large variety of drill bits, the proper selection of these tools determines the efficiency of drilling and tool life. Depending on the type of drilled rocks is chosen the type of drill bit, adapting to the drilling technology. The roller cone allow the use of large axial thrust, which in conjunction with a suitable rotational speed and the washer flux pumped into the hole, gives the possibility of using high speed drilling method, and thus can shorten the time of drilling.

5.1. Design features of the roller cone and their purpose

Structurally different types of the roller cones differ in the type of teeth, their number and the way of distribution on the rims, coverage ratio, type of bearing and method of flushing the bottom of the hole. Characteristic properties of drill design capable of achieving a maximum drilling performance in a variety of geological conditions. Different types of teeth is varied depending on the purpose for each category of rock hardness. The roller cone teeth can be done in the form of molded bars or milled teeth. Profiled bars are made of cemented carbide (e.g. tungsten carbide), which ensure high strength and

* Dr inż. Piotr JAREMEK, Wydział Mechaniczny, Politechnika Lubelska, ul. Nadbystrzycka 36, 20-816 Lublin, Polska, tel. (81)5384583, p.jaremek@pollub.pl

abrasion resistance of mining parts, especially at work in very hard rocks. Sample button bits (TCI) are shown in Figure 5.1. Cemented carbide bars are embedded in holes drilled previously in the tapered bite (core cutter). They crumble around the cross hole, hitting more and more changes in the other place on the bottom of the hole during the drilling.

In the first phase of the introduction of cemented carbide bars it was used mainly for hard and very hard rocks. Nowadays, with the development of construction drill bites, improving workmanship and setting the bars, there is a tendency to shift their use of softer rock formations. The teeth of the roller cones can also be made in the form of milled tooth with carbide surfaced.

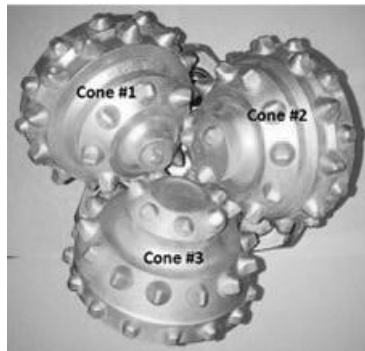


Fig. 5.1. Tricone with TCI bits

In the production of drilling tools the high – alloy nickel – molybdenum steel is used due to the technical specifications and placed requirements. The segments of drills are made of steel grade 20HNM, while drills – 17N3MA and 20HN3A. The milled teeth are made in the form of a wedge, shaped close to prism and parallel with the cutter shaft by its cutting or gouging. The teeth are arranged on the bite (milling cutter) in the form of concentric circles or rims. The rims are marked with letters of the alphabet – A, B, C. The last is called the peripheral rim. Peripheral teeth are subjected to a double load. They take part in the demolition of rock formations in the forehead and calibrate drilling wall of the shaft. Very often the peripheral teeth are made in the form of L, U, T. Their surface and calibrating side of the bit additionally enhances by hard sintered carbide. In order to increase the resistance to lose diameter and to reduce the use of cutting teeth, the bits are carburized and hardened. Carburizing depth is 1.5 to 3.0 mm depending on the drill bit diameter. The surface bites hardness after hardening should not be less than 56 HRC and a core hardness not less than 32 HRC. The characterizing values of the teeth are height, length, tightening angle tooth, pitch (i.e. the distance between the tops of the teeth) and their number in each bit (milling cutter) and the rims. The drills with higher teeth bites with a small apex angle but with less of their number on the rims are used

for soft rocks. While average hardness of the rocks, drills have lower teeth but a greater number of the rim (are densely located). With increasing hardness of the rocks, the number of teeth on the rims are also increases. The roller cones for very hard and abrasive rocks characterized by a large number of the rims and blades with a big apex angle.

Another very important element influencing the selection of the drill is its shape and geometry of the bites and their alignment with the axis of the drill. At present day, each bite is composed of several (two or three) truncated cones having on its periphery a number of teeth arranged on the rims (rows). The diameter and the angle at the vertex is selected from the condition for the largest volume of the rolling element bearing drill. These values also depend on the angle of the axis of pins feet to the axis of the drill and the angle of the bit to the axis of the hole. The axis angle inclination of feet pins for drills to the rocks of soft to medium-hard is 57 °, while for the drills to rock hard and very hard from 51 to 52 °. The roller cones are also characterized by a variable factor of cover the bottom of the borehole by the teeth, which is a quotient of the sum of the length throws of the teeth on any bites on a horizontal plane and the radius of the drill according to the formula:

$$\eta = \frac{2 \cdot (L_I + L_{II} + L_{III})}{D}$$

where:

L_I, L_{II}, L_{III} - length throws teeth of the drill on a horizontal plane, spaced at different bits,

D - drill bit diameter.

Proper selection of this factor determines the efficiency of the drilling process. The soft rock drills have the fewer rims on individual bits than the drills for hard rock. The coverage ratio of the bottom of the hole for the drills for hard rocks is greater than for the drills to soft rocks. Another characteristic, resulting from the cutting mechanism of the different hardness rocks is the position of the bit axis to the axis of the roller cone and the hole axis, called shift. The roller cones designed for drilling in soft and plastic rocks are highly teeth with a sharp apex angle and large scale (small number of teeth on the rim) and a smaller number of rims. In these drills axes of the bits are shifted so that in addition to rolling we obtain their slip, which gives the beneficial effect of soft rock cutting (Fig. 5.2a). Another factor increasing the slip of soft rock drills is to shift the point of intersection of cones forming beyond the axis of the roller cone (Fig. 5.2b). Increased angle of the teeth in the case of the hard rock, reduces the height and scale (large number of teeth and rims) and the shift of the axis of bites, which for the very hard rock tends to zero. This prevents intensive wear of roller cone when drilling hard and abrasive rock.

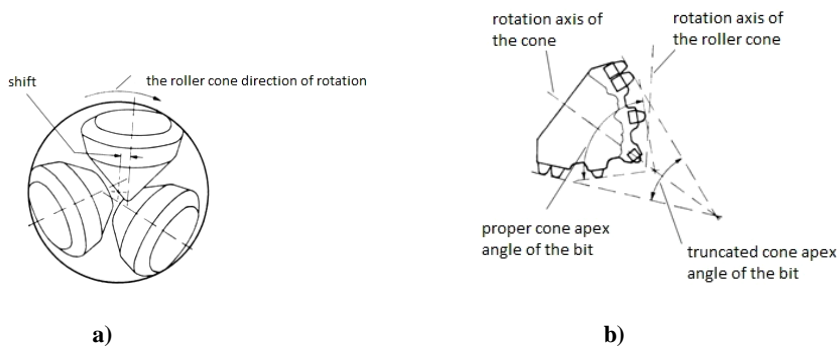


Fig. 5.2. Factors affecting the slip of roller cones [1]

The rims of roller cones with his teeth milled for soft and medium-hard rocks are so arranged that they provide additional self-purification. What happens is that the rim of one bite falls between two rims cooperating with the second bite. Such an arrangement of the teeth also increases the coverage of the hole, thus ensuring a better mining of the bottom surface. This also prevents allow leaving not mined the bottom, which could cause abrasion or cut a bite [1].

5.2.The ways of roller cones identification

At the moment, in the world there are many companies producing the roller cones for the mining industry. We may here mention such companies as Atlas Copco Secoroc, Bit Brockers International Ltd, Hughes Christensen, ReedHycalog, Smith Tool, Varel International and China's Hejian City Drilling Accessories Co. Xingtai. Ltd. or the Kiev Factory of Drilling Techniques. At our home, the Polish market, the production of these tools occupies the company Drilling Tools & Equipment Glinik Sp. z o.o, continuing the tradition of "Glinik" – the company was founded in 1883. by Canadian entrepreneur Mr. Mac William Garvey.

A huge variety of the roller cones produced in the world has forced the International Association of Drilling Contractors (IADC) to create a drills code. IADC is standard classification for tooth and button bits.

This system of roller cone identification was established in 1987 and expanded in 1992 to include more features. The division of the drills by IADC code is based on adapting their design to the hardness and abrasive of the rocks. There are six rocks formation categories corresponding to the IADC formation types [2]. The formations are:

- Soft and soft sticky. Low compressive strength and high drillability, such as clay, marl, gumbo, unconsolidated sand.
- Soft-to-Medium. Low compressive strength, inter-bedded with hard layers, such as sand, shale, anhydrite.

- Medium Hard with moderate compressive strength, such as shale, chalk, anhydrite, sand.
- Medium-to-Hard. Dense with increasing compressive strength but non-or semi-abrasive, e.g., shale, siltstone, sand, lime, anhydrite.
- Hard. Hard and dense with high compressive strength and some abrasive layers, such as sand, siltstone.
- Extremely hard. Very hard and abrasive, like quartzite and volcanics.

IADC code consists of four characters, indicating bit design and formation type being drilled (Fig. 5.3).

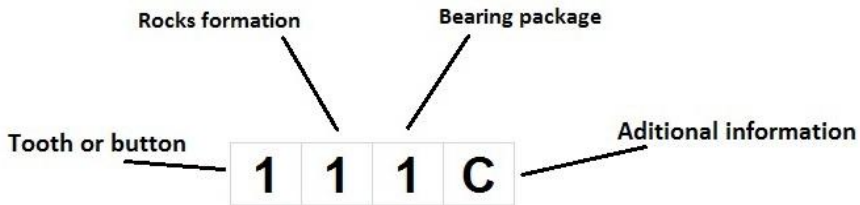


Fig. 5.3. IADC code

First three characters are numerical, fourth one – literal. Fourth literal code character defines "additional features". The numerical code characters sequence is determined as "series-type-bearing/gauge".

There are four common primary types of tricone bearings designs (Fig. 5.4):

- Standard open roller bit bearings are bearings without a seal. This means that the bearings are open to outside debris, which can enter through the cone. The advantage of an open bearing bit is that they are usually cheaper. They are ideal for drilling shallow holes, in the hundreds of feet. If drilling deeper holes with an open bearing bit you will probably have to pull it out every couple hundred feet to clean out the debris in the cones to free them up (Fig. 5.4a).
- Air blast roller bit bearings are equipped on air circulation bits. These bits have air passages that supply air to the bearings for cooling and lubricating of the bearing, and for cleaning of the bearing from the drilling debris (Fig. 5.4b).
- Sealed roller bit bearings have some of the features of the non - sealed open bearings, but longer lifetime because the bearings are sealed with an O' Ring Seal. A lubrication and compensator system prevents leakage into the bearing system and stops the possibility of debris blocking the bearing as well as leakage of gears (Fig. 5.4c).
- Journal roller bit bearings have very good durability and wear resistance. Instead of rollers inside the cone there is a floating bushing. The bushing is usually made out of special material that is highly resistant to heat and surface damage (Fig. 5.4d).

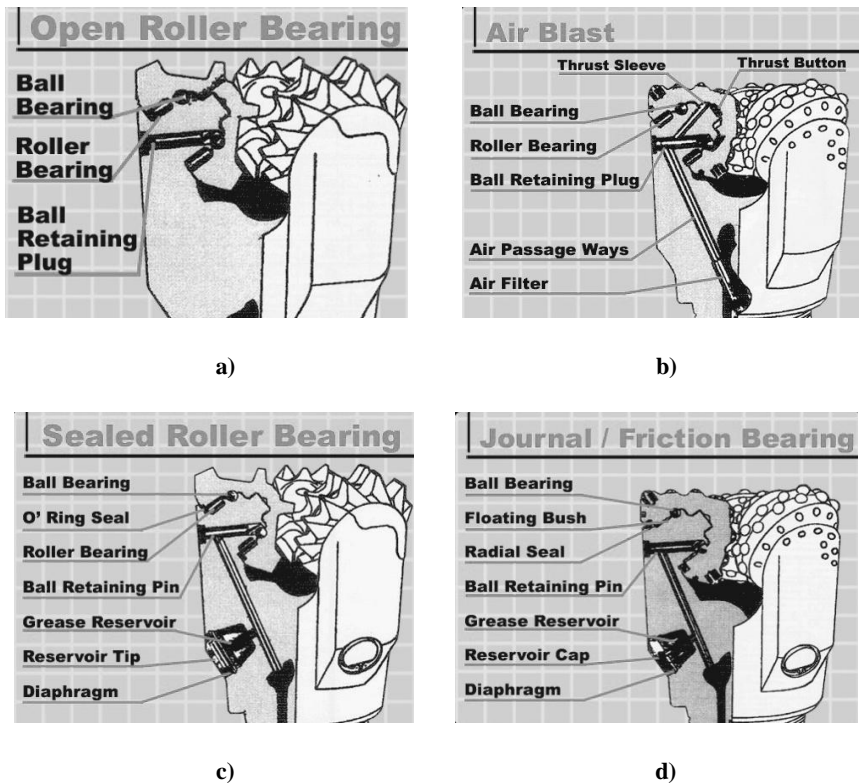


Fig. 5.4. Tricone bearings explained [3]

The first digit in IADC code (Fig.5.5) actually denotes two different things: tooth or button and hardness of formation the tooth or button bit was designed to drill [3,4,5].

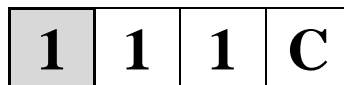


Fig. 5.5. First digit of IADC code

Thus, the numbers 1, 2 and 3 indicate a steel tooth bits with 1 being used for soft formations, 2 for medium, and 3 for hard. While the numbers 4, 5, 6, 7 and 8 are tungsten carbide inserts bits (TCI bits) designed for different hardness with 4 being softest and 8 being the hardest.

For instance the roller cone with steel tooth bits (IADC 116) for soft formation rocks like clays, salt, soft limestone and unconsolidated sands is shown on Fig. 5.6a, while the roller cone (IADC 316) for hard formation rocks like hard sands, chert or dolomite is shown on Fig. 5.6b.

Roller cone with button bits (IADC 427) is used in very soft formation rocks like shale, salt, soft limestone, clay or red bed is shown on Fig. 5.7a and roller cone (IADC 837) is used in very hard and high strength abrasive formations like sand, chert, quartzite, pyrite or granite (Fig. 5.7b). The figures show a clear difference in the number of the teeth or buttons on the rims, and their density and method arrangement on the cone according to the rocks formation.

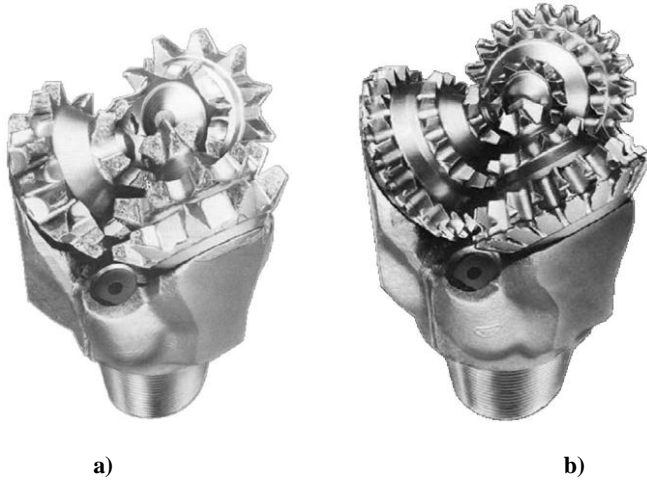


Fig. 5.6. Roller cone steel tooth bits a) IADC 116, b) IADC 316 [4]

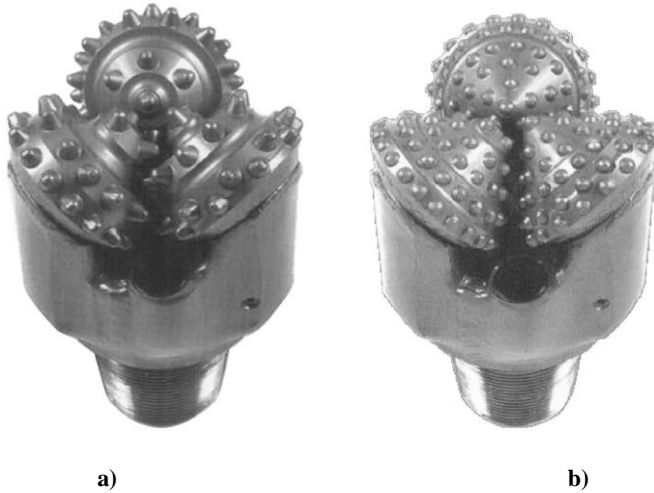


Fig. 5.7. Roller cone button TCI bits a) IADC 427, b) IADC 837 [4]

The second digit (Fig. 5.8) indicates formation hardness the bit was designed to drill. The number 1 is the softest formation and 4 the hardest.

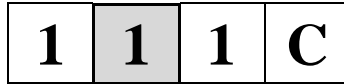


Fig. 5.8. Second digit of IADC code

The third digit (Fig. 5.9) will classify the bit according to bearing/seal type (Fig. 5.4) and special gauge wear protection as follows:

1. Standard open bearing roller bit.
2. Standard open bearing bit for air drilling only.
3. Standard open bearing bit with gauge protection which is defined as carbide inserts in the heel of the cone.
4. Roller sealed bearing bit.
5. Roller sealed bearing bit with carbide inserts in the heel of the cone.
6. Journal sealed bearing bit.
7. Journal sealed bearing bit with carbide inserts in the heel of the cone.

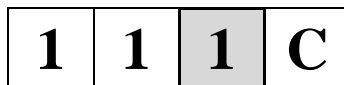


Fig. 5.9. Third digit of IADC code

Fourth literate code (Fig. 5.10) character additional features (unrequired). Sixteen letters are used to describe specific cutting structures, bearings, jets and gauge protections of a bit. If bit has more than one additional feature the only most significant one is to be indicated.

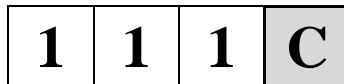


Fig. 5.10. Fourth literate of IADC cod

It looks like this:

- A - air application (journal bearing with air nozzles),
- B - special bearing seal,
- C - center jet,
- D - deviation control,
- E - extended jets (full length),
- G - extra gauge/body protection,
- H - horizontal/steering application,
- J - jet deflection,
- L - lug pads,
- M - motor application,

S - standard steel tooth model,
T - two cone,
W - enhanced cutting structure,
X - predominantly chisel tooth inserts,
Y - predominantly conical inserts,
Z - other shape inserts.

The symbolism of the roller cones manufactured by our only native company Drilling Tools & Equipment "Glinik" Sp z o.o. differs slightly from IADC code. Depending on the type of rock roller cones divided into five main types as shown in Table 5.1 [6].

Table 5.1. Depending on the type of rock roller

Symbol depending on the hardness of the drilled rocks		Category of the rock hardness
BM		very soft
M		soft
S		medium
T		hard
BT		very hard
Symbol depending on the design of the roller cone		Structural features of the roller cone
T	toothing	T-shaped teeth on the calibration rims
Z		the calibration rims reinforced with bits
G		TCI bits
GY		cone-shaped TCI bits
-	bearing	unsealed
X		sealed
SX		sealed slide bearing
M (at the beginning of indication)	stabilizing insert	reinforced teeth with additional stabilization for directional drilling
P	scrubber	additional central nozzle
C		drilling with air scrubber

This company. products mainly for the following industries: oil exploration, geology, hydrogeology, geophysics, engineering drilling and coal mining. The main products are tricone bits, available in a wide range of types and diameters. Figure 5.11 shows the tricone bits produced by Glinik, with its own symbols and the corresponding symbols in the IADC code.

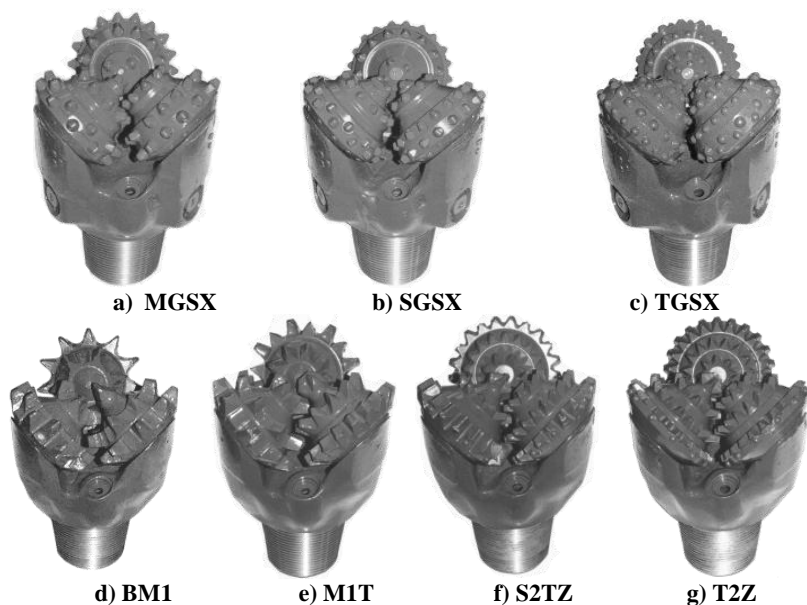


Fig. 5.11. Tricone drill bits used in rotary drilling [6]

The tricone bit MGSX (Fig. 5.11a) is used in the soft and layered rocks, medium concise and medium - hard with hard inserts. It is the equivalent of 537 in IADC code. The next tricone is SGSX (Fig. 5.11b). Is is used in the hard rocks and medium abrasive, very hard concise and abrasive. It is the equivalent of 627 in IADC code. Another tricone TGSX (Fig. 5.11c) is used as SGSX and in addition to the very hard and highly compact rocks and it is the equivalent of 737 in IADC code. The BM1tricone shown in Fig. 5.11d is used in the rocks very soft, powdery and loose. It is the equivalent of 111 in IADC code. The next MIT tricone (Fig. 5.11e) is used in layered and soft rock. The corresponding symbols is 131 in the IADC code. Another next one is S2TZ (Fig. 5.11f). It is used in hard and medium abrasive rocks. It is the equivalent of 243 in IADC code. The last one is T2Z (Fig. 5.11g) and is used in hard, abrasive and highly cohesive rocks. The corresponding symbols of this tricone is 333 in the IADC code.

Conclusions

Introduced IADC standard code that uniquely identifies the structure and purpose of the roller cones, helps potential buyers their correct identification regardless of manufacturer or brand. IADC is a code for every information bearings design and any other design features: shirt, tail, leg, section, cutter. The above classification of roller cones by IADC code was based on the alignment, design feature, the hardness and abrasive mined rock and uniquely allows for proper identification and optimal selection of this tool suited for the physical and geological conditions.

Reference

- [1] Szostak L. Wiertnictwo. Wydawnictwo Geologiczne. Warszawa 1989.
- [2] Drill Bit Classifier. World Oil's. September 2006.
- [3] Webpage <http://www.bitbrokers.com>
- [4] Webpage <http://www.iadc.org/>
- [5] Webpage <http://www.rock-drill-bit.com/>
- [6] Webpage <http://www.glinik.pl>

The roller cones selection criteria and the ways of their classification

Summary: This article presents the roller cone, which is the main tool used in drilling. Describes the characteristic parameters of the construction and design features that determine its use in specific mining and geological conditions. Presented and characterized IADC standard that facilitates the proper selection of tools for hard and abrasive drilled rock.

Keywords: drilling, roller cone, IADC code, rock hardness, rock abrasion, selection criteria

Kryteria doboru świderów gryzowych oraz sposoby ich klasyfikacji

Streszczenie: Przedstawiono świder gryzowy, który jest głównym narzędziem stosowanym w wiertnictwie. Opisano charakterystyczne parametry budowy i cechy konstrukcyjne decydujące o jego zastosowaniu w konkretnych warunkach górniczo-geologicznych. Przedstawiono oraz scharakteryzowano standard IADC, który ułatwia prawidłowy dobór narzędzia do twardości i ścierności przewiercanych skał.

Słowa kluczowe: wiertnictwo, świder gryzowy, kod IADC, twardość skały, ścieralność skały, kryteria doboru

VIKTOR MARCHUK*
ANATOLIU TKACHUK**
STANISLAV PRYSTUPA***

6. Thermophysical analysis process diamond smoothing

A study of thermal processes during diamond smoothing. Based on the calculation scheme of distribution of heat that is released during processing. Determined the resulting heat flows and their value.

Diamond smoothing surfaces are widely used in manufacturing. Low coefficient of friction of diamond on the work piece, its high hardness and wear resistance and high purity diamond surface, can be obtained by smoothing, surfaces of low roughness and hardened layer, which formed the residual compressive stress. Smoothing operation is often done by a tool working part which has a spherical shape of radius $R_{JIP} = 0,5...4\text{mm}$. It also uses the indenter functional part which is designed as a cylinder, cone, or torus [1].

Efficiency of the diamond smoothing depends on the speed of the spindle V , the applied force and the tool feed P_y , S . Studies have shown that the speed has little influence on the quality of the work piece, but it determines the nature and wear resistance of diamond indenter. For rational organization smoothing process, which provides the highest performance and create optimal conditions for crystal diamond, to determine the temperature that occur on tangential surfaces.

For thermo physical analysis we consider aspects that will come to the schematic form bodies involved in heat transfer during diamond smoothing and schematic form and character of distribution of heat. Consider the scheme for determining the area and configuration of the contact surface between the working part of the tool, which has a spherical and cylindrical surface detail (Fig. 6.1).

* Prof. Wiktor MARCZUK, Łuck Narodowy Uniwersytet Techniczny ul. Lwów, 75 Łuck, Wołyniu. 43018, Ukraina, e-mail: AspirantAA@gmail.com

** Anatoliu TKACHUK, Łuck Narodowy Uniwersytet Techniczny ul. Lwów, 75 Łuck, Wołyniu. 43018, Ukraina, e-mail: AspirantAA@gmail.com

*** Stanislav PRYSTUPA, Łuck Narodowy Uniwersytet Techniczny ul. Lwów, 75 Łuck, Wołyniu. 43018, Ukraina, e-mail: AspirantAA@gmail.com

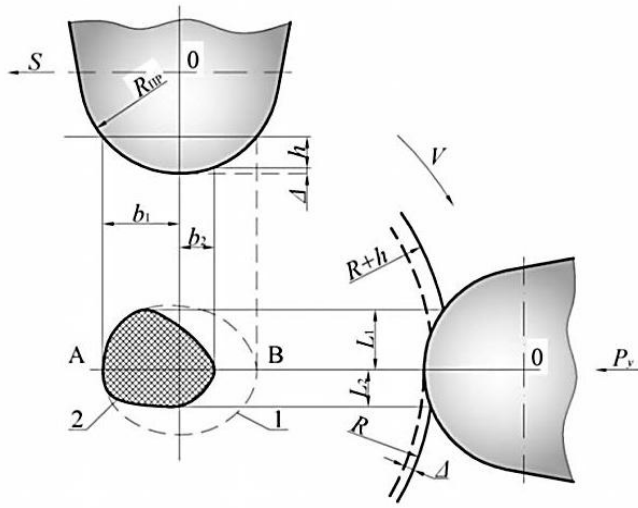


Fig. 6.1. Shape of the contact surface in the smoothing processing cylindrical parts with spherical indenter working part

During static view projection contact area between the indenter and the cylindrical surface detail is shaped ellipse 1 (Fig. 6.1). However, given the indenter movement and that in the process of smoothing the processed material gets permanent deformation and elastic recovery h , Δ , the shape of the contact surface takes the following form 2 (Fig. 14.1). To calculate the size of the contact area of this type just following formula [2]:

$$l_1 \approx \sqrt{\frac{2RR_{IP}}{R+R_{IP}}(h+\Delta)}; \quad l_2 \approx \sqrt{\frac{2RR_{IP}}{R+R_{IP}}\Delta}. \quad (6.1)$$

$$b_1 \approx \sqrt{2R_{IP}(h+\Delta)}; \quad b_2 \approx \sqrt{2R_{IP}\Delta}. \quad (6.2)$$

The value of h and Δ depend on the properties of the material and smoothing regime, they are determined by calculation-experimental method [1]. To determine h in the first approximation using data on contact angles ε_1 between the front surface of the indenter and the details of these parameters are given in Table 1 [4]. Taking the value ε_1 according to modes of processing and material, and also assuming that $\varepsilon_2 \approx 0,5 \varepsilon_1$, size of contact area can be calculated by the formula:

$$l_1 \approx 0,017R_{IP}\varepsilon_1; \quad l_2 \approx 0,009R_{IP}\varepsilon_1. \quad (6.3)$$

$$b_1 = l_1 \sqrt{\frac{R+R_{IP}}{R}}; \quad b_2 = l_2 \sqrt{\frac{R+R_{IP}}{R}}. \quad (6.4)$$

These formulas should be applied to the calculation of the area of contact during running-layer because angles ε_1 here have the same meaning as when smoothing [2].

Tab. 6.1. Contacts diamond smoothing angles during

Mode of processing:	Angle ε_1 , deg	
	for hardened steel	for soft materials
smoothing	6...7	2...3
firming-smoothing	8...9	4...5
strengthening	11...12	6...7

As shown in Fig. 6.1. Contact surface has a form that with sufficient accuracy for our purposes can be replaced by a rectangle $(l_1 + l_2) \cdot (b_1 + b_2)$ (Fig. 6.1). A more complex situation with schematic distribution laws intensity heat forming flows. The stress state that occurs in the area of smoothing, causes complex law intensity distribution of heat generation on the surface area of contact between the indenter and the work piece. However, given the assumption that:

- in terms of the contact placed above the line AB (Fig. 6.1) is mainly plastic deformation, and the part is under this line, elastic recovery;
- laws of intensity distribution similar in shape sources relatively little effect on the temperature in the contact zone. Thus thermogenesis allocated as follows (Fig. 6.2):

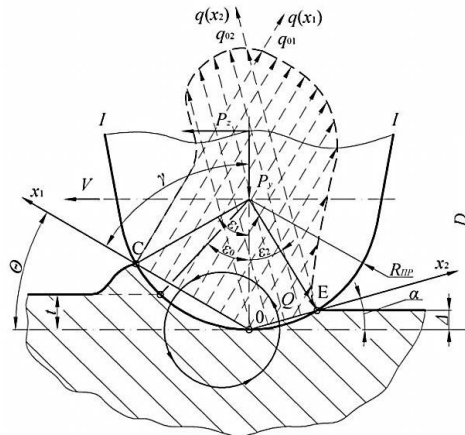


Fig. 6.2. The distribution of thermal stress during plastic deformation of the surface (heat is given in diamond indenter)

The area source distributed according to the law in the direction of the velocity vector smoothing V , and evenly – in the direction of the vector serve S (Fig. 6.4). Similarly, the area intensity is distributed according to the direction of the reciprocal vector V , and evenly – in the direction of the vector S . The extraction of heat to the indenter depicted as evenly distributed flow of heat.

In the event of such a schematic for the calculation of average temperatures in areas of contact with the sides of the work piece can apply formula (6.5), (13.6) in which to enter a correction factor to be considered limited sources of width $b_1 + b_2$.

$$\theta_1 \approx 0,066 \frac{\sqrt{\omega l_1}}{\lambda \sqrt{v}} (q_{01} - 2,78q_1) \quad (6.5)$$

$$\theta_2 = 0,1 \frac{\sqrt{\omega l_1}}{\lambda \sqrt{v}} \left[q_{02} \sqrt{\beta + 1,38\xi_1 q_{01}} - 1,84q_2 \sqrt{\beta} - 2,76\xi_2 q_1 \right] \quad (6.6)$$

where: $\beta = l_2 : l_1$.

Graphs of functions ξ_1, ξ_2 shown in Fig. 6.3.

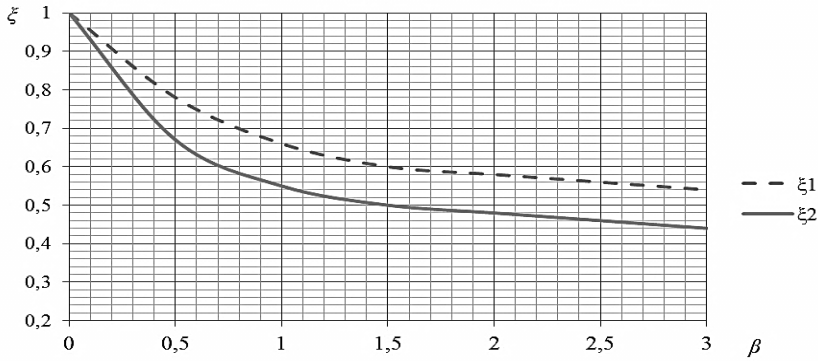


Fig. 6.3. To determine the correction factor

Values of correction factors ξ_1, ξ_2 , Considering the shape of the sources depend on the dimensionless variables:

$$u_1 = \frac{b_1 + b_2}{l_1} \sqrt{Pe_1}; u_2 = \frac{b_1 + b_2}{l_2} \sqrt{Pe_2} \quad (6.7)$$

where: $Pe_1 = \frac{vl_1}{6\omega}$; $Pe_2 = \frac{vl_2}{6\omega}$.

Since the calculations show that in practically used modes and smoothing radius indenter for processing steel with heat-resistant material $u_1 > 10, u_2 > 10$. Used a correction factor for all sources $\xi \approx 0,87$, to be fair the following equation:

$$\theta_1 \approx 0,057 \frac{\sqrt{\omega l_1}}{\lambda \sqrt{v}} (q_{01} - 2,78q_1) \quad (6.8)$$

$$\theta_2 = 0,87 \frac{\sqrt{\omega l_1}}{\lambda \sqrt{v}} \left[q_{02} \sqrt{\beta + 0,86\xi q_{01}} - 1,84q_2 \sqrt{\beta} - 2,76\xi q_1 \right] \quad (6.9)$$

At what value $\beta = l_2 : l_1; \xi_1; \xi_2$, and intensity of heat fluxes are determined by the formulas:

$$q_{01} = 7,62 \frac{P_z v}{l_1(b_1 + b_2)} - 1,92 \sigma_{-B} \mu_2 v \frac{l_2}{l_1} \text{ cal}/(\text{cm}^2 \cdot \text{s}); \quad (6.10)$$

$$q_{02} = 1,92 \sigma_{-B} \mu_2 v \text{ cal}/(\text{cm}^2 \cdot \text{s}). \quad (6.11)$$

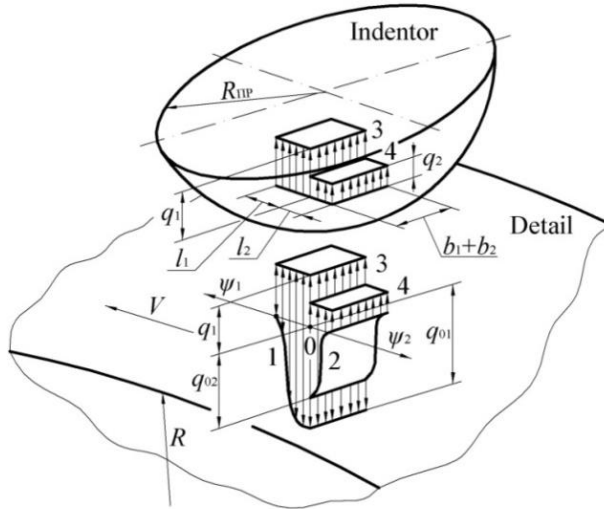


Fig. 6.4. Thermal scheme of diamond smoothing

The value of tangential force P_z which occurs during smoothing can be calculated or determined experimentally [1]. It depends on the radial force P_y , which indenter pressed against the work piece, and in general $P_z = kP_y + c$. For example, while smoothing 100Cr6 hardened steel (HRC 60...62) indenter with spherical working surface: $P_z = 0,085$; $P_y = 0,425$ [1].

In turn, the optimum value and depends on the hardness of the work piece (by Vickers HV), diameter D parts and labor radius of the indenter R_{IP} . To calculate the optimal values of P_y during the processing of hardened steels and recommend using the following formula:

$$P_y = 0,013HV \left(\frac{DR_{IP}}{D + R_{IP}} \right)^2, \quad (6.12)$$

who used to practice the values D and R_{IP} when $D \gg R_{IP}$, simplified to the expression: $P_y = 0,013HVR_{IP}^2 \text{ kgf}$.

Given the high thermal conductivity of diamond and sufficiently large length smoothing process heat exchange between the work piece and indenter installed quickly. Therefore, to calculate the temperature in the contact side indenter will be valid the following relationship:

$$\theta_1 = \frac{q_1 l_1}{\lambda_i} J_1 + \frac{q_2 l_2}{\lambda_i} N_2; \quad (6.13)$$

$$\theta_2 = \frac{q_2 l_2}{\lambda_i} J_2 + \frac{q_1 l_1}{\lambda_i} N_1. \quad (6.14)$$

In equation (6.13), (6.14) the coefficients describing the influence of shape sources at an average temperature of contact zones. Factors determining influence on appropriate sources of temperature zones of contact.

Formulas for calculating values and are as follows:

$$J_{1,2} = 0,061 + 0,033 \eta_{1,2}^{0,5} \lg \eta_{1,2}; \quad (6.15)$$

$$N_{1,2} = 0,0573 \eta_{1,2} \rho_{1,2}^{-1/\eta_{1,2}^{0,68}}, \quad (6.16)$$

where: $\eta_{1,2} = \frac{b_1 + b_2}{2l_{1,2}}$; $\rho_1 = 1 + \frac{l_2}{l_1}$; $\rho_2 = 1 + \frac{l_1}{l_2}$.

Pair wise equating the expressions (6.8) and (6.13), (6.9) and (6.14) to calculate the intensity of the resulting heat flow q_1, q_2 further define the temperature at the surface of contact with the work piece indenter.

The drawback of previous researchers [3] is that in the studies did not take into account the growth temperature parts caused by heat, which brought indenter on previous revs details. We describe the heat released in each of the previous momentum components in the form of one-dimensional source that moves with speed $V_1 = \frac{Sn}{600}$, where n – rotational details. This schematization is quite acceptable, as each smoothing V many times the feed rate of V_1 , and heat in the contact zone is concentrated in a narrow band width $b_1 + b_2$ (see Fig. 4). Contents getting a moving coordinate system with the source. Axis is directed along the axis of the details in the opposite direction of the vector V_1 . Then to calculate the additional temperature rise using the following formula, taking $x_i = y_i = 0; y = 0; x = -S$:

$$\theta' = \frac{q'}{\pi \lambda} \exp\left[-\frac{V_1 S}{20\omega}\right] K_0\left[\frac{V_1 S}{20\omega}\right]. \quad (6.17)$$

For used in practice mode smoothing different materials argument Bessel functions is rather small value, which allows the use of an approximate formula $K_0[u] \approx 1,4u^{-0,27}$. In this connection, temperature θ' represented as:

$$\theta' = 1,2q' \left(\frac{\omega D}{S^2 V} \right)^{0,27} \quad (6.18)$$

Here work piece diameter D is substituted in mm, S – in mm/rev, speed smoothing V – at m/min. Intensity q' is calculated by the formula obtained by analyzing the heat balance in the process of smoothing:

$$q' = \frac{10}{\pi D} \left[0,039 P_z V - \frac{b_1 + b_2}{100} (q_1 l_1 + q_2 l_2) \right] \text{ cal/(cm}\cdot\text{s)} \quad (6.19)$$

Analysis of specific examples for the conditions and modes of smoothing used in practice showed that both the resulting heat flow in the contact zone between the tool q_1, q_2 and work piece are directed into the tool.

Conclusions

Consider the scheme of temperature distribution on the arc AOB (Fig. 6.5), which is the diametrical plane indenter. Curves $\theta(\psi_1), \theta(\psi_2)$, describing the temperature distribution on the front and inner surfaces of the indenter are the sum of the ordinates of curves 1-4, each of which reflects the impact of a stream or source of heat. Sources and streams are numbered the same as in Fig. 6.4. Growth temperatures delayed the axis in the direction $\theta(+\theta)$ (Fig. 6.5), falling – in the direction $(-\theta)$.

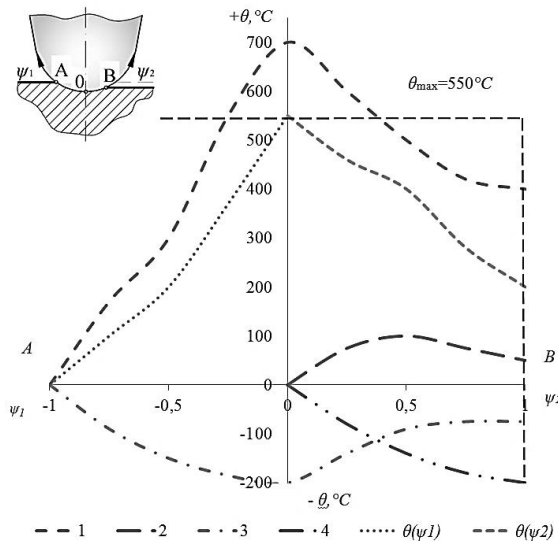


Fig. 6.5. Temperature distribution on the arc of contact with the work piece diamond indenter steel 100Cr6, (treatment conditions: $P_y=17$ kg·f; $R_{HP}=1$ mm; $V=200$ m/min; $S=0,005$ mm/rev)

As shown in Fig. 6.5, the temperature on the inner surface of the indenter on average higher than in the front (in the example under $\theta_2 = 330^\circ C$ and $\theta_1 = 210^\circ C$). So, in terms of the thermodynamic pressure inside surface indenter is more stress, and under extreme conditions can be expected to zone OB agents will have less resistance to wear. It is in this area will occur burn or other surface defects details associated with heat release during smoothing.

Thus, studies found that the temperature in the contact zone can reach very high values (Fig. 6.5). It should also be noted that the calculated value $\theta_{\max} = 550^\circ C$ which corresponds to the values obtained by experiment, and confirms that the admissibility of the schematic.

References

- [1] Абразивная и алмазная обработка материалов. ред. Резников А.Н. М.: Машиностроение, 1977, 392с.
- [2] Папшев Д. Д.: Упрочнение деталей обкаткой шариками. М.: Машиностроение, 1968. 132с.
- [3] Боков Е. М., Табачников Ю. Б. Усилия при алмазном выглаживании закаленных сталей. – Вестник машиностроения, 1970, №10, с. 60–62.
- [4] Резников А. Н., Барац Я. И.: Применение алмазного выглаживания для отделочно-упрочняющей обработки. Вестник машиностроения, 1970, №1, с. 15–17.

Thermophysical analysis process diamond smoothing

Abstract: A study of thermal processes during diamond smoothing. Based on the calculation scheme of distribution of heat that is released during processing. Determined the resulting heat flows and their value.

Keywords: diamond smoothing, tension, durability, residual deformation, intensity thermal circuit

Analiza termofizyczna procesu wygladzania diamentowego

Streszczenie: Na podstawie modelowania procesów cieplno-fizycznych określono rozkład temperatury podczas wygladzania diamentowego.

Słowa kluczowe: Diamentowe wygladzanie, wytrzymałość na rozciąganie, odkształcenie reszkowe, intensywność termicznego obwodu

MAREK SUKOP*
MIKULASH HAJDUK**
VLADIMIR BALAZ***
RUDOLF JANOS****

7. Higher speeds of data between computers and mobile robots based on increase in the number of transmitters (robosoccer)

Introduction

Robot soccer is an application for testing multi-agent systems consisting of multiple mobile robots. Each team, consisting of five robots, have a camera attached above the playground in height of 2 to 2.5 meters. Camera is connected to the control computer in which image processing algorithms is recalculating, and then algorithms strategy. Then the robot player instructions sent through the transmitter. In this article is described to decrease the response by adjusting the transmitting part.

7.1. The standard configuration the transmitting device

The system is very sensitive to the speed of response (time from shooting scenes to perform interventions in the scene) and the number of hits per unit of time (usually a specified frequency framing cameras around 50–100 fps). The speed of response in general is mainly dependent on the system parameters: speed image acquisition (camera shutter, the speed of data transfer to a computer), the speed of image processing (to obtain required positional data on all participating entities), speed over the strategic calculations (to generate commands for robots), the data rate to transmit module (eg. via RS232 or USB), the speed of data transfer between the RF transmitter module and robots (eg. 433MHz, ZigBee, Bluetooth), the processing of the data microcontroller robot and finally change the robot speed parameters.

* doc. Ing. MAREK SUKOP, PhD., , Department of Production Systems and Robotics, Faculty of Mechanical Engineering, Technical University of Kosice, 042-00 Kosice, st. Nemcovej 32, tel./fax.: (+421) 55 602 21 93, e-mail: marek.sukop@tuke.sk

** prof. Ing. Mikulash Hajduk , Department of Production Systems and Robotics Faculty of Mechanical Engineering, Technical University of Kosice, 042-00 Kosice, st. Nemcovej 32, tel./fax.: (+421) 55 602 21 93, e-mail: mikukash.hajduk@tuke.sk

*** Ing. VLADIMIR BALAZ, PhD. , Department of Production Systems and Robotics Faculty of Mechanical Engineering, Technical University of Kosice, 042-00 Kosice, st. Nemcovej 32, tel./fax.: (+421) 55 602 21 93, e-mail: vladimir.balaz@tuke.sk

**** Ing. RUDOLF JANOS, PhD., Department of Production Systems and Robotics Faculty of Mechanical Engineering, Technical University of Kosice, 042-00 Kosice, st. Nemcovej 32, tel./fax.: (+421) 55 602 21 93, e-mail: rudolf.janos@tuke.sk

One of the ways to positively affect the rate of response was applied to non-standard transmitting data in category MiroSot. The standard configuration transmitter link to the transmitter requires a computer with RS232 or USB interface (Fig.7.1).

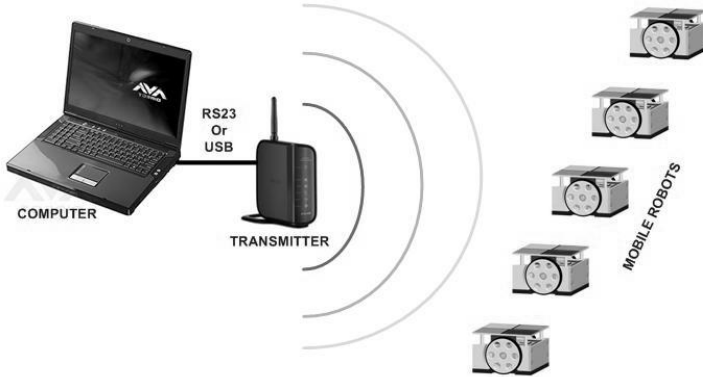


Fig. 7.1. The standard configuration the transmitting device

As a final member to use modules with free frequencies 433MHz (418MHz in some countries), or 915MHz. The disadvantage of these modules is normally quite low bit rate of RF parts. Modules can transfer data up to 115.2 kbit/s. Data is sent with the sequence for all mobile robots. Each robot receives data with a delay of:

$$t_n = \frac{n * BM}{TR} * 10 \quad (7.1)$$

n...ID of robot (n=1,2,3,4,5, large league n=1,2,...,11)

BM...number of bytes in message for one robot

TR...transfer rate v bit/s

When using the maximum possible transmission speed 115.2 kBaud number of bytes being transferred and 4 for each robot (speed 16 bit, 16 bit angular velocity), the resulting delay complete information for the last robot in the chain of 1.74 ms. But it delays the ideal situation is that using conventional transmitter cannot be achieved. Transmitters operating with a carrier frequency hundred MHz are limited data transfer by the ratio of ones and zeros in a short time should it be 1:1, 1:3 in the worst case. Sjf TUKE Robotics team was due to technological limitations, and with the help of using coding delay amounted to around 870us per robot, which is 4.35 ms for the fifth robot.

7.2. Using more transmitters

The philosophy of arrangement more transmitters in transmission chain is shown on Fig. 7.2. To shorten the time of data transmission modules were used, based on the nRF24L01 chip. Its advantage is the data transfer speed of up to 2 Mbit/s. Communication with the control processor runs over SPI at up to 8MHz.

Minimum configuration is sent bytes: 1 byte preamble, 3 byte address, data transferred 1–32 bit, 1 CRC byte. The non-standard configuration, we achieved a delay of sending data to capture all the data about the last robot. 300–320 μ s.

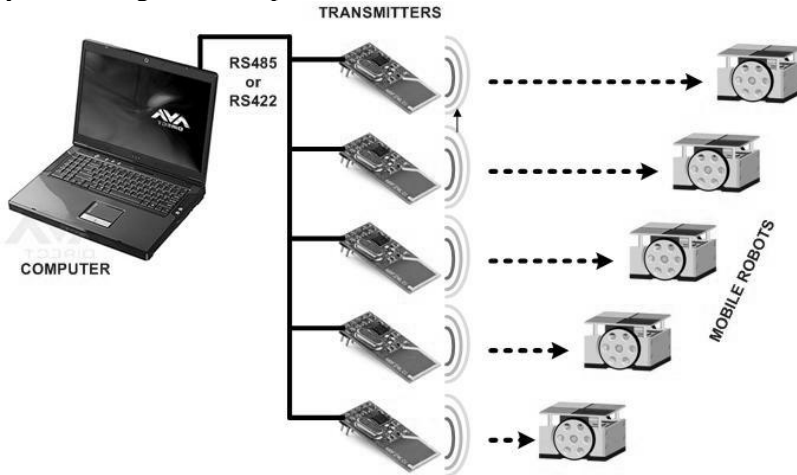


Fig. 7.2. Non-standard arrangement of devices in the data transmission chain

There was room for repetition level data microcontroller, which ensures repeat transmission to reception of new data. Using the principle of that problem is eliminated accidental data loss. If the robot does not capture the first data pack, then catch the second resp. third etc. Of course there is a longer delay, but that would not be still, so long as the standard broadcast. Time display data transfer from PC to microcontroller and RF module is then to Fig. 7.3.

The big advantage is visible in the graph is constant delay for all robots. The delay does not depend on the number of robots, but only from faults in transmission. In the earlier arrangement, however, there has been a complete failure in the data processor for the image, if there is a failure of transmission between the transmitter robot. The complete block diagram of the implemented data transmission between the control computer and the mobile robot is shown on Fig.7.4.

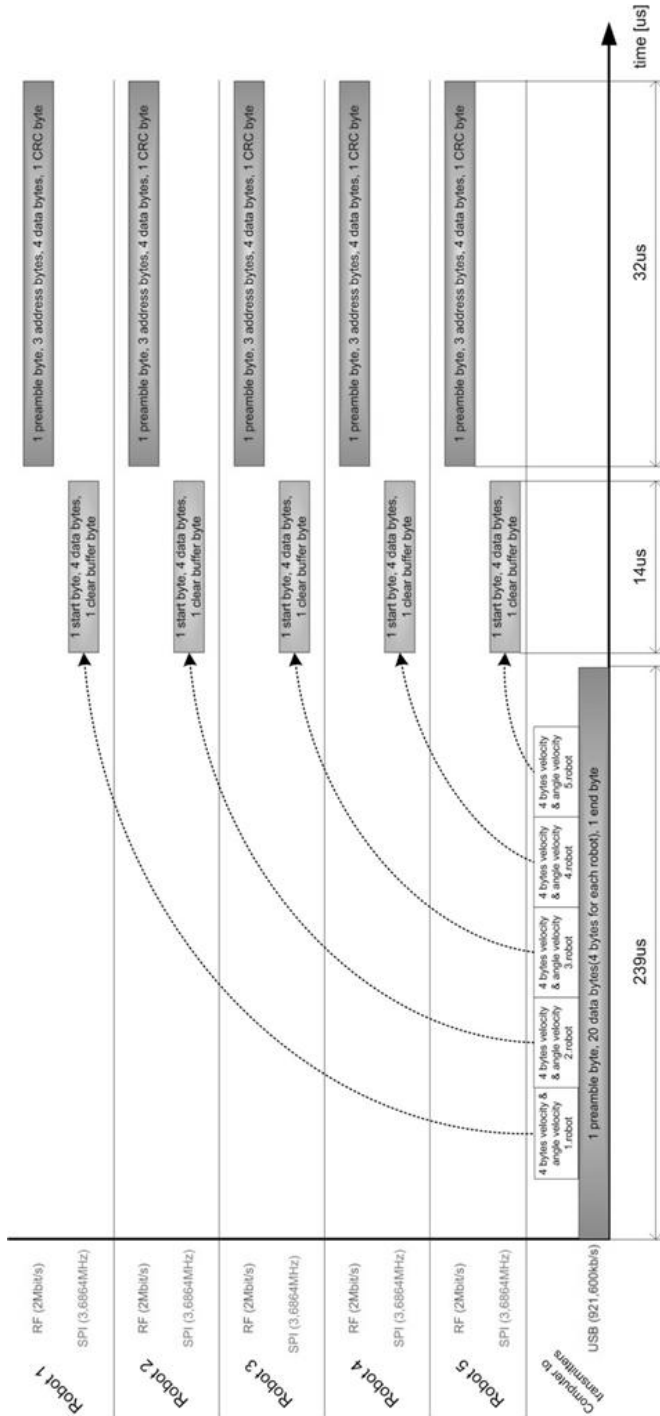


Fig. 7.3. Time display data transfer

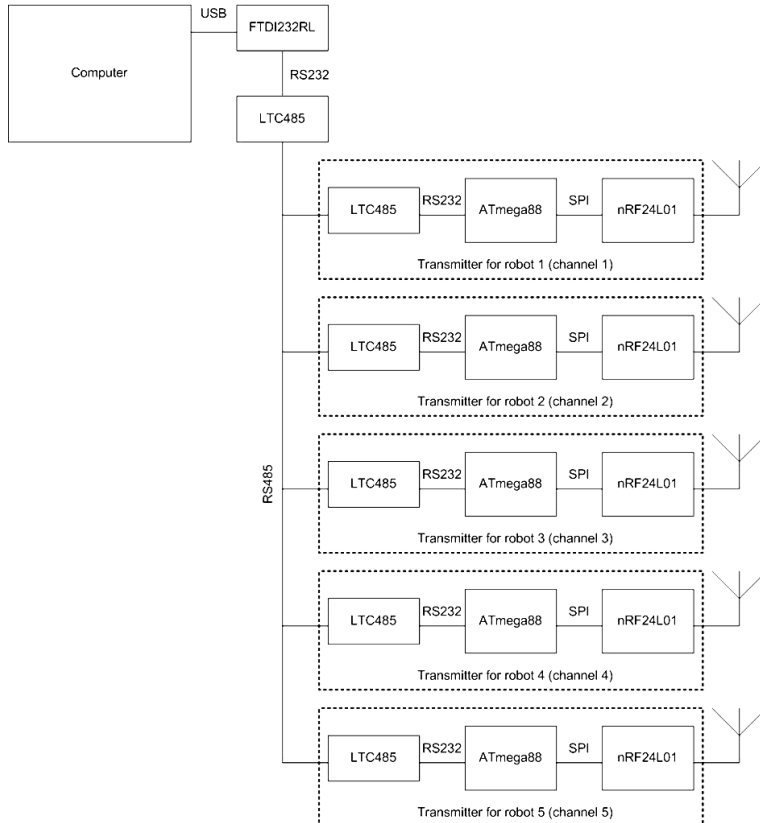


Fig. 7.4. Block diagram of transmission system

Part of the algorithm in the control computer, which is responsible for transferring data from a software module strategic calculations to the transmitter via USB, remained unchanged. After filling the system as shown in Fig.16.4, it was necessary to change the algorithms in microcontrollers upstream transmitter module and also part of the algorithms in the robot which processes data from the receiving module.

Conclusions

The advantage of applying the method described in shortening the response time of mobile robots to load images from a camera positioned above the playground. For optimal transmission, we reduced the time required for data transmission speed and the desired yaw rate compared to our old system of approx. 4ms, so we reduced the total delay in the control loop by more than 20%. It is a delay that is constant for all 5 robots. This latter feature is another important advantage. With such transmitters arranged in a chain, our team Sjf TUKE Robotics presented at the 2009 World Championships in Korea.

This contribution is the result of the project implementation: Research modules for intelligent robotic systems (ITMS: 26220220141) supported by the Research & Development operational Program funded by the ERDF.

References

- [1] Fedák V., Bačík J.: Hardware Design for State Vector Identification of a Small Helicopter Model. In: Applied Mechanics and Materials, Vol. 282, ISSN 1660–9336, 2013, p. 107–115.
- [2] Sukop M., Hajduk M., Varga J.: Aplikácia robotického futbalu: 1. Použitie softvérové a hardvérové moduly. In: ATP Journal PLUS 1/2013, ISSN 1336-5010, 2013, p. 66–68.
- [3] Sukop M., Varga J., Jánoš R., Svetlík J.: Aplikácia robotického futbalu: 2. Robot ako hráč. In: ATP Journal PLUS 1/2013, ISSN 1336–5010, 2013, p. 69–71.
- [4] Sukop M., Páchniková L.: Aplikácia robotického futbalu: 3. Spracovanie obrazu. In: ATP Journal PLUS 1/2013, ISSN 1336-5010, 2013, p. 72–75.
- [5] Swic, A., Zubrzycki, J. Taranenko W.: Modelling and Systemic Analysis of Models of Dynamic Systems, Robotics in Theory and Practice, ROBTEP 2012
- [6] Piotrowski, A., Nieszporek T.: Setting up a work centre based on the Profibus network, Robotics in Theory and Practice, ROBTEP 2012.
- [7] Sukop M.: Aplikácia robotického futbalu: 4. Modul stratégií. In: ATP Journal PLUS 1/2013, ISSN 1336–5010, 2013, p. 76–82.

Higher speeds of data between computers and mobile robots based on increase in the number of transmitters (Robosoccer)

Abstract: A very important feature in the management of robotic soccer is the response time of the system. This article is one of the possible ways of reducing the time and using concatenation transmitters. This way to the first team (under MiroSot) used by FME TUKE Robotics World Championship 2009 in Korea. The first section describes the conventional method of data transmission as it said it applied. The second part describes the hardware and software method by which transmitters and finally compare responses with conventional manner.

Keywords: robot soccer, transmitter, receiver, mobile robot

JOZEF VARGA*
KAMIL MADÁČ**
LADISLAV VARGOVCIK***

8. Walking and turning of swivel walker

Introduction

Swivel walker is defined as a support walking equipment for long term paraplegic patients (Motloch and Elliot, 1966; Edbrooke, 1970; Rose and Henshaw, 1972; Stallard et al., 1978; Butler et al., 1982; Farmer et al., 1982). Swivel walker not only allows patient to walk but it also ensures his stability, without any other aids such as crutches. It was primarily designed and has a high potential for use by a patient suffering from muscular dystrophy, which are able to move their legs, but their muscles are not strength enough to manage walking alone. A wheelchair would be the only possible option for these patients in case there was no swivel walker.

The construction of first swivel walkers ever built (Fig.8.1) was not very successful, but however it verified the basic principle. Deficiencies and weak points of initial construction were eliminated by later development but there are still several details that need to be solved to provide full functionality – comfortable and effective walking for patient diagnosed with muscular dystrophy.

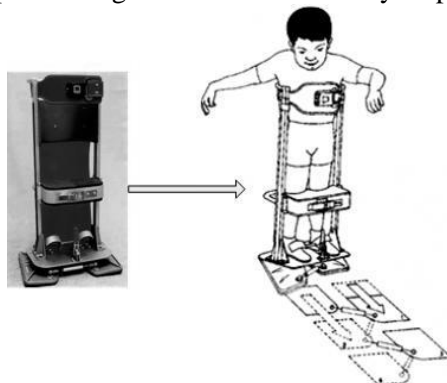


Fig. 8.1. Swivel walker

* Ing. Jozef Varga, , Department of Production Systems and Robotics, Faculty of Mechanical Engineering, Technical University of Kosice, 042-00 Kosice, ul. Nĕmcovej 32, tel./fax.: (++421) 55 602 21 93, e-mail: jozef.varga.l@tuke.sk

** Doc. Ing. Kamil Madáč,CSc., Department of Production Systems and Robotics, Faculty of Mechanical Engineering, Technical University of Kosice, 042-00 Kosice, ul. Nĕmcovej 32, tel./fax.: (++421) 55 602 21 93

*** Ing. Ladislav Vargovcik, Department of Production Systems and Robotics, Faculty of Mechanical Engineering, Technical University of Kosice, 042-00 Kosice, ul. Nĕmcovej 32, tel./fax.: (++421) 55 602 21 93

8.1. Analysis of walking for swivel walker

The walking principle is based on mechanical shift of a pad, limited by springs and mechanical backstops located on each foot plate. Swivel walking itself is caused by human body CoG left-right movement Fig. 8.2. The tilt of construction is limited by the angle between foot plate and ground, which equals 4° in our case. In fact 4 degree tilt angle limitation and sufficiently large surface of the foot plate prevents platform from overbalancing.

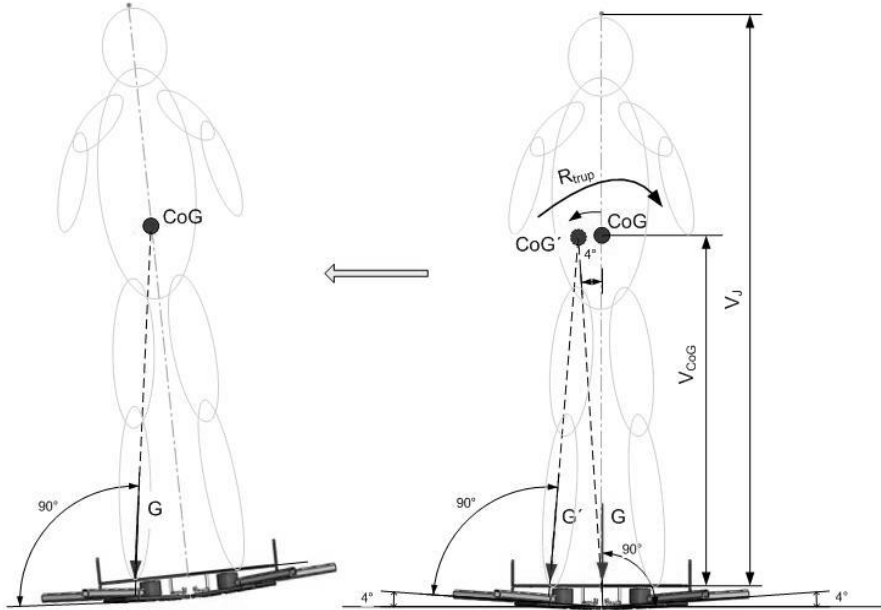


Fig. 8.2. Transmit of CoG Swivel walker

Full weight of body is concentrated alternatively on left or right foot, while moving from side to side (Fig. 8.3). This is illustrated as phase 0 to phase 2. One step is completed after phase 3 and 4, when CoG is concentrated above opposite foot. It is also possible to rotate whole platform about its foot axis by combination of side and back movement of body.

Walking movement of platform is consequently achieved by cyclic repeating of phases 0-4, but the trajectory is not completely straight. Deviation β depends on mutual distance of right and left footplate as well as angle of axis foot plane α

Equal for length of step: $k = \sin \alpha \times l$

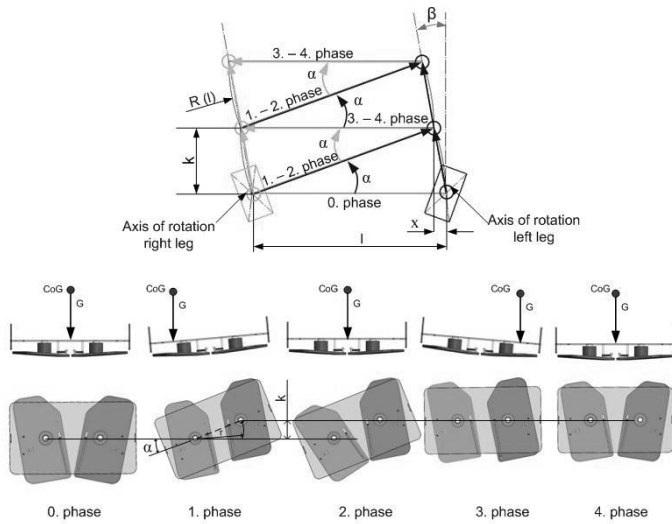


Fig. 8.3. Analysis of walking for swivel walker

Deviation from straight walking β :

$$l^2 = (l - x)^2 + k^2$$

$$x = l - \sqrt{l^2 - k^2}$$

$$\tan \beta = \frac{x}{k}$$

$$\beta = \arctan \frac{x}{k}$$

8.2. Analysis of turning swivel walker

Radius of turning circle equals mutual distance of left and right foot $l = R(l)$. Maximum angle of platform rotation is limited by mechanical backstops and α angle, see Fig. 8.4.

As mentioned before, full weight of body is concentrated alternatively on left or right foot. Platform is rotating about foot axis, whilst loaded foot plate remains in place. It is necessary to shift unloaded foot plate back to basic position before repetition of next step. This is done by means of spring mounted directly between foot plate and standing platform.

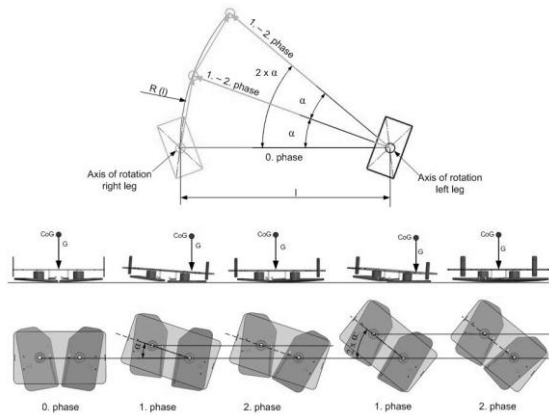


Fig. 8.4. Turning of Swivel walker

8.3. Modular conception of swivel walker

Fig.8.5 shows the conception of Swivel walker. It is modular and depends on degree of patient disability.

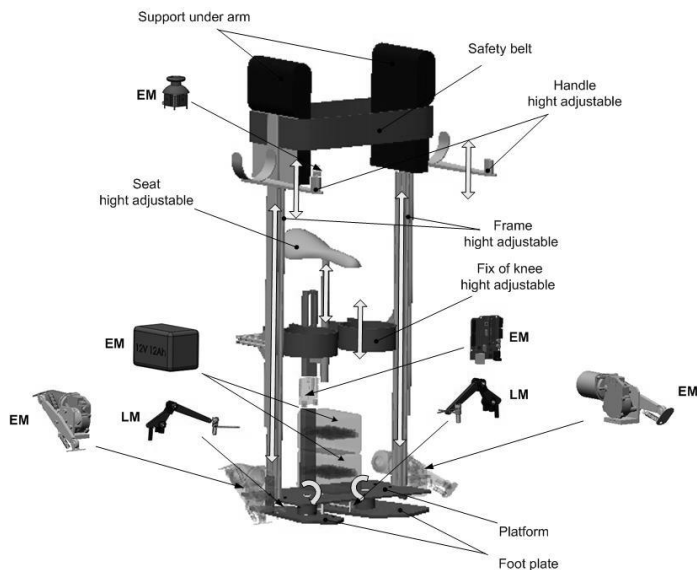


Fig. 8.5. Modular conception of Swivel walker

The core of construction includes platform and foot plates. Two different extensions are possible:

- Lever module LM, which allows step transition by pushing lever system caused by patient bodyweight while leaning form side to side,

- Electro motoric module EM consisting from two motors. Aluminum profile, located on motor axis, supports step transfer, so leaning of patient is not necessary Joystick located on upper part of the construction allows patient to control the movement.

Lever module is intended for use by lower degree disabled patients whilst electro motoric module is for patients suffering from higher degree of disability.

Conclusions

Modular conception of swivel walker is innovative and modern approach of swivel walker solutions. Despite mentioned extension modules, basic idea and original swivel walker construction won't be affected. The main advantage lies in possibility to choose module which fits the patient needs the most. The Swivel walker basically helps people suffering with muscular dystrophy and other paraplegics problems to extend period of individual walking ability.

This publication is the result of the project implementation: Research modules for intelligent robotic systems (ITMS: 26220220141) supported by the Research & Development Operational Programme funded by the ERDF.

References

- [1] Chih-Hsiu Ch, Liang-Wey Ch., Kwan-Hwan L., Determination of foot-plate spacing for swivel walkers by an optimization method, *Biomedical engineering: Applications and Communications*, Vol. 22, No. 3 213–221, 2010.
- [2] Stallard J, Lomas B, Woollam P, et.al., New technical advances in swivel walkers, *Prosthet Orthot Int* 27: 132-138, 2003.
- [3] Butler P. B., Farmer I. K., Poiner R., Patrick J. H.: Use of the ORLAU swivel walker for the severely handicapped patient. *Physiotherapy* 68, 324–326, (1982).
- [4] Edbrooke H.: The Royal Salop Infirmary "Clicking Splint". *Physiotherapy* 56,148–153, (1970).
- [5] Farmer I. R., Poiner R., Rose G. K., Patrick J. H.: The adult ORLAU swivel walker – ambulation for paraplegic and tetraplegic patients. *Paraplegia* 20, 248–254, (1982).
- [6] Motloch W. M., Elliot J.: Fitting and training children with swivel walkers. *Artificial Limbs* 10 (2), 27–38, (1966).
- [7] Rose G.K., Henshaw J.T.: A swivel walker for paraplegics: medical and technical considerations. *Biomed Eng* 1,420–42, (1972).
- [8] Stallard J., Farmer I.R., Poiner R., Majorre Rose G.K.: Engineering design considerations of the ORLAU swivel walker. *Eng Med* 15, 3–8 , (1986).
- [9] Stallard J., Rose G. K., Farmer I. R.: The ORLAU swivel walker. *Prosthet Orthot Int* 2, 35–42, (1978).

- [10] Smrček J. Kárník, L.: Robotika. Servisné roboty. Navrhovanie, konštrukcia, riešenie. Edícia ved. A odb. Lit. Sjf TU v Košiciach. Vydavateľstvo Vaško Prešov. Košice 2008.
- [11] Hajduk M.: Present status and evolution trend of service and humanoid robotics. In. Service and Humanoid Robotics, Košice, 2007.
- [12] Hajduk M., Sukop M., Marko L., Varga J., Balaz V.: Design of Humanoid's Lower Limb Model for Walking, Advanced Materials Research, ISSN:1022-6680, 2012.
- [13] <http://www.prowalk.de/Swivel-Walker/440/>
- [14] <https://www.rjah.nhs.uk/Our-Services/ORLAU/Rehabilitation-Engineering/The-ORLAU-Swivel-Walker.aspx>

Walking and turning swivel walker

Abstract: The aim of this article is to introduce modular concept of walking mechanism Swivel walker. In translation means Swivel – rotary from German language and walker from English. It is prosthetic equipment for children, who are not able to hold their body weight on their legs. The largest groups for using Swivel walkers are children with nervous and muscular diseases. Their common symptoms are gradual development of muscle weakness, often accompanied by reducing their volume. Nervous disease is progressive muscle disease that is worsening over time. Thanks to modular design is possible through the degree of disability determine a necessary type of module, mechanically or electromotive module.

Keywords: swivel walker, CoG – center of gravity, modular design of swivel walker

Chodzenie i obracanie swivel walker

Streszczenie: Celem niniejszego artykułu jest przedstawienie koncepcji modułowej spaceru za pomocą mechanizmu Swivel walker, czyli swivel - obrotowy i walker - pieszy, z języka angielskiego. Jednym z nich jest urządzenie protetyczne dla ludzi, którzy nie są w stanie udźwignąć swojego ciężaru ciała na nogach. Największą grupą stosującą Swivel walker są dzieci z chorobami nerwów i mięśni. Ogólnym objawem choroby jest stopniowy rozwój osłabienia mięśni, któremu często towarzyszy zmniejszenie ich objętości. Aby umożliwić ruch w rzeczywistości, w celu ułatwienia przemieszczania zostały opracowane różne urządzenia. Większość z nich jest zaprojektowana jako urządzenia jednofunkcyjne. Artykuł opisuje podejście rozwiązania opartego na koncepcji modułowej. To właśnie dzięki modułowej konstrukcji może być określony właściwy typ modułu w zależności od stopnia niepełnosprawności: moduł mechaniczny lub elektromotoryczny.

Keywords: swivel walker, CoG – center of gravity, modular design of swivel walker

*VLADIMÍR BALÁŽ**
*MAREK VAGAŠ***
*MIKULÁŠ HAJDUK****
*JÁN SEMJON*****

9. Modular training system in virtual reality environment - MSEVR

Introduction

MSEVR is an education system designed for training at automated and robotized systems for employees of small and medium –sized enterprises as well as for professional trainers. One of its parts is a virtual laboratory, which is intended to teach in virtual reality environment. Created laboratory simulates real environment of workplace, where you can insert mechanical equipment and then makes experiments with it.

Basic building component for virtual laboratory is VRML language. By this language are created models that form 3D view of laboratory. Laboratory has a certain level of interaction. This feature is secured by using of VRML language sensors in cooperation with ECMA script (standard form language of JAVA script). This solution allows to retain ongoing events in virtual reality and respond to their processing in any way.

Virtual laboratory can be run directly in VRML browser, or distributed through web site. In this case is VRML browser integrated as plug-in web browser. Created virtual laboratory has been developed and tested at configuration: Cortona3D Viewer v6 and MS Internet Explorer 8.

Virtual laboratory does not support a Mozilla Firefox of Google Chrome yet. At the beginning of the starting page is checked a configuration at client site to prevent an unresponsiveness of system. In case of inappropriate configuration of system follows next steps:

- If laboratory does not start at MS IE browser follows a starting block.
- If client does not have a plug-in of VRML viewer Cortona3D from Parallel Graphics firm follows an instruction to download and half-automatic installation.

* Ing. Vladimír BALÁŽ, PhD., Department of Production Systems and Robotics, Faculty of Mechanical Engineering, Technical University of Kosice, 042-00 Kosice, ul. Nĕmcovej 32, tel./fax.: (++421) 55 602 21 93

** Ing. Marek VAGAŠ, PhD., Department of Production Systems and Robotics, Faculty of Mechanical Engineering, Technical University of Kosice, 042-00 Kosice, ul. Nĕmcovej 32, tel./fax.: (++421) 55 602 21 93

*** Prof. Ing. Mikuláš HAJDUK, PhD., Department of Production Systems and Robotics, Faculty of Mechanical Engineering, Technical University of Kosice, 042-00 Kosice, ul. Nĕmcovej 32, tel./fax.: (++421) 55 602 21 93, e-mail: Mikulas.Hajduk@tuke.sk

**** Ing. Ján SEMJON, PhD., Department of Production Systems and Robotics, Faculty of Mechanical Engineering, Technical University of Kosice, 042-00 Kosice, ul. Nĕmcovej 32, tel./fax.: (++421) 55 602 21 93

9.1. Virtual Laboratory

From the design point of view to virtual environment built through VRML language, which visually introduce a space of built workplace with empty feature of ground (see Fig. 9.1) basic view to environment system MSEVR). From the user design point of view is system before starting of experiment similar to status, when are finished building treatments of workplace and begins installation processes of mechanical equipments in real situations. In real situations is necessary at this moment proceed to buy, to import and to build all machines. In virtual environment we will follows similar steps, but without any costs and mainly much easier. Instead suppliers we have a gallery of machines, robots and equipments (see right part of Fig. 9.1). From it we can choose and move objects by drag & drop method to ground of workplace. Similarly we can edit properties of feature structure of ground workplace. For better orientation is possible to move textures, which have dimensions as an indicative lines from 1m x 1m to 0,1m x 0,1m.

Basic equipment MSEVR contains, (Fig.9.2):

- models of robots,
- models of machines,
- models of transport equipments,
- models for trajectory optimization of robot,
- auxiliary models,
- textures for better orientation

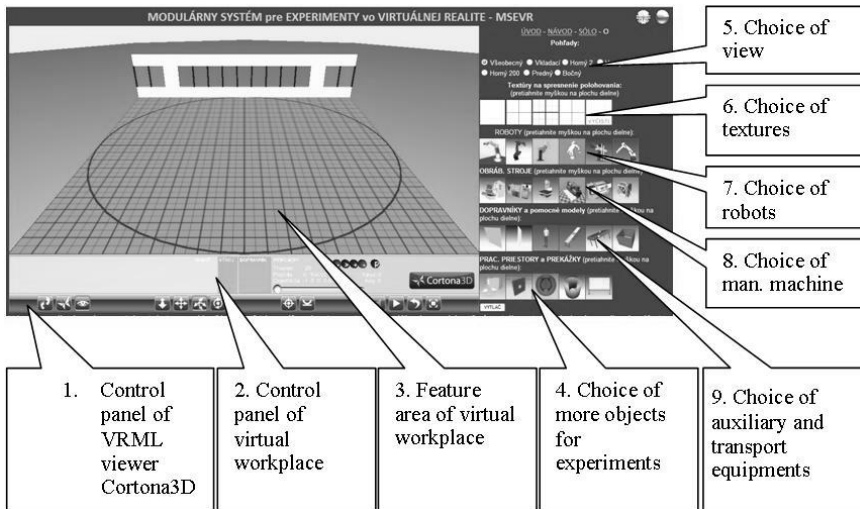


Fig. 9.1. Basic view to environment system MSEVR



Fig. 9.2. Detail of MSEVR menu for select object at workplace

MSEVR allows to experiments in virtual reality quite simply through simply controlling of similar activities to real build of automated and robotized systems, see Fig. 9.3. So teacher can directly on lecture placed machines and equipments into feature ground of workplace with relative position and created automated and robotized systems from them. Students can saw not only results of its work, but also watch its progress, that is mainly increasing of effectively education process. For creating workplace is available pre-prepared models, but system allows using also external models. Due to creating of workplaces from individual models MSEVR will laboratory provides follow functions:

1. Visual

- representation at 3D virtual reality,
- freedom in movement at 3D space,
- change the type of motion at 3D space,
- set of view (cameras),
- to record trajectory of movement and then to start movement in automatic mode

2. Preparatory

- change textures of feature ground area – guides lines for better orientation,
- insert (also remove) individual objects (machines, fixtures and other equipment),
- multiple insert,
- insert the foreign objects with minimal requirements to their adaptation

3. Implementing

- movement with models,
- rotation with models,

- through scaling to change dimensions of inserting objects (only at necessary models),
- measurement of feed movement (axis X and Y) also rotation of objects, (around axis Z) for accurate determining their position,
- to retrieve all functions of own machines.



**Fig. 9.3. Building phase of workplace in MSEVR system
(Mutual position setting of equipment)**

Except for those functions is possible for created virtual workplace also more functionality because each model by inserting to the workplace brings not only its own shapes, but also all properties, which were assigned during its creating including interactive properties. Some standard models of workplace brings to us possibility for control, for example, also performance technology movements, controlling of movement speed, programming by teach method, sound and visual effects, possibility for extended edit and manipulation with model and so on. Complete list of functions from created workplace is depended on using models and their functions. Algorithm for building of virtual workplace in MSEVR environment can be seen at Fig. 9.4.

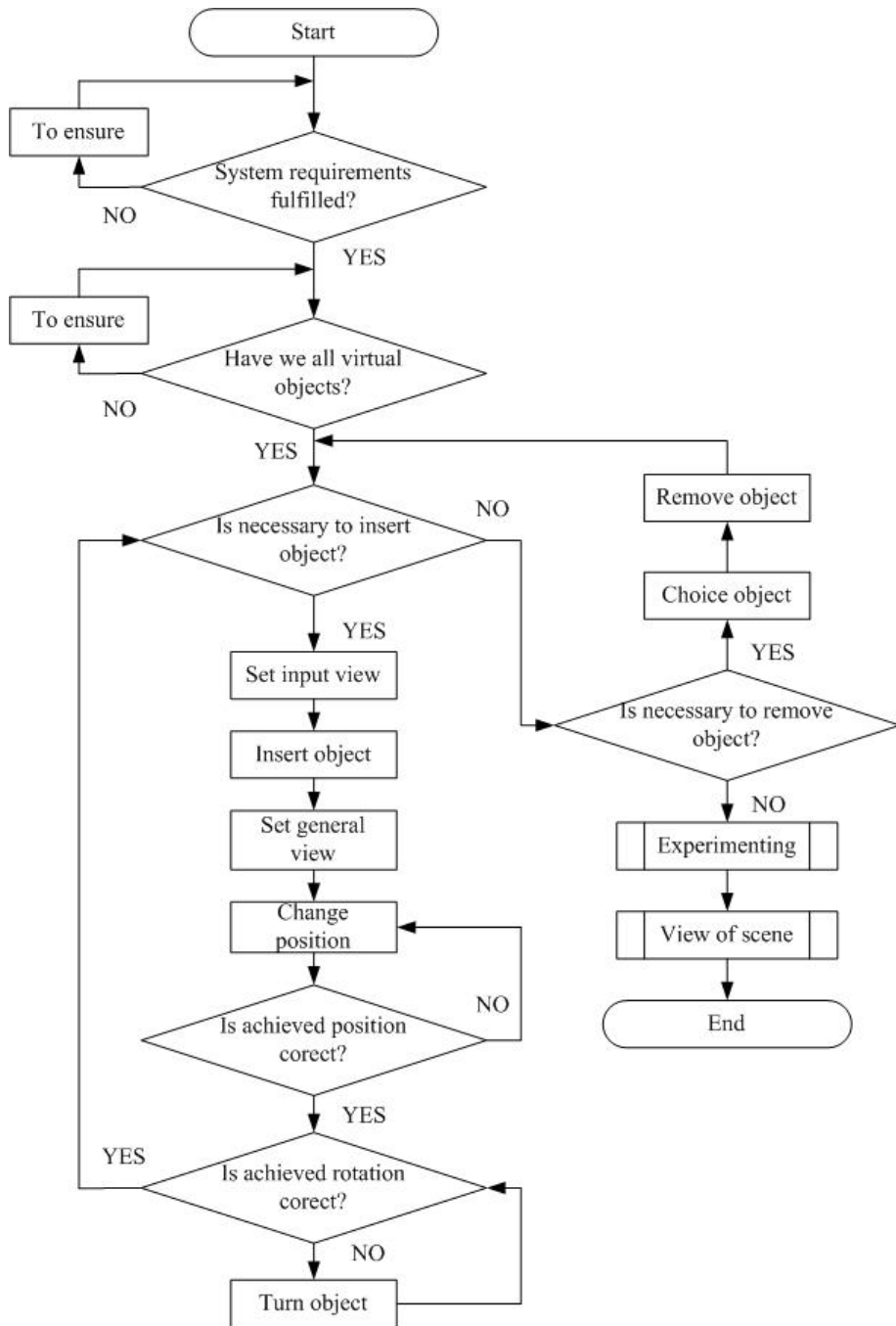


Fig. 9.4. Algorithm for building of virtual workplace in MSEVR environment

If we want to optimize the layout of machines is convenient to will be visualized some of them, because in real situation is not visible some spaces. Most of them are envelopes of machines, what is the reason how we can without any problems solve situation if are input / output places in its range. Visualized envelope is technically realized similarly as standard model, for example models of machines. Due to this we are able to their edit similarly as for standard models. Only different is their transparency set. It depends on the user, which invisible envelopes (in real situation) to display (in virtual reality) and for what purpose we use them. For us are preferred to display not only working envelopes, but also security zones and creating some fixtures to built virtual reality. MSEVR models have also dynamic characters. Working movement is animated, manually scheduled and controlled by program. All this cases were experimented. The use of dynamic properties allow to accurate optimization at layout of workplace. Fig. 9.5 shows virtual workplace built during development of MSEVR system. MSEVR system allows addition of modules, which brings some new properties, so it is possible to their adapt at however implementation, if is virtual reality deployed.



Fig. 9.5. Example of virtual workplace in MSEVR system

In its early it was tested to implementation in education process and optimized to automated and robotized systems. By most of verification experiments were confirmed our assumptions. In next we show our researched possibilities for MSEVR system:

- dispositional solution of workplace,
- use of animation on technological movements,
- use of visualization of security and technological envelopes,
- optimizing of robot trajectory for circumvent obstacles

Conclusions

Virtual laboratory brings virtual reality into education process, what changed to better quality. Its interactive components allow to teacher and students are active part same as persons in real practice. This form of education process is in maximum volume similarly to real situation, and all costs for its realisation are negligible in compare of real reality. Due to the fulfilment of targets, which were set before its design, still exist the scope for its next improvement. Here is also possibility to insert free available models from different internet sources. Their disadvantage is necessary adaptation for inserting to MSEVR system for more effectively way as its own creating, because some firms that produce industrial robots (for example, ABB, KUKA, MOTOMAN) provides 3D models their products as support for designers without any conditions.

This contribution is the result of project implementation: KEGA 047TUKE-4/2011 E-learning robotiky s implementáciou virtuálneho laboratória s diaľkovým riadením reálnych zariadení na báze internetu.

References

- [1] Baláž V., Vagaš M., Semjon J.: Využitie štruktúr informačných systémov pre pružné výrobné bunky – 2013. In: Atp journal plus 1/2013, p.42–44 ISSN 1336–5010.
- [2] Baláž V., Belovežčík A., Páchniková L.: Virtuálne laboratórium – Vitralab 2012. In: International Scientific Herald. Vol. 4, no. 23 (2012), p. 43–47. ISSN 2218–5348.
- [3] Belovežčík A.: Využitie virtualizačných prostriedkov pri projektovaní robotických pracovísk, Písomná práca k dizertačnej skúške, Košice, SjF, 2010
- [4] Craig A. B.: Understanding virtual reality, Morgan Kaufmann, p. 448, ISBN 978–0123749437, 2003.
- [5] Hajduk M.: Dva spôsoby spriahnutia vizuálny system robot 2011. In: Zborník príspevkov z 11. medzinárodnej konferencie ROBTEP 2011, Automatizácia / Robotika v teórii a praxi, p.87-90, ISBN: 978-80-553-0846-3.
- [6] Nieszporek T., Piotrowski A.: Parametric Programming of CNC Machine Tools – 2013. In: Applied Mechanics and Materials Vol.282, Robotics in Theory and Practice, p.203-210 ISSN 1660-9336.
- [7] Swic A., Zubrzycki J., Taranenko V.: Modelling and Systematic Analysis of Models of Dynamic Systems of Shaft Machining – 2013. In: Applied Mechanics and Materials Vol.282, Robotics in Theory and Practice, p.211–220 ISSN 1660-9336.
- [8] <http://www.parallelgraphics.com/products>
- [9] <http://wwwvrl.umich.edu/>
- [10] <http://www.web3d.org/x3d/specifications/>

Modular Training System In Virtual Reality Environment – MSEVR

Abstract: MSEVR is a system created for teaching of automated and robotic systems by means of new advanced teaching aids, including virtual reality. One of its constituents is also virtual laboratory that has been created as a specialized website. The presented paper acquaints with structure and performance of the virtual laboratory created by a work team at KVTaR Sjf TU at Košice. It is a laboratory that is segmented to a set of independent robots for learning basics of industrial robots and Modular system for experimentation in virtual reality. The Modular system has been designed for work with bigger, easily configurable workplaces.

Keywords: Automated and robotic system, robot, simulation, teaching, virtual reality

10. Stock price forecasting using collective intelligence

10.1 Introduction

Owning stocks is, without a doubt, one of the greatest tools ever invented for building wealth. Stocks are a part, if not the cornerstone, of nearly any investment portfolio.

Stock prices change every day as a result of market forces action. If more people want to buy a stock (demand) than sell it (supply), then the price moves up. Conversely, if more people wanted to sell a stock than buy it, there would be greater supply than demand, and the price would fall.

Understanding supply and demand is easy. What is difficult to comprehend is what makes people like a particular stock and dislike another stock. This comes down to figuring out what news is positive for a company and what news is negative. The principal theory is that the price movement of a stock indicates what investors feel a company is worth.

The most important factor that affects the value of a company is its **earnings**. Of course, it's not just earnings that can change the sentiment towards a stock. Literature [6] points on over 200 factors that may influence traders decision and in consequence stock prices. These factors range from economical and political, global and local situation, internal business environment, company's financial situation, its business and marketing strategy, possessed know-how and management forces.

Last but not least we need to consider all hardly measurable factors that influence traders decisions and in consequence stock price as professional analysis provided by experts, newspaper news, market trends, traders psychology and behavior – particularly so called psychology of crowd.

Nobody really knows for sure why do stock prices change. The only thing we do know is that stocks are volatile and can change in price rapidly.

10.2. Efficient Market Hypothesis

The main question contained in this article is whether stock prices are at all predictable? One common argument against the possibility of forecasting stock prices is the *Efficient Market Hypothesis* (EMH).

The EMH was developed in 1965 by Fama [7], and states that the current market price reflects the assimilation of all the information available. This means that given the information, no prediction of future changes in the price can be made. As new information enters the system the unbalanced state is immediately discovered and quickly eliminated by a correct change in market price. In the long run, a new

* Dr inż. Krzysztof Jędrzejek, e-Tower Group, 30-051 Kraków, ul. Urzędnicza 20/12, e-mail: kj@e-tower.pl

prediction technique becomes a part of the process to be predicted, i.e. it influences the process to be predicted. According to this point of view, if any method based on generally available information really worked then enough people would begin using it so that any advantage would disappear. The monopoly on "better prediction ability" will cease to exist [24].

In recent years, the philosophy of EMH has become controversial due to many reasons. Some researchers have pointed out that the very fact that traders are willing to pay for information indicates that markets cannot be informational efficient [10]. The most reasonable argument against the EMH deals with the different time perspectives different traders have when they do business [25]. For example, a majority stock owner will react quite differently than a floor trader when a stock suddenly drops in value. These differences in time perspectives will cause anomalies in the market prices even if no new information has entered the scene. It may be possible to identify these situations and actually predict future changes.

Most arguments against the EMH refer to a time delay between the point when new information enters the system and the point when the information has been assimilated globally and a new equilibrium with a new market price has been reached. Viewed this way, the controversy is only a matter of how the word immediately in the EMH definition should be interpreted.

Presented above arguments against EMH convince us that under certain conditions, when we consider behavior of investors, social networking and wisdom of crowds it is possible to develop efficient forecasting method.

10.3. Stock price forecasting

There are two major types of analysis for predicting stock prices: fundamental and technical.

Fundamental analysis of a company is the examination of underlying forces that affect the well-being of the company. It involves the examination of financial data in order to derive the current fair value of a company's stock. The fundamental analysis measures the intrinsic value of a particular stock by studying everything from the overall economy and industry conditions, to the financial condition and management of companies [1]. It uses revenues, earnings, future growth, return on equity, profit margins, and other data to determine a company's underlying value and potential for future growth. Fundamental analysis is mainly used for long-term (months, even years) stock analysis.

A significant body of research has shown that various valuation and financial statement indicators predict subsequent returns. In [14] authors show that valuation factors, such as P/E ratio and B/M ratio predict future returns, other research [22] documents a strong association between accruals and future returns or claim that information contained in fundamental analysis is related to both future earnings and returns. These studies argue that investors can earn "abnormal" returns by trading on various signals of financial performance, as the market fails to fully incorporate the information in historical financial data into

prices in a timely manner. Moreover, a significant portion of investors' focus is on short-term, recurring gains, for which fundamental analysis is not necessary.

Whilst fundamental analysis involves analyzing the characteristics of a company in order to estimate its value, technical analysis takes a completely different approach. Technical analysis is a method of evaluating stocks by analyzing statistics generated by market activity, past prices, and volume. It looks for peaks, bottoms, trends, patterns, and other factors affecting a stock's price movement. Technical analysis helps to visualize and anticipate the future trend of the stock market and is suitable for short-term (days or weeks) analysis [20]. The field of technical analysis is based on the assumptions that at any given time, a stock's price reflects everything that could affect the company – including fundamental factors and price movements [4]. Technical analysis believes, that stock price follows trends and that history tends to repeat itself, mainly in terms of price movement. The odds of an indicator based predicting future stock price turns out to be not much better than a coin flip over time as most indicators are built on a single set of data – the price [12].

In this paper we consider short term stock price forecasting. Regardless of technical analysis approaches, there are many different methods and tools, mainly for short-term prediction of stock market behavior.

Stock markets are complex, nonlinear, and dynamic [27]. Traditionally, forecasting research and practice had been dominated by statistical methods [18] and regression analysis [4]. Other methods include, ARIMA, Box-Jenkins and stochastic models take as input huge amounts of numeric time series data to find a model extrapolating the financial markets into the future [21]. Some promising results were achieved by Group Model of Data Handling algorithms that give possibility to find automatically interrelations in data and to select optimal structure of financial models [16].

The domain of financial time series prediction is a highly complicated task because financial time series often behave nearly like a random-walk process, i.e. statistical properties of the time series are different at different points in time and are usually very noisy, with a large amount of random variations [17].

The use of artificial intelligence had made a big influence on the forecasting and investment decision-making technologies and it was proved that some efficient results can be obtained [19]. Artificial neural networks (ANNs) have been successfully applied in time-series problems to improve multivariate prediction ability [26]. In the comparison with conventional statistic tools the main advantages of ANNs are that they are able to learn to recognize patterns in the data set, they are flexible in changing environments and they can build models when more conventional approaches fail [5].

ANNs have good generalization capabilities by mapping input values and output values of given patterns. They are usually robust against noisy or missing data, all of which are highly desirable properties in time series prediction problems.

Undoubtedly being much more powerful than traditional time series processing techniques, ANNs have several disadvantages from their complexity and a more difficult testability as ANNs require very large number of previous cases and for more complicated networks, reliability of results may decrease. Last but not least, there is also a problem of interpretability of the results produced by ANNs [19]. To conclude, the potentially superior predictive power of ANNs can be exploited only if specific properties of the time series data are accounted for by means of appropriate pre- and post- processing mechanisms.

The main disadvantage of both statistical and AI methods are that they analyze numerical, historical data not taking into account investors' behavior in making trade decisions and daily news about company and business environmental situation.

10.4. Investor psychology and human interaction in forecasting process

There is a growing body of evidence that the key to forecasting the stock market lies neither in value analysis nor in technical analysis. Rather, investor psychology seems to be the critical factor. This, so called behavioral finance, was a subject of various research [9].

Instead of treating investor psychology as noise, we should recognize that it is actually the signal that drives much of the day-to-day price fluctuations. In fact, when researchers have conducted experimental studies of investors, they find that people do not seem to take a random walk down Wall Street. Instead they behave in predictable ways, which can be captured by models that incorporate psychological assumptions [3].

People tends to expect rising prices, miss price jumps, and learn from experience. Apparently, over time, people forget that crashes can happen and eventually get carried away with "irrational exuberance". The question is if there is a way to instantly gather and synthesize all of the complex variables that comprise investor psychology, and then distil them into a single number – a forecast of a future stock price.

In fact, each individual investor is doing exactly such a synthesis in his own brain before making an investment decision. However, the synthesis is imperfect in large measure, because no investor has access to all relevant information, no investor has the brainpower to process all information rapidly enough to make optimal decisions, and individual investors make mistakes in judgment.

All these shortcomings might be overcome by groups. Groups, collectively, have access to more information than an individual does, have the brainpower to process much more information than an individual can and generally have better judgment than a single individual.

Many people emphasize the aspect of social networking. With more than a billion individuals around the world connected by a new multimedia high – bandwidth medium of human communications, collaboration and teamwork have become the business world's biggest drivers of success.

With than many brains the transformation forged by the Internet has morphed from quantitative to qualitative. The new and potent “We” is smarter than any singular “Me”. For the first time, humans can act in mass collaboration, using the kind of collective intelligence. The result is a quantum increase in the world’s ability to conceive, create, compute and connect.

10.5. Methodology

10.5.1. Collective Intelligence

The processes that a human trader executes when making prediction about the future convince us that human factor in stock price prediction is remarkable. Firstly, a human trader is able to process newspaper articles, news related to the company or industry of interest, and other external information which in most cases is available in form of text. Secondly, a human trader has a profound economic education, which allows him to extract important causal connections (patterns) in the information he receives. Thirdly, a human trader has a long experience as trader. This means that through long experience he learned certain general rules using which he manages to make decision even with incomplete or false information at hand. Fourthly, a human trader has powerful statistics software at hand, which allows him to develop an understanding of current market situation from the statistician’s point of view. Since human species usually work in teams and the work of one person is often verified by other team members, it can be assumed that most random mistakes are ruled out provided that the team as a whole works efficiently. This is the fifth feature of a human trader. The proposed in this paper forecasting method mimics most of these features.

The collective intelligence methods that will be used here arise from several different traditions concerning the facilitation of citizen participation, the study of social groups, the use and development of survey methods, and investigation of the new possibilities provided by the Internet [11].

There are a variety of techniques for analyzing information about the beliefs or opinions of a social group, organization, or community. Much of the knowledge in these networks is tacit, as no individual in the group is aware of its shared global structure.

This tacit knowledge enables groups to solve much more complex problems than individuals could solve on their own. The study of semantic networks dates back to the networks form the core of most expert systems and traditional artificial intelligence applications [2]. And new ways to use the Internet to examine the structure of communities are being continuously developed [11].

The Internet is changing the way all kinds of social groups deal with the critical issues that they face. The Internet is a medium of human information exchange with enormous depth and breadth. Its depth consists in capturing the full complexity of human use and creation of information and knowledge, and its breadth consists in its integration of machines, information, and people.

When the full diversity of the society's intellectual dynamics is combined with the Internet's ability to quickly and accurately link information, large groups can quickly and efficiently pool their resources and coherently analyze issue complexes that were very difficult to cope with in other ways [11].

The social psychology literature offers a number of empirical studies demonstrating the phenomenon of Collective Intelligence CI [11,13,15]. Results in these studies generally indicate that group solutions are at least as good as the average quality of individuals' solutions.

From many definitions of CI available it follows that at the best the CI may be defined as: *The group of independent people, who act through collaboration and/or competition for their individual goals, but whose group actions may result in a higher than any member of the group ability to solve problems for benefit of the community.*

In this paper we consider the problem how to use CI for effective stock prices forecasting. Our main aim is designing of a CI system that makes stock forecasting based on investor group input with better accuracy that results obtained by investing in major stock indices. Through a series of experiments we are going to prove the following two hypotheses:

- the CI system used for stock prices forecast outperforms results of major stock indices (i.e. investment based on CI system leads to greater revenue that investing in stock index),
- the overall performance of the group decision is better that the performance of any CI group member.
- Having in mind EMH, in our approach we assume that:
- our forecasting method is available to limited number of individuals so that their trading cannot influence significantly stock price,
- all individuals participating in the test have an access to sufficient market information.

10.5.2. User collaboration methods

There are several methods using collaboration of group of people to make decisions, to find optimal problems' solutions or to predict events. The most important are: unstructured face-to-face meetings, the nominal group technique, Delphi method and prediction markets. We will try to show the difference between these methods and our, based on CI approach.

Unstructured face-to-face meetings (FTF) allow any form of direct interaction between group members. Although meetings are most common for group decision-making in organizations, they have been shown to be subject to many biases and drawbacks [8]:

- groups tend to aim to reach 'speedy decisions' and do not consider all problem dimensions, and thus tend to pursue a limited train of thought, which leads to so called 'groupthink',

- less confident group members, may keep silent about their reservations because of either group pressures for conformity or implied threats of sanctions,
- dominant personalities tend to exert an excessive amount of influence on the group.

Nominal group technique (NGT) tries to avoid some of the drawbacks of FTF by adding a structured format to the direct interactions. This process is conducted in three steps. First, group members work independently to generate individual estimates for a problem. Then, the group enters an unstructured discussion to deliberate on the problem. Finally, the group members again work independently to provide their final individual estimates. The group result is the aggregated outcome of these final individual estimates. The idea of NGT is that direct interactions during the assessment or evaluation phase can have a positive impact on estimation or problem solving [8].

Delphi method (DM) is a multiple-round survey in which the participants anonymously reveal their individual estimates and provide comments on a problem. After each round, the individual estimates and comments are summarized and reported to the participants as feedback. Taking this information into account, the participants then provide their new estimate in the following round. The group result is the aggregated outcome of the individual estimates of the final round. Unlike FTF and NGT, which require the physical proximity of the group members, the participants in DM are physically dispersed and do not meet in person. In general, DM functions somewhat similarly to NGT. The main difference is that written interactions are utilized throughout the process, in order to avoid direct interactions between the group members. The strengths of the method are seen in its structured communication process, which enables discussion and helps groups to achieve a consensus, but limits the drawbacks associated with direct interactions [8].

Prediction markets (PM) are gaining attention in various fields of forecasting. The idea is to set up a contract whose payoff depends on the outcome of an uncertain future event. This contract, which can be interpreted as a bet on the outcome of the underlying future event, can then be traded by participants. As soon as the outcome is known, the participants are paid off in exchange for the contracts they hold. Based on their individual performances, participants can win money. If one thinks that the current group estimate is too low (high), one will buy (sell) stocks. Thus, through the prospect of gaining money, the participants have an incentive to become active in the group process whenever they expect the group estimate to be inaccurate. As in DM, the participants are mutually anonymous, and thus are not subject to the social pressures connected with direct interactions. The main difference is that the participants exchange information continuously through the price signal of the market, but do not share comments or reasons as to why they buy or sell a contract [26]. The disadvantage of this method lies in the fact that its members meet only their goals and are not paying attention on the group objective.

The main difference between the method based on CI, and presented NTG, PM, FTF and DM approaches follows from conditions that characterize CI [23]:

- diversity of opinion – each person should have some private information,
- independence – people’s opinions are not determined by the opinions of those around them,
- aggregation – some mechanism exists for turning private judgments into a collective decision.

The CI approach eliminates the disadvantages of the previous methods, mainly resulting from the communication between the members, the impact of the stronger on the weaker members of the group and subjective determination of the final result by a single person or group of people.

10.6. Methodology and experiment

10.6.1. Experiment principle

In order to develop CI system and for the purpose of checking its operation we assumed that:

- we can gather together CI members who are not necessarily professional investors but at least they possess some experience in stock trading,
- members will participate in forecast of selected stock portfolio, day-by-day within assumed testing period.

We addressed our method not only to professionals but also individuals who claimed themselves as occasional investors. Our reasoning was that if we could get results by tapping the collective intelligence of members of the general population, then the results would only get better if we tapped selected stock trading professionals only.

To analyze CI performance the main question is to compare CI results to some existing performance indicators. Therefore, the following CI performance models have been tested:

- Predicting of the value of WIG20, index of top 20 Polish companies. Prediction quality of our CI method, seen as investment return based on CI algorithm was compared to investment return based on WIG20 index,
- Predicting of the stock price of companies selected from top 20 Polish companies. Prediction results of CI method were compared to WIG20 index and indices of selected companies.

In our CI method we assumed that forecasters did not exchange information with each other before making forecast and they have access to all information available. Test participants have been recruited from users who were identified as stock investors in Polish internet portal user database. Throughout the test we were communicating with participants through the developed for experiment purposes website. We registered 1959 traders willing to participate in the experiment. According to their declarative personal data they were representing

experienced individual investors (1091 persons), occasional investors (670 persons), professional investors (137 persons), financial analysts (61 persons).

10.6.2. Algorithm

For an experiment we selected group of active investors (197 individuals) that were able to trade for selected stock continuously for 23 trading days. Our system weighted each individual's forecast accordingly to the past track record of forecasts. The collective forecast was calculated based on weighted average of all forecasts. Here is how it works.

Let the set of forecasts $[x_1, x_2, \dots, x_n]$ has wages $[w_1, w_2, \dots, w_n] > 0$ then the waged average forecast is equal to:

$$\bar{x} = \frac{\sum_{i=1}^n w_i x_i}{\sum_{i=1}^n w_i} \quad (10.1)$$

Weights of individual predictions were calculated as follows:

- if the participant correctly estimated the trend of the stock price, and the projected stock price did not exceed the real stock price then the weight of the next prediction was increased by 0.1 for each 10% of the difference between the forecasted and real stock price,
- if the participant correctly estimated the trend of the stock price, but the estimated share price exceeded the real share price then the weight for the next prediction was reduced by 0.05 for every 10% difference between the forecasted and real stock price,
- if the participant incorrectly estimated the trend in the stock price then the weight for the next prediction was reduced by 0.1 for each 10% difference between the forecasted and real stock price.

The test period was scheduled for 23 consecutive trading days. Due to relatively small number of active investors (197 persons were trading day by day) we requested them to trade only for 3 stocks from WIG20 companies – TVN, PKOBP and PKN ORLEN, representing media, banking and oil sectors.

Here is how the CI system operated during the test. As individuals entered their stock forecasts, the system processed these and generated collective forecasts. Each collective forecast represented the processed intelligence of all individuals regarding the closing price of a particular stock the next day. For example, the collective forecast, TVN 24.25, means that based on the input of all individual forecasts for TVN, the system has produced a single collective forecast that TVN will close at 24.25 the next day.

Each day, just before the market closed, we simulated trading on all available collective forecasts for the next day and offered it for all participants.

10.6.3. Experiment results

Our first hypothesis was that the results obtained by the CI system would be better than WIG 20 index. We compared the actual return that would have been generated by trading on the system's collective forecasts with the actual return that would have been generated by investing in the WIG20 stock indices at the beginning of trade. The results of this comparison are shown of Fig. 10.1.

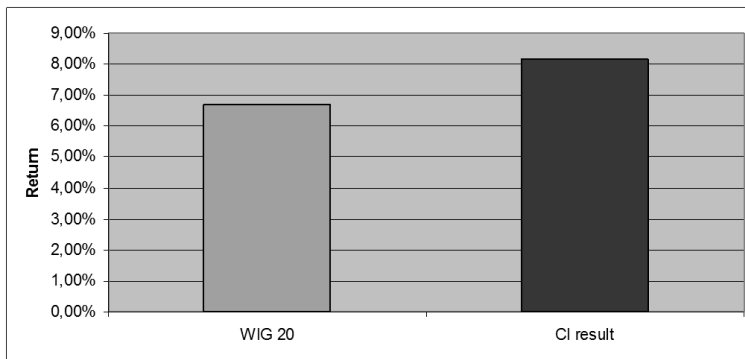


Figure 10.1: WIG20 vs. CI forecast

The CI system received 8,15 % return during the twenty three trading day period whilst the WIG20 received 6,69% return. The CI system outperformed the WIG20 stock index by 21,82%. It was possible to get better profit if investing (buying stock at the beginning of experiment and selling at the end of experiment) only in TVN stock (15,47% return) but it is worthy to note that investing equally in TVN, PKO, ORLEN portfolio lead to return of 7,03% what gave worse result than that given by CI system.

It is also worthy to mention that within the testing period while CI system achieved 8,15% investment return, the best individual performed at the level of 6,9% investment return. Considering daily forecasting for 23 days CI algorithm outperformed the best individual forecast by 18%. CI algorithm also proved its performance for each of selected stock (see Fig. 10.2) performing better by 14,09%, 12,88% and 24,37% for TVN, PKOBP and PKN ORLEN respectively.

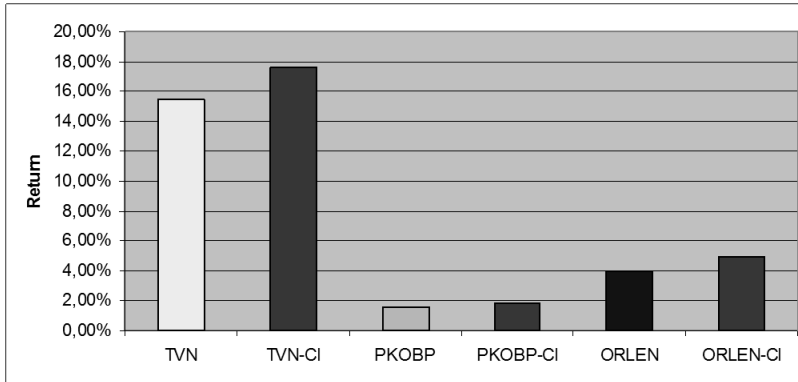


Figure10.2. CI forecast performance for each selected in experiment stock

If collective intelligence is responsible for the better performance of the system, then as more people use the system it should perform better. The best way to test this hypothesis would be to run a follow-up test with a very large number of participants to see if the CI system performs even better.

Due to limited number of experiment participants we divided all collective forecasts into three groups – first group counted up to 50 individual forecasts (Low CI), second group counted from 51 to 100 individual forecasts (Mid CI), and third group counted from 101 to 150 forecasts (High CI) within experiment period (groups were selected randomly). We then compared the return made by collective forecasts by all groups (All).

In Fig. 10.3 we can see that when the system’s collective predictions were based on more forecasts, the result was more accurate, i.e. led to higher investment return.

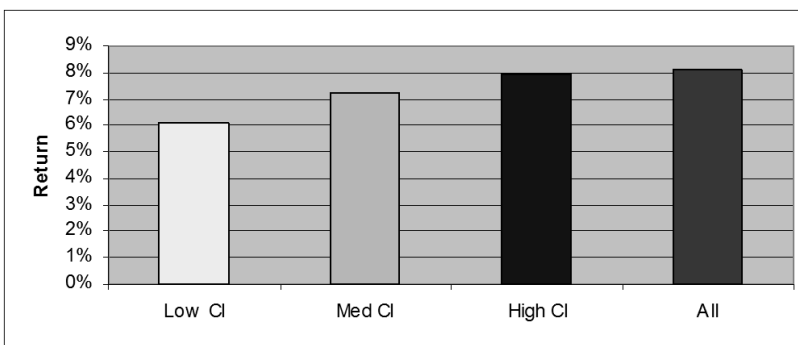


Figure10.3. Return results by no of individual forecasts

Conclusions

We proved that under the right circumstances, groups are remarkably intelligent, and often smarter than the smartest people in them. Groups do not need to be dominated by exceptionally intelligent people in order to be smart. Even if most of the people within a group are not especially well-informed or rational, it can still reach the collective wise decisions.

Our results stand in opposition with Efficient Market Hypothesis and gave examples against perfect market. Human beings don't have complete information. They have private, limited information. It may be valuable information and it may be accurate, useless or false, but it is always partial. Human beings are not perfectly rational either. They may want, for the most part, to maximize their self-interest, but they are not always sure how to do that, and they're often willing to settle for less-than-perfect outcomes.

It was shown that CI method is well suited and accurate for stock price forecasting. The important question about accuracy of the market's forecast is of course, "is accurate compared to what?". We proved in this paper that the CI prediction result outperformed WIG20 stock index.

We demonstrated that CI results in better forecast than any individual member of the group can produce and that performance of the group is proportional to the number of participants.

CI system used for stock price forecasting has one disadvantage. It is suitable for "next day" forecast while most of now-a-days stock trading is executed several times a day, immediately after trader discovers signal about possible stock price movement.

The proposed CI system might be improved. For CI the important factor that takes a lot of effort is to build a community. The whole point of crowd sourcing is to access fresh, powerful ideas and instinct from community. It is extremely important how the group of individuals is selected and how are their results managed. The community must be large and smart enough to ride herd on the content it produces, catching and correcting mistakes as they occur. The bigger the collective brain, the greater the variety of viewpoints and information. Since the members of the communities are sharing themselves and their talents, they deserve acknowledgment and reward to keep them working for the group. Also the method of reducing so-called flammers, who seek to entertain themselves by creating trouble must be improved.

There is also room for CI algorithm improvement – at least different weighting system should be tested.

The following CI models should be subject of further research:

- CI where participants communicate/cooperate while making a decision,
- CI where there exist a hierarchy with decision making, i.e. some managers in the hierarchy decide what prediction goes to the next level in prediction tree,
- CI when participants make decisions only based on selected set of data.

The CI method presented in this paper has proved its power in stock price forecasting and it does not raise a big surprise that similar methods have found its application in commercial systems, e.g. www.marketocracy.com (farm of analysts), www.predictwallstreet.com (stock price prediction system), www.mystock.pl (Polish investor community).

References

- [1] Abarbanell J.S., Bushee B. J.: Abnormal Returns to a Fundamental Analysis Strategy. *The Accounting Review*, Vol. 73, No 1, 1998, pp. 19–45.
- [2] Andreassen P.: On the Social Psychology of the Stock Market: Aggregate Attributional Effect and the Regressiveness of Predictions. *Journal of Personality AND Social Psychology*, Vol. 53, 1987, pp. 490–498.
- [3] Caginalp G., Porter D., Smith V. L.: Overreactions, Momentum, Liquidity, and Price Bubbles in Laboratory and Field Asset Markets. *The Journal of Psychology and Financial Markets*, Vol. 1, No. 1, 2000, pp. 24–28.
- [4] Colby R. W., Thomas A.: *The Encyclopedia of Technical Market Indicators*. Dow Jones-Irwin, Homewood, IL, 1988.
- [5] Dorffner G.: Neural networks for time series processing. *Neural Network World*, Vol. 6, No 4, 1996, pp. 447–468.
- [6] Fabozzi F.J., Modigliani F.: *Capital Markets: Institutions and Instruments*. Prentice Hall International, New Jersey, 1992.
- [7] Fama E. F.: Efficient capital markets. *The Journal of Finance*, Vol. 46, No 5, 1991, pp. 1575–1617.
- [8] Graefea A., Armstrong J, S.: Comparing face-to-face meetings, nominal groups, Delphi and prediction markets on an estimation task. *International Journal of Forecasting*, No 27, 2011, pp. 183–195.
- [9] Granovetter M.: Threshold Models of Collective Behaviour, *American Journal of Sociology*, Vol. 83, 1978, pp. 1420–43.
- [10] Grossman S., Stiglitz J.: On the Impossibility of Informationally Efficient Markets. *American Economic Review*, Vol. 70, 1980, pp. 393–407.
- [11] Heylighen F.: Collective intelligence and its implementation on the Web: algorithms to develop a collective mental map. *Computational & Mathematical Organization Theory*, Kluwer Academic Publishers, Vol.5, No 3, 1999, pp. 253–80.
- [12] Irwin S. H., Park Cheol-Ho.: What Do We Know About the Profitability of Technical Analysis?. *Journal of Economic Surveys*, Vol. 21, No. 4, 2007, pp. 786–826.
- [13] Kaplan C. A: *Tomorrow Ticker: A System for Using Collective Intelligence to Forecast Future Values of Financial or Other Quantifiable Information*, USPTO, 2001.
- [14] Lakonishok J., Shleifer A., Vishny R.: Contrarian investment, extrapolation, and risk, *Journal of Finance*, Vol. 49, 1994, pp. 1541–1578.

- [15] Libert B., Spector J.: We are smarter than me. How to unleash the power of crowds. Wharton School Publishing, 2007.
- [16] Madala H.R., Ivakhnenko A.G.: Inductive Learning Algorithms for Complex System Modeling. CRC Press, 1994.
- [17] Magdon-Ismael M., Nicholson A., Abu-Mustafa Y. S.: Financial Markets: Very Noisy Information Processing. Proceedings of the IEEE, Vol. 80, No 11, 1998.
- [18] Nazmi N.: Forecasting Cyclical Turning Points with an Index of Leading Indicators: A Probabilistic Approach. Journal of Forecasting, Vol.12, No 3&4, 1993, pp. 216–226.
- [19] Pavlidis N.G., Tasoulis D., Vrahatis M.N.: Financial Forecasting Through Unsupervised Clustering and Evolutionary Trained Neural Networks, 2003 Congress on Evolutionary Computation, Canberra Australia, 2003.
- [20] Pring M. J.: Technical Analysis Explained. McGraw-Hill, 1991.
- [21] Reynolds S.B. and Maxwell A.: Box-Jenkins Forecast Model Identification. AI Expert, Vol. 10, No 6, 1995, pp. 15–28.
- [22] Sloan R. G.: Do stock prices fully reflect information in accruals and cash flows about future earnings?. The Accounting Review, Vol. 71, 1996, pp. 289–315.
- [23] Surowiecki J.: The Wisdom of Crowds, Random House, 2004.
- [24] Swingler K.: Financial prediction, some pointers, pitfalls, and common errors. John Wiley and Sons, 1994.
- [25] Tsibouris G., Zeidenberg M.: Testing the efficient market hypothesis with gradient descent algorithms. In Refenes, A. editor: Neural Networks in the Capital Markets. John Wiley and Sons, 1995.
- [26] Versace M., Bhatt R., Hinds O., Shiffer M.: Predicting the exchange traded fund DIA with a combination of genetic algorithms and neural networks. Expert Systems with applications, Elsevier, 2004.
- [27] Yoon Y., Swales G.: Predicting stock price performance. Proceeding of the 24th Hawaii International Conference on System Sciences, Vol. 4, 1997, pp. 156–162.

Stock price forecasting using collective intelligence

Abstract: In this paper we consider the problem of predicting stock prices. In contrast to the existing methods for predicting stock prices that use past figures, patterns and trends, we propose method that is based on the use of non-numerical factors that influence the price of shares, as investors' knowledge, insight, and their assessment of the market behavior. We argue that, contrary to the theory of Efficient Market Hypothesis, which involves the inability to effectively predict stock prices, it is possible to predict stock prices using a methodology based on the wisdom of crowds. For this purpose, we have developed a system of forecasting stock prices that uses Collective Intelligence (CI), where the stock price is calculated as the resultant estimates of investors participating in CI system.

Based on a series of experiments conducted on the Warsaw Stock Exchange we have shown that the quality of CI prediction exceeded the results offered by the stock market index, and that the results achieved by CI are better than the results of individual people involved in the experiment. We also demonstrated that the performance of the system CI system increases with the number of CI members.

The results look promising and will be the basis for further work on the use of CI systems, not only in predicting stock prices, but also in predicting the phenomena in other areas

Keywords: stock price forecasting, collective intelligence, social networking, behavioral finance, efficient market hypothesis

Prognozowanie cen akcji giełdowych przy wykorzystaniu zbiorowej inteligencji

Streszczenie: Przedmiotem badań jest tutaj problem przewidywania cen akcji giełdowych. W przeciwieństwie do istniejących metod prognozowania, które używają historycznych danych, wzorców i trendów proponujemy metodę, która jest oparta na wykorzystaniu czynników wpływających na cenę akcji, które nie dają się wyrazić ilościowo ponieważ obejmują wiedzę inwestorów, ich intuicję i subiektywne oceny zachowanie rynku.

W artykule polemizujemy z teorią o rynkach efektywnych, mówiącą, że w dłuższym okresie czasu nie istnieją efektywne metody prognozowania cen aukcji giełdowych. W tym celu opracowaliśmy system prognozowania cen akcji, który wykorzystuje zbiorową inteligencję (ZI), gdzie prognoza ceny akcji jest wypadkową szacunków wszystkich inwestorów prognozujących ceny akcji w oparciu o system ZI. Na podstawie serii eksperymentów przeprowadzonych na GPW w Warszawie pokazaliśmy, że trafność prognoz systemu ZI jest lepsza niż wyniki oferowane przy inwestowaniu opartym o indeksy giełdowe oraz, że wyniki osiągnane przez ZI są lepsze od wyników poszczególnych osób biorących udział w eksperymencie. Wykazano również, że skuteczność systemu ZI wzrasta wraz z liczbą uczestników ZI.

Rezultaty badań będą podstawą do dalszych prac nad wykorzystaniem systemów ZI, nie tylko do przewidywania cen akcji, ale także do prognozowania zjawisk w innych dziedzinach

Słowa kluczowe: prognozowanie cen akcji, zbiorowa inteligencja, sieci społecznościowe, finanse behawioralne, hipoteza rynku efektywnego

11. Automation of shafts machining about low rigidity

Introduction

Methods of building mathematical model (MM) of the control object significantly depends on the capacity of apriorical information available from the moment of starting investigating of the given object. Task of developing a model can be realized in two stages. In the first stage, basing on this apriorical information regarding physical processes occurring in technological process, structure of the object is developed. Usually, this model includes unknown parameters, which are hard or impossible to be found basing on apriorical data. Initial structural model can contain certain elements that are not necessary in next stages of MM development. During second stage, basing on the experimental tests, unknown parameters are defined and model structure is improved. In many cases it is possible to simplify initial model structure. Dynamic system (UD) of the machining process is a Technological system (UT) – OUPN i.e. machine tool with realized technological process (UT) of the turning processing.

11.1. Identification of dynamic system of cutting processing for shafts with control realized using longitudinal feed

Basic goal of developing model of turning process in designing control system is minimization of measurement-shape errors of the machined tools. Taking into account the fact, that main cause of these errors in case of longitudinal turning is elastic deformation of the technological system and due to functional dependence of cutting force, these parameters are to be considered as input values of controlling object (OS).

Turning process is nonlinear. However, due to assumed use of the model to control and, in particular, to realize a task of stabilizing cutting forces in time (where output variables change slightly) one can linearize nonlinear dependencies near statistic point of operation.

Basing on the analysis of cutting layer geometry, cutting forces, elastic properties, technological system and process of forming section area of cut surface with taking into account phenomenon of cutting “along trace”, a system of dependencies in an operator form describing dynamic features of the machining process is obtained (Fig. 11.1) [1,2].

* dr inż. Jarosław Zubrzycki, Instytut Technologicznych Systemów Informacyjnych, Wydział Mechaniczny, Politechnika Lubelska, 20-618 Lublin, ul. Nadbystrzycka 36, tel. (81)5384585, e-mail: j.zubrzycki@pollub.pl

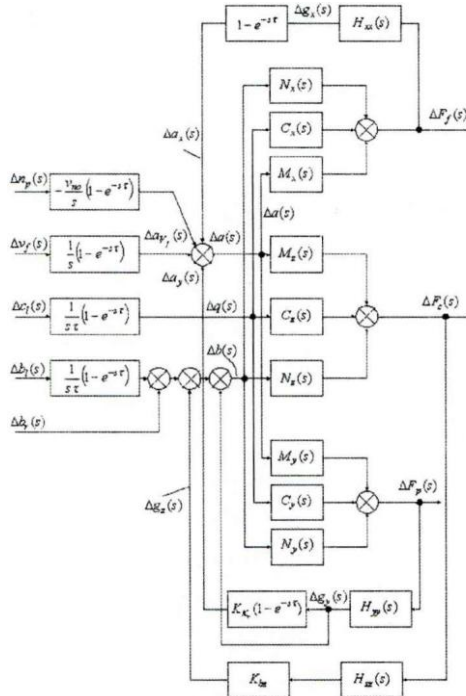


Fig. 11.1. Output structural diagram of the control object

In turning process influence of machining traces on the process course is characteristic – it is so called cutting “along trace”. It occurs since the parameters of cut metal layer in a moment t are determined both by instantaneous position of the edge and both by its coordinates in a moment of previous rotation of parts $t-\tau$, i.e. in a moment delayed by time of one rotation.

Denotation of variables on the structural diagram are: s – Laplace transformation operator, F_f – feeding component of cutting force, F_c – main component, F_r – radial component, n_{cz} – rotational speed of the speed part, v_r – speed of longitudinal feed, c_1 – material hardness, b_1 – processing allowance, $\tau=1/n_{cz}$ – delay.

Relations between value of elastic deformation and components of cutting forces in the operator form are described with linearized equations:

$$\Delta g_i(s) = \Delta H_i(s) \Delta H_i(s), i = \{x, y, z\}, \quad (11.1)$$

After taking into account that time constants of chip formation for different components of cutting forces do not differ much, we can assume:

$$M_x(s) N_x(s) = M_y(s) N_y(s). \quad (11.2)$$

Using above equations, a function of object transition (after transformations) can be written for i -th component of cutting force in a following form:

$$G_{v_f F_i}(s) = \frac{M_i(s)G_\tau(s)}{s[1 + N_y(s)H_{yy}(s) + G_\tau(s)[M_x(s)H_{xx}(s) + K_k M_y(s)H_{yy}(s)]]} \quad (11.3)$$

Assuming transition function of chip forming process in a form of non-periodic element with time constant T_c and assuming oscillating secondary element with constant T_{us} and attenuation coefficient ξ as a model of dynamic properties of control system we get:

$$G_{v_f g_i}(s) = \frac{m_x(s)G_\tau(s)}{s[(T_c s + 1)(T_{us} s^2 + 2\xi T_{us} s + 1) + B_1 G_\tau(s) + n_y h_{yy}] \quad (11.4)$$

or, after taking into equation (11.1):

$$G_{v_f g_i}(s) = \frac{m_x h_{xx}(s)G_\tau(s)}{s[(T_c s + 1)(T_{us} s^2 + 2\xi T_{us} s + 1) + B_1 G_\tau(s) + n_y h_{yy}] \quad (11.5)$$

Due to the above, forming process of cut layer section is significantly affected by cutting “along trace” and by elastic deformation of the technological system. Process of forming section of cut layer can be described by a system of integral-differential equations with delayed argument. The variables characterizing section of cut layer depend on input variables and elastic deformations of the technological system.

11.2. Output mathematical model

Controlling activity, in a form of longitudinal feed, is used in the most effective way to optimize the processes of machining the parts with relatively high rigidity. Preliminary analysis shows that in this case one can take into account only own susceptibilities of the elements of technological system.

According to the set of equations [1] and equations (11.2-11.4) the output diagram of the structure of control object can be presented in a form like in Fig. 1. It shows that current value of thickness of the section and its increment are determined by three components:

$$\Delta a(s) = \Delta a_{v_f}(s) - \Delta a_x(s) - \Delta a_y(s)$$

where: Δa_{v_f} - a component that depends on the speed of longitudinal feed (width of the section of cut layer without taking into account elastic deformations), Δa_x and Δa_y - components conditioned by elastic deformations for X and Y coordinates.

Increment of a current value of section width depends on elastic deformations of the technological system for Y and Z coordinates.

In that way, in case of the considered MM it is characterized by the presence of internal closed circuits in its structure – they are conditioned by an influence of the elastic deformations on the elements of the section of cut layer and singularities of cutting “along trace”.

In the further analysis influence of elastic deformations for Z coordinate on the width of a section as insignificant. Considered structure can be transformed assuming speed of longitudinal feed as input value. Resulting form is shown in Fig. 11.2.

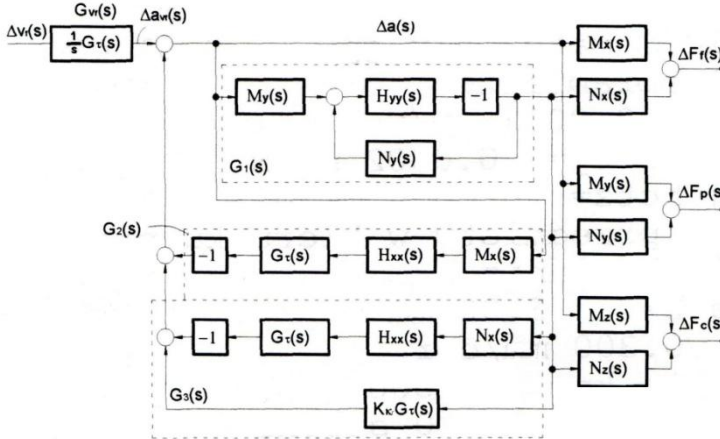


Fig. 11.2. Structural diagram of the control object

Equivalent transition functions marked in Fig. 11.2 as $G_1(s)$, $G_2(s)$, $G_3(s)$ are equal to:

$$G_1(s) = -M_y(s) \frac{H_{yy}(s)}{1 + N_y(s)H_{yy}(s)}, \quad (11.6)$$

$$G_2(s) = -G_\tau(s)M_x(s)H_{xx}(s), \quad (11.7)$$

$$G_3(s) = G_\tau(s)[K_{\kappa_r} - N_x(s)H_{xx}(s)]. \quad (11.8)$$

Transition function for the components of cutting forces, e.g. F_f :

$$G_{v_f F_x}(s) = \frac{\Delta F_f(s)}{\Delta v_f(s)} = \frac{G_\tau(s)[M_x(x) + G_1(s)N_x(s)]}{s[1 - G_{sz}(s)]} \quad (11.9)$$

The following diagram of indices has been assumed for (here and later) denoting coefficients of gain and transition functions. First letter index indicate input coefficient (in the given case v_f), second – output value (F – cutting force, g – elastic deformation), third (if necessary) shows component of a cutting force or elastic deformation $i=\{x,y,z\}$. Transforming dependency for $G_{v_f g_i}(s)$. and applying the last expression for its denominator, we obtain:

$$G_{v_f g_i}(s) = \frac{m_x h_{xx} G_\tau(s)}{s[(T_c s + 1)(T_{us}^2 s^2 + 2\xi T_{us} s + 1) + B_1 G_\tau(s) + n_y h_{yy}]} \quad (11.10)$$

where $B_1 = m_x h_x + K_{\kappa_r} m_y h_y$ (11.11)

11.3. Analysis of the possibilities of simplifying mathematical models

An analysis of the obtained dependencies of transition function of the control object has been performed for their simplification. Mathematical model of the control object in a form of transition function (11.10) takes into account inertia of the chip formation process and elastic system together with delay caused by singularities of cutting “along trace”. Characteristic singularity of the mathematical model is presence of internal, closed circuit in its structure. Thus, it is important to investigate features of the closed circuit and analyze its stability.

Stability of the mentioned circuit is determined by so called “vibro-stability” of the machine [3]. If the stability conditions are not met, during cutting in dynamic system self-excited vibrations occur. While developing mathematical model of the dynamic machines system it was assumed that “vibro-stability” of the machines is ensured i.e. closed circuit is stable.

Relation between time constants of the elastic system T_{us} , chip formation process T , and delay time τ were investigated. Delay τ , inversely proportional to the rotational speed of a part is not less than 0,1 to 0,2s in case of lathes. For medium size machine tools rotational speed of a spindle is 2000 rpm, thus minimum τ value is 0,03 s. Own resonance frequencies of equivalent elastic system of a machine tool and of a part for medium size lathes are within a range of frequencies higher than 50 Hz, i.e. the largest equivalent time constant T_{us} does not exceed 0,003s. Computations of the time constant of chip formation show that in ordinary cutting conditions values of T do not exceed 0,005 to 0,001s hence delay τ in (10), contained in a transition function $G\tau(s)$, exhibits the largest value and exceeds (by an order of magnitude) time constants T_{uc} and T_c [1,2]. Properties of equivalent closed circuit (if its stability conditions are met) are determined mainly by an element with the highest inertia – in this case an element with transition function:

$$G_{\tau}(s) = 1 - e^{-s\tau}.$$

In later part a possibility of neglecting “small” time constants regarding transition function of the investigated object was evaluated. In order to verify formed errors frequency domain was used – frequency characteristics.

Frequency characteristics of a model are obtained by substituting in (11.10) $s=j\omega$ and by using Euler’s formulas for exponential function:

$$e^{-j\omega\tau} = \cos \omega\tau - j \sin \omega\tau.$$

After transformation of a dependency for amplitude characteristics (ACH) and phase characteristics (FCH) one can write:

$$A(\omega) = m_i h_{ij} \frac{\left| 2 \sin\left(\frac{\omega\tau}{2}\right) \right|}{\omega \sqrt{C_1^2 + D_1^2}} \cdot \varphi(\omega) = -\frac{\omega\tau}{2} - \arctg\left(\frac{D_1}{C_1}\right) \quad (11.12)$$

where:

$$C_1 = 1 + n_y h_{yy} + B_1 - B_1 \cos \omega \tau - (T_{us}^2 + 2\xi T_{us} T_c) \omega^2,$$

$$D_1 = B_1 \sin \omega \tau - (T_c + 2\xi T_{us}) \omega - T_{us}^2 T_c \omega^3.$$

Fig. 11.3 shows functions of frequency characteristics (dashed lines) $A_1(\omega)$, $L_1(\omega)$ and $\varphi_1(\omega)$ of the mathematical model of output transition function (11.9) that were obtained from numerical calculations for the following data: $m_i n_i = 1$, $\tau = 1$, $B_1 = 0,6$, $T_{us}/\tau = 0,1$, $T_c/\tau = 0,05$. Thanks to assumed unit values $m_i n_i$ and τ , presented relations can be considered as generalized characteristics of the mathematical model in relative units. Their form does not depend on the particular values of the time constants but their ratio and coefficient B_1 . An argument in frequency characteristics is relative frequency $\omega^\circ = \omega / \omega_b$, where value $\omega_b = 1/\tau$ [1] is assumed as base frequency. Full lines in Fig. 11.3 show characteristics of a simplified model $A(\omega^\circ)$, $\varphi(\omega^\circ)$, $L(\omega^\circ)$, obtained by neglecting time constants of the elastic model and chip formation processes: $T_{us}=T_c=0$.

Analysis of the obtained relations show that output and approximated ACH and FCH are periodical functions of frequency. For the critical values of frequency $\omega_k^\circ = 2\pi k / \tau$ ($k=1,2,3, \dots$), amplitude characteristics assumes zero values and the coordinates of logarithmic amplitude characteristics $L(\omega_k) \Rightarrow -\infty$. Phase shift reaches -180° .

Reduction of the object equivalent gain coefficient to zero for the critical frequencies is explained by singularities of cutting “along trace”. In case of critical frequencies trajectory of blade motion on developed surface for current rotation remains equally distant to the trajectory of motion in previous rotation. Consequently, increment of section thickness, cutting forces and elastic deformations equals zero.

For frequencies higher than first critical $\omega_k^\circ = 2\pi k$ maximum value of $A(\omega^\circ)$ does not exceed $(0,08 \text{ to } 0,18)A(0)$ with changing B_1 coefficient in a range 0,1 to 1. Logarithmic phase characteristic is a discontinuous, periodic function. Points of their discontinuity overlaps with critical values of the frequency. Values of the logarithmic phase characteristics of an approximated model change within a range from 0 to $-\pi$. Taking into account inertia of the chip formation process and elastic system leads to changing value of logarithmic amplitude characteristics and phase characteristics. Moreover, it leads to additional phase shifts value and to the first critical frequency the difference between output and approximated logarithmic phase characteristics does not exceed 3 to 4dB. In this range of frequencies deviation of approximated $\varphi(\omega^\circ)$ phase characteristics from output $\varphi_1(\omega^\circ)$ occurs only near critical frequency value. Within the range of frequencies higher than critical one deviation between phase characteristics is significant.

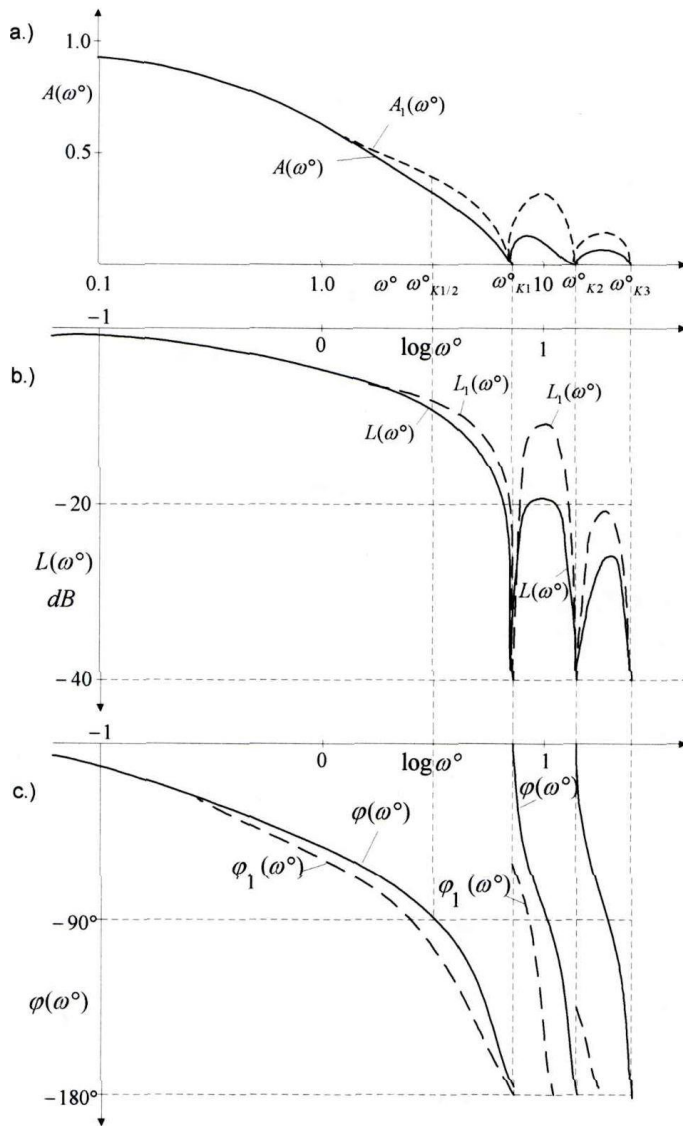


Fig. 11.3. Frequency characteristics of mathematical model of a dynamic system

During synthesis of the corrective elements of the automatic control system the cut-off frequency is chosen on the left side of the first critical frequency of mathematical model of control object. It allows to consider frequency characteristics of the mathematical model limiting frequency range to smaller ones than first critical equal to $2\pi/\tau$.

For the given frequency range, as performed analysis showed, inertia of the chip formation process and elastic deformation can be neglected without significant error and assume at the end:

$$H_{ii}(s) = h_{ii}, M_i(s) = m_i, N_i(s) = n_i, C_i(s) = c_i, \quad (11.13)$$

Then, the approximated dependencies of the object transition function for recognized control activity and for the output values in a form cutting forces and elastic deformations are as follows:

$$G_{v_f F_i}(s) = \frac{\Delta F_i(s)}{\Delta v_f(s)} = \frac{K_{1v_f F_i} G_\tau(s)}{s(1 + BG_\tau(s))} \quad (11.14)$$

$$G_{v_f g_i}(s) = \frac{\Delta g_i(s)}{\Delta v_f(s)} = \frac{K_{1v_f g_i} G_\tau(s)}{s(1 + BG_\tau(s))} \quad (11.15)$$

where:

$$K_{1v_f F_i} = m_i \left[1 - \frac{m_y h_{yy} n_i}{(1 + n_y h_{yy}) m_i} \right], K_{1v_f g_i} = K_{1v_f F_i} h_{ii} \quad (11.16)$$

$$B = \frac{m_x h_{xx} + m_y h_{yy} K_{K_v}}{1 + n_y h_{yy}} \quad (11.17)$$

In this way, while developing mathematical models for control over dynamic system of machine tools with met condition of “vibro stability” it is allowed to describe the properties of the elastic system and chip formation process with gain coefficient. It means that mentioned elements can be considered as proportional.

One has to note that dependency between output coordinates (components of the cutting force and elastic deformations) and intermediate coordinate – thickness of a cut layer Δa_{v_f} as an input is presented by transition function of the closed circuit:

$$G_{zkF}(s) = \frac{\Delta F_i(s)}{\Delta a_{v_f}(s)} = \frac{m_i}{1 + n_y h_{yy}} \cdot \frac{1}{[1 + BG_\tau(s)]} \quad (11.18)$$

$$G_{zkg}(s) = \frac{\Delta g_i(s)}{\Delta a_{v_f}(s)} = \frac{m_i h_{ii}}{1 + n_y h_{yy}} \cdot \frac{1}{[1 + BG_\tau(s)]} \quad (11.19)$$

In rough processing, when values of B coefficient are larger than 0,1, in order to obtain simplified relations one has to use development of the exponential function into Pade series. Limitation to the first two components of the Pade series one obtains:

$$G_{v_f F_i}(s) = \frac{\Delta F_i(s)}{\Delta v_f(s)} = \frac{K_{v_f F_i}}{(T_{o1}s + 1)(T_{o2}s + 1)}, \quad (11.19)$$

$$T_{o1, o2} = 0,5\tau \left[0,5 + B \pm \sqrt{(0,5 + B)^2 - \frac{1}{3}} \right]$$

Empirical investigations showed that obtained simplified models ensure precision equal 15% to 20% of time constants evaluation [2].

11.4. Empirical investigation of the static and dynamic characteristics of machine dynamic system

Investigation of the dynamic characteristics was performed using methods of active experiment. In order to obtain time characteristics curves of output coordinates of the object during cutting the semi-finished product with blade were registered.

It is worth noting that a process of cutting product with a blade at constant values of longitudinal feed and rotational speed of a product can be considered as transient process for control value and as transient process for a disturbance. Simultaneously, first and second operation can be considered as abrupt if main cutting edge is parallel to the cut surface and thickness of the cut layer remains constant after cutting in.

Mentioned transient processes are characterized by zero initial conditions. Transient object characteristics for a disturbance with non-zero initial conditions would be registered during turning semi-finished products with abrupt change of allowance (Fig. 11.4).

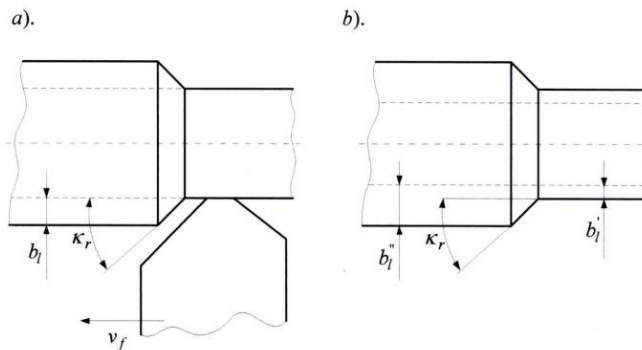


Fig. 11.4. Sketches of semi-finished products for determining transient function:
a – controlling longitudinal feed, b – disturbance in a form of allowance

During experimental tests a tangent component of cutting force as object output value. To its measurement two-component dynamometer was used. Tangent cutting force moves “movable” part of the force gauge (to which blade is fitted) with respect the solid part located on a support due to elastic

deformations of an element with reduced section. Values of the elastic deformations were measured with inductive sensor of linear displacements. Results showed that value of the displacement of "movable" part with respect to the solid one, thanks to high longitudinal and radial stiffness of the element with reduced section depends practically only on the tangent cutting force.

In order to register static characteristic of the mentioned dynamometer, the blade fitted in the device using special lifting tool was loaded with a force equivalent with equivalent direction to tangent cutting force. Thanks to that dynamometer gain coefficient was found and it was established that nonlinearity of its static characteristics does not exceed 2%. Dynamic characteristics of the gauge were obtained using oscilloscopic recording of curves of transient processes caused by increase and decrease of load. Inertia of the gauge, as shown by performed experiments, is smaller by an order of magnitude than inertia of an object what allows considering the device as proportional element (fig. 11.5).

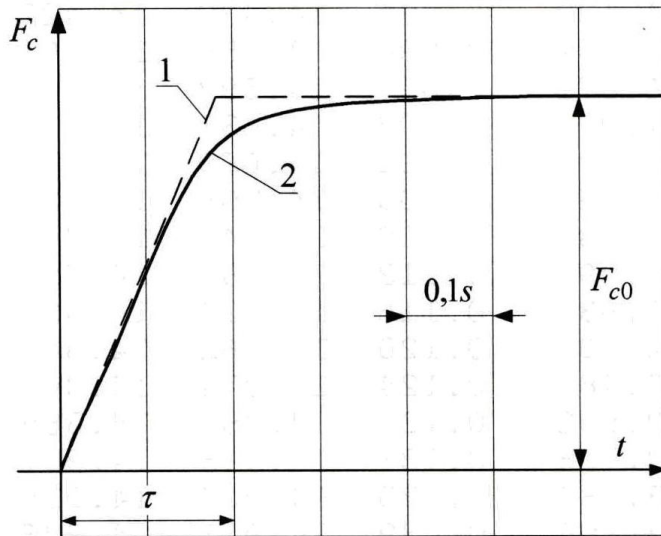


Fig. 11.5. Experimental transient characteristics of the control object

In order to obtain indicator of the beginning of transient process during oscillographic recording exactly in a moment of cutting the blade into a semi-finished product, low voltage was delivered to the blade (isolated from grip) – second pole was connected to the machine body. Moment of contacting the edge and machined semi-finished product was detected by closing mentioned electrical circuit.

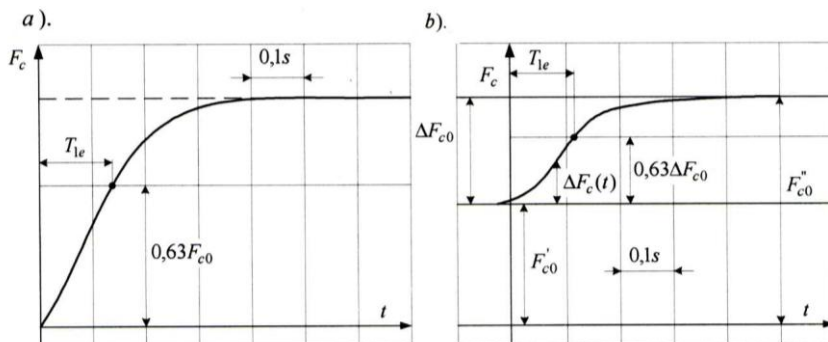


Fig.11.6. Experimental transient characteristics of the control object

Example: Fig. 11.5 and 11.6 show oscillographs of the transient processes, obtained during experimental testing dynamic lathe system. First was obtained for cutting process in the following conditions: semi-finished product material – steel C45, blade Ti15Co6, blade normal angle $\kappa_r = 90^\circ$, cutting speed $v_c = 90$ m/min, cutting depth $a_p = 1$ mm, speed of longitudinal feed $v_f = 60$ mm/min, thickness of a cut layer in a stationary state $a = 0,2$ mm, value of tangent cutting force in a stationary state $F_{c0} = 350$ N, product rotation time $\tau = 0,2$ s, product diameter $d = 30$ mm. Calculation of the cutting gain coefficients (taking into account literature data) gives $m_x = 0,66 \times 10^6$ N/m, $m_y = 0,14 \times 10^6$ N/m. Susceptibility of the semi-finished product, as shown by calculations, can be neglected in this particular case. Using static characteristics (Fig. 11.5 and 11.6) it was determined: $h_{xx} = 1,5 \times 10^{-7}$ m/N, $h_{yy} = 0,66 \times 10^{-7}$ m/N. Value of the coefficient B , computed using formula (11.16), $B = 0,099$ and approximated mathematical model can be assumed in a form of integrating element with a transition function (11.19).

Response of an element to abrupt change of input value, as shown above, theoretically presents linearly increasing signal in time τ (curve 1 in Fig. 11.5). Real curve 2 of the output value is sufficiently close to the theoretical one; maximum deviation is 12%.

Fig. 11.6a shows transient characteristics obtained during cutting time in the following conditions: semi-finished product - steel C45, blade Ti15Co6, $\kappa_r = 45^\circ$, $v_c = 96$ m/min, $a_p = 1$ mm, $v_f = 100$ mm/min, $a = 0,2$ mm, value of tangent cutting force in a stationary state $F_{c0} = 1450$ N, $\tau = 0,12$ s. Similarly as above, cutting process gain and elastic system coefficients were found and value of coefficient $B = 1,2$ was calculated. Model (11.18) should be assumed as approximated one (it takes into account value of a B parameter) in a form of non-periodic element of second order.

Time constants determined using equation (11.20) are equal $T_{o1} = 0,2$ s, $T_{o2} = 0,006$ s. Taking into account that second time constant of an object is smaller by an order of magnitude than the first one, it can be assumed in further calculations that $T_{1p} \approx T_{o1}$ and approximate experimental curve with exponent

and establish time constant to be $T_{1e} = 0,18s$ - as a time after which output value reaches 0,63 of its value in stationary state. Evaluation error of computed time constant is:

$$\delta = \frac{T_{1e} - T_{1p}}{T_{1e}} \cdot 100\% = -11\% \quad (11.21)$$

Fig. 11.6b shows oscillograph of object time characteristics obtained during processing of a product with abrupt change of cutting depth from $a_{p1} = 1,5mm$ to $a_{p2} = 3mm$, i.e. change of allowance by $\Delta a_p = 1,5mm$. Semi-finished product – steel C45, blade Ti15Co6, $\kappa_r = 45^\circ$, $v_c = 98$ m/min, $v_f = 100$ mm/min, $a = 0,2$ mm, $\tau = 0,075s$, $B = 1,44$ value of tangent cutting force in a stationary state $F'_{c0} = 620N$, $F''_{c0} = 1240N$ (fig.11.7).

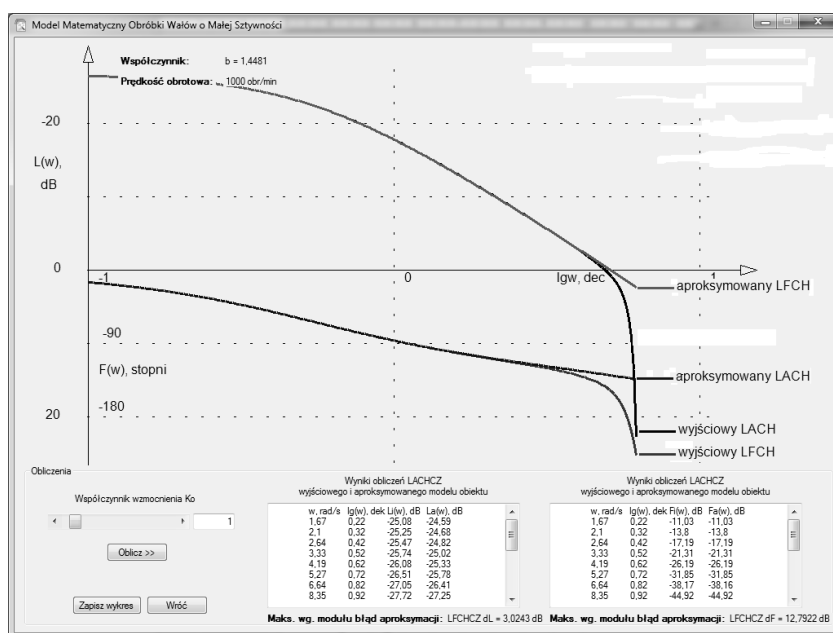


Fig. 11.7. Graphs for calculation of time characteristics of a control object

According to the dependency described above average computed coefficient value is $B = 0,9$. Time characteristics was approximated with an exponent with computed time constant $T_{1p} = 0,106s$. Transient process can be characterized with non-zero initial conditions and experimental value of a time constant according to formula (11.21) equals 6%.

Listing experimental and calculated curves of transient processes was performed according to the methodology described below. Experimental time characteristics were approximated according to the following formula:

$$F_c(t) = F_{c0} [1 - \exp(-t/T_{1e})]$$

where: F_{c0} – established output value or its increment, T_{1e} – equivalent time constant determined basing on the oscillograph as a time, after which output value or its increment reaches 0,63 of value in stationary state. Found values of T_{1e} were compared with computed T_{1p} that were defined as time, after which computed transient characteristic, described by above dependencies, reaches 0,63 of value in stationary state. Relative values of T_{1p} depend on B coefficient and they can be determined basing on the curves shown in Fig. 11.8.

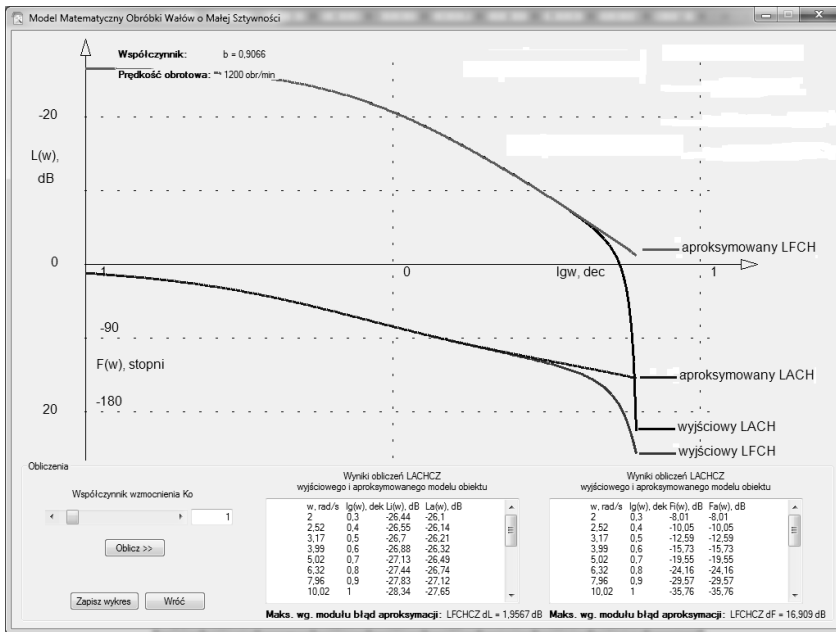


Fig. 11.8. Graphs for calculation of time characteristics of a control object

Given results were obtained during processing of semi-finished products made of steel C45 with a blade Ti15Co6 working at normal angles 45^0 and 90^0 . Values of time constants given in Table 1 were calculated as averaged results of three or four obtained oscillographs in steady conditions.

Analytic determination of time constants was performed using values of the gain coefficients corrected by performed experiments. Errors of the computed time constants basically do not exceed 20%. Results of investigating experimental object characteristics for controlling values in a form of speed of longitudinal feed and spindle rotational speed together with disturbing value in a form of allowance on a part perimeter show that mathematical models, obtained after analytic analysis, are useful. Research confirmed introduced conclusion about possibly wide range of changes in case of control object parameters.

Table 11.1. Listing of cutting parameters and experimental and calculated time constants

Nr	τ [s]	χ_r	V_c [m/s]	a_p [mm]	a	F_{c0} [N]	T_{1c} [s]	T_{1p} [s]	δ [%]
1	0,48	45	0,8	2,0	0,2	900	0,59	0,55	7
2	0,48	45	0,8	3,0	0,2	1380	0,7	0,625	11
3	0,375	45	0,85	1,0	0,2	480	0,3	0,3	0
4	0,375	45	0,85	2,0	0,25	1140	0,46	0,43	7
5	0,375	45	0,85	3,0	0,2	1400	0,55	0,48	13
6	0,24	45	1,3	1,5	0,25	855	0,23	0,215	7
7	0,24	45	1,3	2,0	0,25	1150	0,34	0,28	18
8	0,24	45	1,3	3,0	0,2	1370	0,36	0,31	14
9	0,12	45	1,6	1,5	0,2	730	0,12	0,13	-8
10	0,12	45	1,6	3,0	0,2	1470	0,18	0,161	11
11	0,095	45	1,65	1,0	0,2	475	0,08	0,076	5
12	0,095	45	1,65	3,0	0,2	1475	0,15	0,13	13
13	0,095	45	1,65	5,0	0,1	1180	0,2	0,19	5
14	0,075	45	1,67	1,0	0,2	470	0,06	0,064	-7
15	0,075	45	1,67	2,0	0,2	981	0,11	0,09	18

Conclusions

Structure and parameters of a control object depend on processing conditions of the machine tool. Time constants of a time object are mainly affected by delay time τ , depending on object rotational speed. Moreover, object inertia depends on a value of B coefficient. Adjustment range of the rotational speed of main motion drive in case of ordinary machines reaches 100 and more - in certain range it can change time constants of a control object.

Object gain coefficient, defined by delay time, parameters of a technological system, gain coefficients of cutting process and also can change by an order of magnitude. Simultaneously it is necessary to take into account that such wide ranges of changes of the parameters of machine dynamic systems characterize their operation in whole technological range. During realization of the part processing its rotational speed usually remains constant and changes of object parameters are caused mainly by changes of allowance what results in changed gain coefficients in cutting process. Moreover, variability of the dynamic properties of an object is affected by changes of parameters of elastic system along product axis what occurs when technological system includes non-rigid part.

Properties of the turning process like nonlinearity, variability of parameters, deterministic and accidental disturbances cause that effective controlling is not possible in case of ordinary adjustment systems. Results of research covering use of developed control models indicate that good quality control can be ensured by adapting algorithms.

References:

- [1]. Taranenko V., Abakumov A.: Dinamicheskiye modeli dlya ocenki tochnosti tehnologicheskikh sistem. WNIITEMR, 1989, vyp. 1. 56 pp.
- [2]. Czachor G., Taranenko W.: Badania eksperymentalne charakterystyk dynamicznego systemu modułu tokarskiego. Rzeszów. Materiały 11 Międzynarodowej Konferencji Naukowo-Technicznej - MTK 2002. Modułowe technologie i konstrukcje w budowie maszyn. Zeszyty Naukowe Politechniki Rzeszowskiej Nr 196. Mechanika z. 59, Rzeszów 2002. pp.159-166.
- [3]. Tomków J.: Wibrostabilność obrabiarek, WNT. Warszawa 1997, 205s.
- [4]. Besekerskiy V. A., Popoy E. P.: Theory of automatic control systems. M.: Nauka, 1975. 768 s.
- [5]. Abakumow A., Taranenko W., Zubrzycki J.: Program modules for the study of characteristics of the dynamic system of machining process. Zeszyty Naukowe Politechniki Rzeszowskiej NR 230 MECHANIKA, z. 67 Modułowe Technologie i Konstrukcje w Budowie Maszyn, Rzeszów 2006. pp. 99 -109
- [6]. Abakumoy A., Taranenko V., Zubrzycki J.: Modeling of characteristics of dynamic system of turning process for axial-symmetric shafts. V-th International Congress "Mechanical Engineering Technologies 06" (MT'06), September 20 -23. 2006, Varna, Bulgaria. PROCEEDINGS. Section III. S.76–78
- [7]. Taranenko W., Szabelski J., Taranenko G.: Fundamentals of Identification of the dynamic system of turning of low-rigidity shafts. Pomiary. Automatyka. Robotyka. Miesięcznik naukowo - techniczny, nr 2/2008, Warszawa 2008.
- [8]. Taranenko G., Taranenko V., Szabelski J., Świc A.: Systemic analysis of models of dynamic systems of shaft machining in elastic-deformable condition. Applied Computer Science. Business Process Optimization. Vol. 3, No 2,2007. Technical University of Zilina, Slovak Republic.
- [9]. Taranenko W., Czachor G.: Badania eksperymentalne charakterystyk układu dynamicznego modułu tokarskiego. Modułowe technologie w konstrukcji maszyn. MTK'02 15-18 październik 2002. Rzeszów 2002.

Automation of shafts machining about low rigidity

Abstract: The article presents rule of identifying dynamic system of the process of longitudinal turning axially symmetric shafts about low rigidity. Generalized mathematical model of the dynamic system of the process of longitudinal turning was developed, systems of equations and generalized structural diagram of the dynamic system is given. Possibilities of simplifying generalized mathematical model of the dynamic system basing on the analysis of frequency characteristics are shown. Neglecting “small” time constants is evaluated depending on the operator transmittances of the frequency series for the investigated object. Evaluation of the approximation errors of the time and frequency characteristics is discussed. Method of experimental research is described and results of this research is given. Features of developed software for investigating dynamic and frequency characteristics of the turning process are shown. Software allows to make possible: establishing the conditions of cutting process basing on the technological parameters of the machine, parts and cutting process, computing (basing on the models of cutting process) basic dynamic characteristics, including transition functions in an operator form, response of cutting forces to abrupt feed change and amplitude and phase frequency characteristics. Basing on the developed algorithms of elastic strains control of the machines dynamic systems that use longitudinal feed as control, a few variants of automatic control for general-purpose lathes, grinders and CNC machines are realized.

Key words: shafts about low rigidity, CNC machines, mathematical model, technological parameters

Automatyzacja obróbki wałów o małej sztywności

Streszczenie: W pracy przedstawiono rolę identyfikacji układu dynamicznego procesu toczenia wzdłużnego wałów osiowo symetrycznych o małej sztywności. Opracowano uogólniony model matematyczny układu dynamicznego procesu toczenia wzdłużnego, przedstawiono układy równań i uogólniony schemat strukturalny układu dynamicznego. Przedstawiono możliwości uroszczenia uogólnionego modelu matematycznego układu dynamicznego w oparciu o analizę charakterystyk częstotliwościowych. Przeanalizowano możliwość pominięcia „małych” stałych czasowych w zależności od funkcji przejścia zmiennych częstotliwościowych badanego obiektu. Omówiono wpływ błędów kolejnych przybliżeń stałych czasowych i charakterystyk częstotliwościowych. Opisano metodykę badań eksperymentalnych i podano wyniki badań. Przedstawiono własności opracowanego oprogramowania przeznaczonego do badania charakterystyk dynamicznych i częstotliwościowych procesu toczenia. Opracowane oprogramowanie umożliwia: ustalenie warunków skrawania bazując na parametrach technologicznych maszyny, części i procesu skrawania, wyznaczenie charakterystyk dynamicznych zawierających funkcję przejścia, odpowiedź siły skrawania na nagłą zmianę posuwu, amplitudy i przesunięcia charakterystyki częstotliwościowej.

Słowa kluczowe: wały o małej sztywności, maszyny CNC, model matematyczny, parametry technologiczne

RUDOLF JANOS*
MIKULAS HAJDUK**
MAREK SUKOP***
VLADIMIR BALÁŽ****

12. Requirements for agent – rescue robot

Introduction

The current negative trend of natural disasters, industrial and environmental accidents, terrorist threats updates the question of how effectively and efficiently rescue the affected human, material and environmental potential, respectively to effectively monitor the risk of such a situation. One of the ways to increase operational capacity, efficiency and effectiveness of interventions and rescue also monitoring of hazards is to deploy these techniques work effectively. This path also eliminates the risk associated with the direct participation of people (rescue team) to rescue work especially in areas of high local risk and danger. Higher ranked in effect rescue operations can be achieved by using multiagent systems. The current reality and trends also support rescue work documenting dynamically increase the deployment of service robots in these activities [1,2].

12.1. Requirements for Rescue Service Robots

Service robot, designed as a technical resource for active citizenship in the subject area surrounding the labor and technological scene plays in your application two categories of basic tasks. [3]

- transport task - move service robot in operational space (mobility subsystem feature - locomotion system) - active autonomous service robot moving in the space of deployment, physical activity level service robot,
- global area (operating space between origin and destination of operational deployment) – physical activity: searching and achieve the goal, obstacle avoidance,
- local area (area of contact with an object on the route of movement, respectively. Workspace area performing work) - physical activity: operational route changes direction of movement, change of position and orientation of the functional subsystem mobility robot, programmed and

* Rudolf Janos, Faculty of Mechanical Engineering, Department of Production Systems and Robotics, Nĕmcovej 32, 042 00 Košice, Slovak Republic, rudolf.janos@tuke.sk

** Mikulas Hajduk Faculty of Mechanical Engineering, Department of Production Systems and Robotics, Nĕmcovej 32, 042 00 Košice, Slovak Republic, mikulas.hajduk@tuke.sk

*** Marek Sukop, Faculty of Mechanical Engineering, Department of Production Systems and Robotics, Nĕmcovej 32, 042 00 Košice, Slovak Republic, marek.sukop@tuke.sk

**** Vladimir Balaz, Faculty of Mechanical Engineering, Department of Production Systems and Robotics, Nĕmcovej 32, 042 00 Košice, Slovak Republic, Vladimir.balaz@tuke.sk

operative movement in the employment scene the needs of routes to reach the destination, programmed and operating labor movement in the scene according to the needs of technology work task,

- deployment of space – performance transport service robot tasks, management and navigation service robot moving in operating a workspace designed for, respectively. induced transport routes, service robot movement in the space provided for transport routes, respectively. service robot motion on the principle of intelligent behavior in space according to the immediate situation,
- working performance at work scene service robots (function subsystem
- action body - actively working autonomously perform tasks specified SR on the scene working its operational area, activity action body at the level of service robots

Above categorizations service robots tasks and factual description schema specifies the desired effects of deployment service robots, as well as the resulting requirements necessary for establishing design concepts of service robots. [3,4]

12.2. Requirements of Transport

Requirements resulting from the transport task needs associated with the implementation of the required service robot motion in the space of deployment. Motion service robot is seen as a continuous time change of the position and orientation of the service robot (movement of the body in physical space representation of the motion of its center of gravity, the distance between the starting and final position of center of gravity) in the designated area, as relating to the reference frame coordinate system operational area. Interpretation of the general patterns of movement to fulfill the role of transport service robot, based on the nature of the movement is the phenomenon of spatial and temporal phenomenon (each movement takes time). [6]

Traffic routes of the service robot in current approaches to the assessment classified from different perspectives to their characters, respectively from different perspectives, requirements on the behavior of service robot for those routes, namely:

- depending on the nature of movement execution service robot for the transport route,
- motion by location (location of transport routes in the global space) service robot in its operating area (X_o , Y_o , Z_o),
- implementation of the strategy and navigation service robot motion control
- the strategy programmatically determined behavior SERVICE ROBOT on the transport route,
- characters according to the operating area and the deployment of service robots nature of the environment movement service robots.

The description of the motion characteristics of service robot, as well as for the design and construction of the subsystem mobility service robot as a base features and parameters are recommended:

- track parameters - minimum width, minimum height, minimum turning radius,
- range - continuous movement time per battery energy,
- motion parameters - minimum and maximum speed, maximum acceleration, minimum motion, motion modes of operation,
- maneuverability - the parameters of rotation (turning radius, surface to rotate on the spot, ...), directional motility (movement in the directions perpendicular to each other, without rotation of the chassis), physical responsiveness (bypassing maneuver geometry or surface bypass routes), motion reversibility,
- precision motion - stopping accuracy, precision motion along the programmed route,
- throughput - overcoming obstacles (maximum climb, descent, moving stairs, maximum inequality, movement along a slope, ...) ratios (roughness height/width robot, roughness height/footprint chassis, ...) [5].

12.3. Working Tasks Requirements

Work tasks of service robots, characterized by their diversity, can be classified from different perspectives, their execution performance, respectively terms of the requirements for their implementation:

- work task in a static position – service robots shall move on path defined by points A (starting position) and B (the target position), the target position after position biased static service robots performed work task, Fig. 12.1.

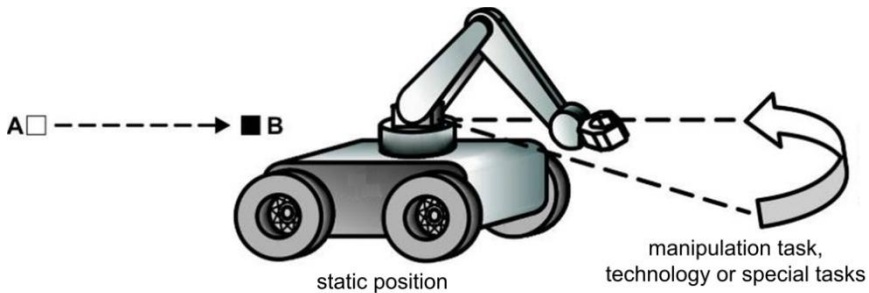


Fig. 12.1. Work task in a static position

- work task in a dynamic position of service robots – performance of the work task is carried at all times moving service robot designed for the transport route represented the starting position and target location.
- technology work task performance - performance of the work task is governed by established technology and related technological conditions of its realization. In carrying out the tasks of service robots must be strictly complied with the conditions set technology applied technology performance task. At the same time required for design and construction service robots

and in particular in the construction of the exposed sub-address "resistance" service robots effects on the performance of the work task (an additional burden, the impact of technological waste, the impact of environmental problems, ...) [4].

12.4. Conclusion

Based on the characterization and practice can be said that service robots compared to industrial robots is much more difficult technical system. In practice, service robots is presented to a wider range of deployment, greater diversity concept and principles of design, which is the result of demands made service tasks, as well as the diversity of the environment of the service robots. Statistical data on the deployment of service robots show that the most widely used solution concept as a mobile service robot. Technical solutions service robots are presented from a relatively simple design to specialized intelligent integrated automation system, where sharp boundaries between technological systems and automatic robot is lost.

This contribution is the result of the project implementation: Research modules for intelligent robotic systems (ITMS: 26220220141), activity 2.2, supported by the Research & Development operational Program funded by the ERDF.

References

- [1] Jánoš, R., Svetlík, J., Dobransky, J.: Design service robot body for handling. In: Acta technica corviniensis : bulletin of engineering. Vol. 3, no. 4 (2011), p. 73-75. - ISSN 2067-3809.
- [2] Vagaš, M., Hajduk, M., Semjon, J., Páchniková, L., Jánoš, R.: The view to the current state of robotics. In: Advanced Materials Research. Vol. 463-464 (2012), p. 1711-1714. - ISSN 1022-6680.
- [3] Niculescu D., Olaru A., Tufan A. D., Diagnosis and maintenance in the spectrum of vibrations, on universal machine for sharpening and grinding In: Robtep 2011, Košice 2011, pp. 135-142.
- [4] Hajduk M, Present status and evolution trends of the service and humanoid robotics, Acta Mechanica Slovaca. – ISSN 1335-2393. – Roč. 11, č. 2-A/2007 (2007), s. 7-10.
- [5] Uhríček J., Popeová V., Zahoranský R., Chochul M.: Control system and simulation software of training robot: SOP, 2000. pp. 165-168, ISBN: 3-901509-16-X.
- [6] Jánoš, R a kol: Design of service robot for rescue operations, in In: Applied Mechanics and Materials. Vol. 282 (2013), p. 123-126. - ISSN 1660-9336.
- [7] Jánoš, R.: Modulárne robotické systémy, In: International Scientific Herald. Vol. 4, no. 23 (2012), p. 83-88. - ISSN 2218-5348.

Requirements For Agent- Rescue Robot

Abstract: Automation service business is characterized by scattering needs and the related diversity and diversity requirements for service robot working in multiagents systems (usually extremely multifunctional requirements), followed by complexity and demands of their transformation into technical characteristics and qualities of service robots, all this creates a different basis for the formulation of system features and characteristics.

Key words: service robot, mobile platform, requirements for robot, agent, mutliagent system

VLADIMÍR BALÁŽ*
MAREK VAGAS**
JÁN SEMJON***
MIKULÁŠ HAJDUK****

13. Design of automated robotized system with two robots

Introduction

The solutions of many problems emerging in production process require a deployment of more robots in present times. Particularly touch in to assembly of complex parts, welding of longer parts etc. Application of more robots at workplace requires a perfect prepare at design area also like at programmed equipment robots area. In operation with more robots is mainly important to avoid their mutual collisions. As solution for these situations are preferred to use off-line system program at programming at robots. These allows to us by detection of collisions to avoid any undesirable conditions.

13.1. Automated robotized system for assembly

Automated robotized system is designed in CAD program. The workplace for manipulation is situated around conveyor belt Bosch. Every object for assembling is transported to required position at pallet size 160x160mm [1]. Every pallet is equipped by RFID element MDT-2K for entry of information. At loading up of object to pallet is through transmitter ID-40 activated a memory MDT-2K and writes data, which determines, where pallet stops and what kind of operation follows at object. The control of conveyor belt is realized by PLC Simatic S7/300 DP. To profibus is connected to RFID elements ID-40 for writing and reading information from memories at pallets. Change direction of pallet movement at conveyor belt is possible by transport units. Conveyor belt is equipped by inductive sensors for monitoring of pallet movement. At places, where is necessary stops the pallet are situated pneumatic stopper, which prevent to their any movement. Pneumatic stopper is fitted by inductive sensor for pallet monitoring at exactly place. The workplace for manipulation is realized with assembling robot by addition of RFID element ID-40, that after reading of information from pallet determines, if objects continue to assembly, or continue at conveyor belt.

* Ing. Vladimír Balaz, Ph. D., Faculty of Mechanical Engineering, Department of Production Systems and Robotics, Némčovej 32, 042 00 Košice, Slovak Republic, vladimir.balaz@tuke.sk

** Marek Vagas, Vladimír Balaz, Faculty of Mechanical Engineering, Department of Production Systems and Robotics, Némčovej 32, 042 00 Košice, Slovak Republic, marek.vagas@tuke.sk

*** Ing. Jan Semjon, Ph. D., Faculty of Mechanical Engineering, Department of Production Systems and Robotics, Némčovej 32, 042 00 Košice, Slovak Republic, jan.semjon@tuke.sk

**** prof. ing. Mikuláš Hajduk, Ph. D., Faculty of Mechanical Engineering, Department of Production Systems and Robotics, Némčovej 32, 042 00 Košice, Slovak Republic, mikulas.hajduk@tuke.sk

The workplace is situated with two robots. Robot OTC Daihen AX-V6 is situated for loading up from stock to pallet that are designed to assembly or storing of finished products to stock. Searching of objects at stock is realized through barcodes. Robot OTC has six degrees of freedom that allows good reachability in envelope to arbitrary point in space [4]. Function of effector is secured by pneumatic two-fingered gripper. In necessary situations is possible to change effector by another one, suction caps etc. Control of robot is realized through control system AX-C with input / output unit and 32 inputs/outputs. The number of inputs / outputs is possible to extend to 2048 value [6]. Accuracy of robot is 0,08mm that is sufficient for manipulation with chosen objects. Robot is equipped by programmed unit (pendant), which allows setting robot to required positions. Robot is programmable at SLIM language. Designed manipulation workplace with robot OTC Daihen Almega AX-V6 is situated at Fig.13.1.



Fig. 13.1. Manipulation workplace with robot OTC Daihen Almega AX-V6

The second one robot is situated to assembly. Robot Motoman SDA 10F is dual arm robot with 15-teen degrees of freedom, Fig. 13.2. Each arm of robot can be loaded at flange by weight 10kg. For assembly purpose is one of arm equipped by two-fingered gripper SMC MHS2-32D and second one by three-fingered pneumatic gripper SMC MHS3-40D. The range of pressure at grippers are from 0,1 – 0,6 MPa [2]. To control of robot was designed control system FS100, where is touch screen programmed unit (pendant) connect. Control system FS100 is equipped by input / output card that allows connecting 16 inputs and 16 outputs. Robot can be programmed in Inform III language.

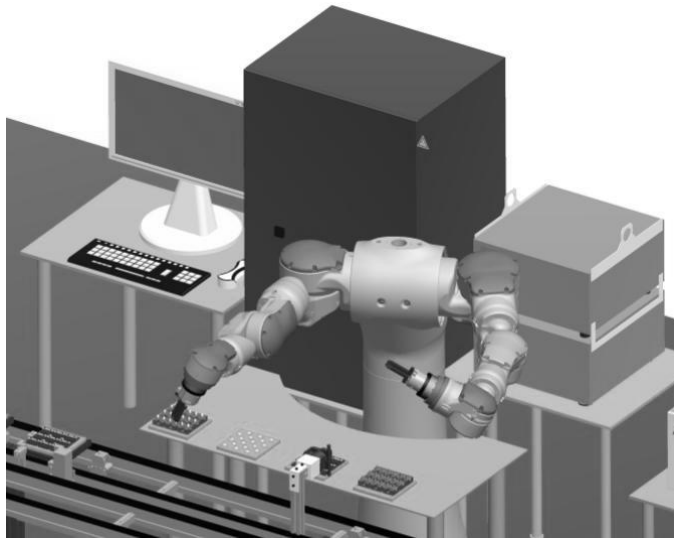


Fig. 13.2. Assembly workplace with Motoman SDA 10F

Design of workplace with conveyor belt tray is on Fig. 13.3. Workplace contains also a superior control system and camera system Omron 150 with two cameras. This camera system allows determining most effective method for off take objects from pallet.

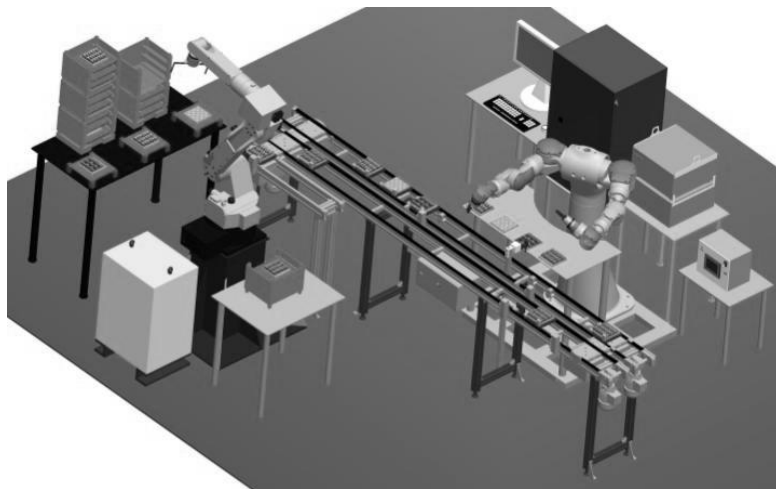


Fig. 13.3. Design of workplace in CAD system

Whole automated robotized workplace is controlled by superior control system on PLC base components [5]. At Fig. 13.4 is presented basic flowchart for information flow of workplace.

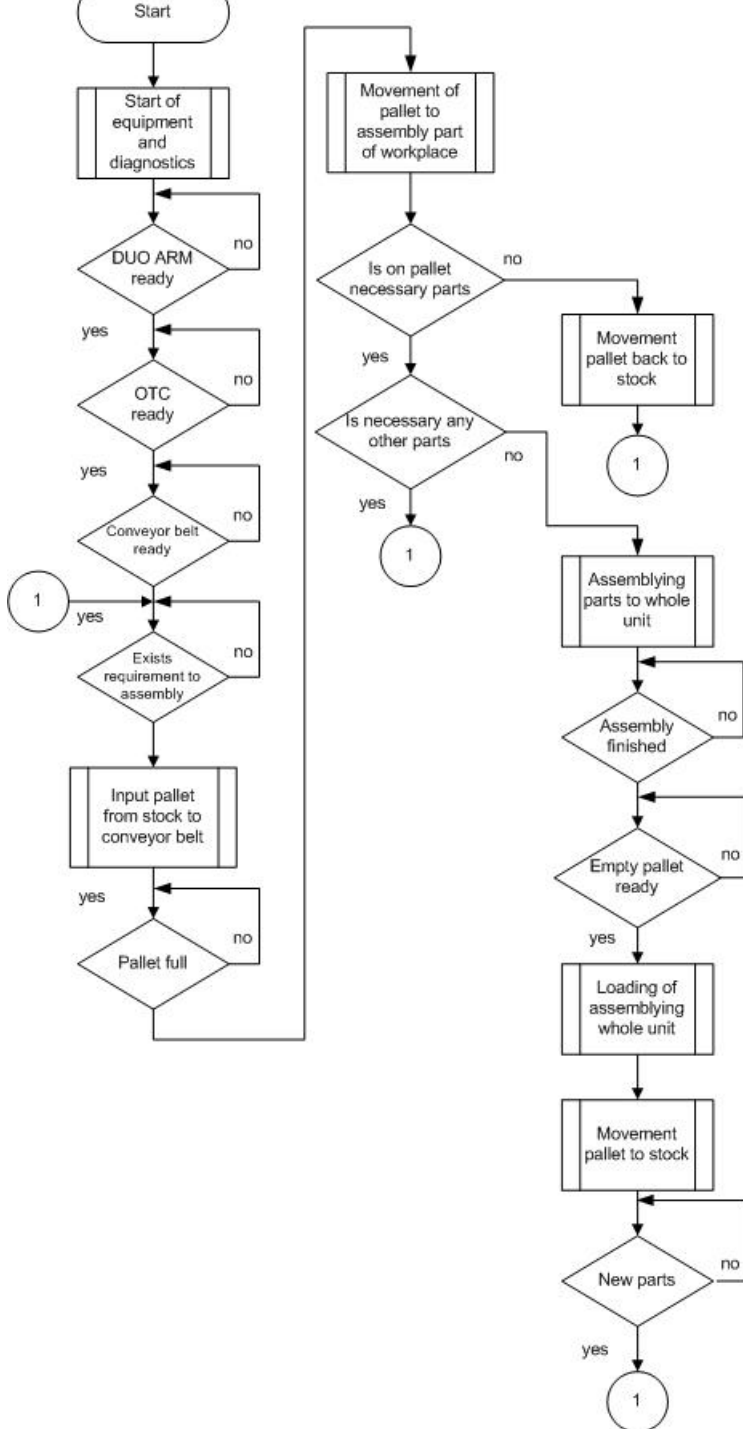


Fig. 13.4. Basic flowchart for information flow of workplace

Block diagram for transmission of information at workplace is on Fig.13.5.

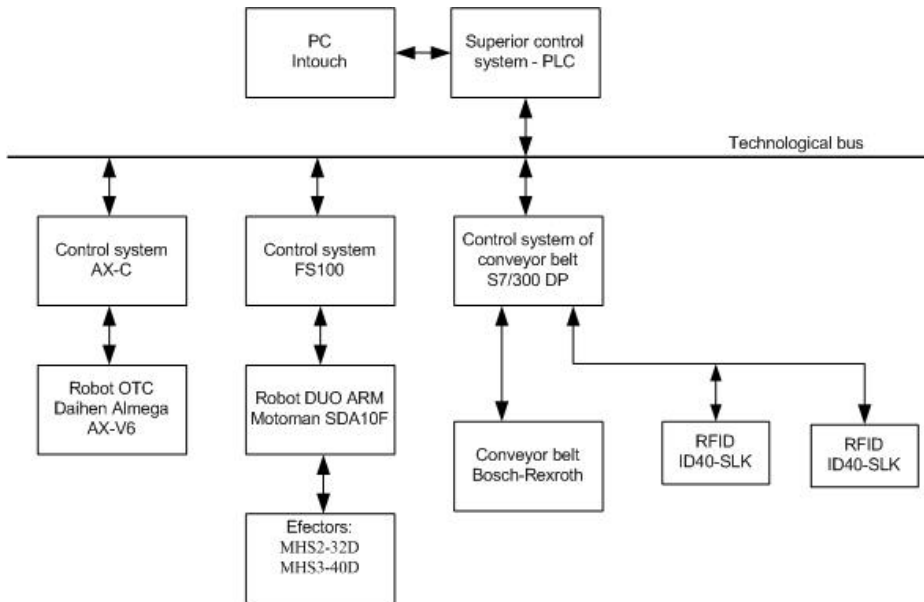


Fig. 13.5. Block diagram for transmission of information at workplace

Conclusions

Automated robotized system is built to verification purpose for behavior of robots designed in more numbers at one workplace. The workplace is built gradually and first phase of solution in present time. Assembling part of workplace will be used for recognition of non-oriented objects through camera system that rapidly increases the possibilities at workplace.

This contribution is the result of the project implementation: Center for research of control of technical, environmental and human risks for permanent development of production and products in mechanical engineering (ITMS: 26220120060) supported by the Research & Development Operational Program funded by the ERDF.

References

- [1] Biľ R., Dovica M., Kaľuch P.: Vývoj v riadení robotických systémov - swarm systémy, ATP Journal plus1, 2008, prístupné na Internet: http://www.atpjournals.sk/buxus/docs/casopisy/atp_plus/plus_2008_1/plus38_41.pdf
- [2] Jánoš R.: Modulárna stavba robotických systémov, Transfer inovácií, č. 19, 2011, p.171-174, ISSN 1337-7094.
- [3] Sukop M., Hajduk M., Varga J., Vagaš M.: Increasing degree of automation of production systems based on intelligent manipulation, Acta Mechanica Slovaca, roč. 15, č.4, 2011, ISSN 1335–2393.
- [4] Hajduk, M, Baláž, V, Sukop, M, Evin, M, Vagaš, M.: Robotized Cell for Palletization with CCD Camera, IN: Optirob 2007: Bren Publishing House, ISBN 9789736486562.
- [5] Buda, J., Kováč, M.: Projektovanie a prevádzka robotizovaných systémov. Bratislava: TU, 1990. 335 s. ISBN 80–05–00680–2.
- [6] Hajduk M., Semjon J.: Methodological approach in robotic cell support implement design, In: Machinery, technology, materials: 7th international congress: Bulgaria – Sofia: Scientific technical union of mechanical engineering, 2010 pp. 108–109.
- [7] Baláž V., Sukop M., Palaščáková D., Páchniková L.: Návrh architektúry riadenia vo výrobných systémoch, In: Eldikom 2009, Žilina, s.110–113, ISBN 9788089072477.

Design of automated robotized system with two robots

Abstract: The article describes a design of automated robotized system with robot OTC Daihen AX-V6 suited for manipulation and robot Motoman SDA 10F that provides assembling of chosen parts. The transport of every part is realized from/to stock through conveyor belt Bosch. Superior control system is equipped by computer with visualization program of whole workplace.

Keywords: automated robotized system, camera, duo robot